Mechanisms associated with rumpling of Pt-modified β-NiAl coatings

by

Joseph Peter Henderkott

A thesis submitted to the graduate faculty

in partial fulfillment of the requirements for the degree of

MASTER OF SCIENCE

Major: Materials Science and Engineering

Program of Study Committee:
Brian Gleeson, Major Professor
Xiaoli Tan
Pranav Shrotriya

Iowa State University

Ames, Iowa

2007

Table of Contents

Acknowledgements

I would like to thank my family, Jim, Pat, and Jesse Henderkott, for their constant support during my entire educational career. I would also like to thank my committee members, especially Brian Gleeson, for their assistance during my research. Many thanks also go out to Dan Sordelt and Matt Besser for their help with x-ray runs and trust with their profilometer and other equipment. Support for this research was funded by the Office of Naval Research, with Dr. David Shifler being the Program Manager. Special thanks are extended to Ram Darolia and Brian Hazel at GE Transportation for their input and oversight of the dilatometry runs. Also thanks go out to Bruce Pint for supplying me with CTE data. Thanks also goes to Dan Balint whose model calculations were used to compare the experimental data I recorded. I would also like to thank Kate Ottesen who, not only corrected my entire thesis, but who offered her support and encouragement over seven years.

IS-T 2726

Abstract

The formation of surface undulations (i.e. rumpling) at the bond coat/thermally grown oxide (TGO) interface has been shown to cause failure by spallation of the ceramic top coat in aero-turbine systems. Many mechanisms have been proposed concerning the cause of these surface distortions; however, there is little agreement on what may be the dominating cause of the rumpling behavior. Of these mechanisms, the reversible phase transformation from a cubic β-NiAl structure to a face centered tetragonal (FCT) martensitic phase was of particular interest because of its ability to form surface rumpling in Pt-modified β bulk alloys. However, the bulk alloys used in obtaining that result were simple ternary systems and not relevant to actual coating compositions as other alloying elements enter the coating due to coating/substrate interdiffusion at high temperature. In the current study, the depletion behavior of a commercial coating was studied. Compositions from the depletion path were determined and bulk alloys representing these coating compositions were prepared. The martensitic phase transformation was then characterized using DSC and XRD. The martensitic start temperature on cooling, Ms, was consistently found to b e significantly lower than previously reported values (e.g. 530°C vs. 100°C). Because of the low Ms temperature, the formation of the martensitic phase was concluded to be unnecessary for the occurrence of rumpling. However, cyclic exposure treatments at low temperature (~400°C) of bulk alloys and commercial coatings did show the detrimental effects of the phase transformation in the form of crack formation and propagation leading to eventual failure of the alloys. The current work also infers that the differences in coefficient of thermal expansion (CTE) mismatch between the coating and substrate are the dominating factor leading to rumpling. Dilatometry measurements were made on bulk alloys representing depleted coatings and the superalloy substrate to determine CTE as a function of temperature. Finally, simulations were completed to help determine the role of CTE mismatch. It was found that these results compared closely to those collected during experimental cyclic exposure treatments; although, modifications to the current model were found to be needed in order to truly simulate rumpling.

Section 1: Introduction

The constant evolution of the gas turbine system has led to a steady improvement in the overall efficiency and service life of jet engines. Over the course of several decades a number of major advances in the turbine industry have led to safer, more efficient turbine engines. A number of these advances are indicated in Figure 1 by the progressive increase in temperature capability of the high-temperature alloys used in the engine. Some of the notable advances include the use of cast nickel-based alloys over wrought alloys (1960s), directional solidification of the superalloy as opposed to conventional casting methods (1970s-1980s), and finally, the use of single crystal superalloys (1990s-present).

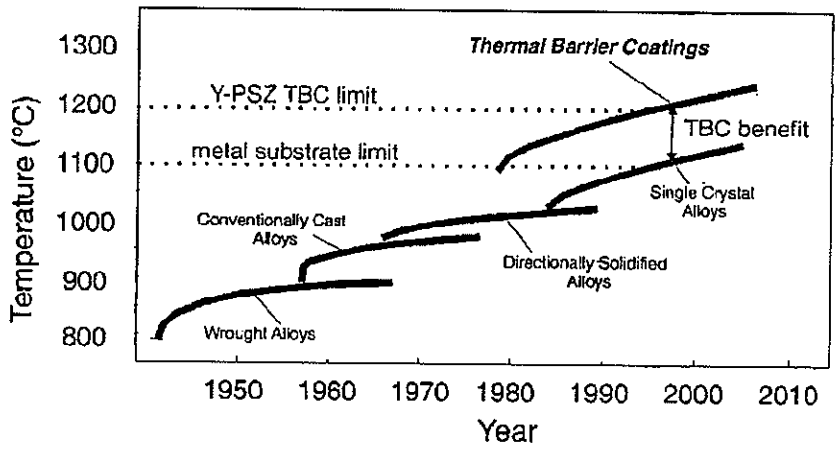

Figure 1: Advances in Gas Turbine Technology Over Time [1]

One of the most important advances in the field of engine production is the use of thermal barrier coatings affixed to the hot-section turbine blades. The beneficial uses of these coatings were first explored in the 1980's and advances continue today. These coatings have the effect of decreasing the overall temperature felt by the metal substrate, thereby, also increasing fuel efficiency. This increased efficiency decreases the cost of operation and allows the engine to be run at higher temperatures for longer periods.

Generally, the temperature in the 'hot zone' of a turbine engine is well above the melting point of the nickel-based superalloy substrate. In some cases, this temperature exceeds 250°C above T_m [1]. The only way for the superalloy to survive, then, is through the use of

some sort of cooling mechanism(s). The major method currently employed is through the use of thermal barrier coatings (TBCs) coupled with internal cooling of the alloy component. Generally, TBCs are made from yittria partially stabilized zirconia (YPSZ), which has a thermal conductivity more than an order of magnitude lower then that of the superalloy substrate [1]. When the coating is added to the superalloy, a high thermal gradient is established within the system. In many cases the gradient is high enough so that a 150 μm layer of a TBC coupled with cooling channels can lead to a minimum 75°C reduction in superalloy temperature [2].

While these TBCs help to achieve more efficient engines, they do suffer from various modes of failure. Some of these failures can be due to causes as simple as debris coming through the engine and hitting the blade. This form of failure is known as foreign object damage (FOD). Part of the coating becomes cracked or sintered together and, eventually, spallation of the TBC occurs. This causes the bare metal to then be exposed to the high temperatures experienced in the engine which can result in severe creep degradation.

Another common type of failure which will occur in lower temperature regimes ($T < 1000^0C$) is due to corrosion experienced when salt deposit attacks the surface of the coating. Salt tends to come from the environment, specifically bodies of water such as the ocean. Therefore, planes that fly across these open waters tend to be more susceptible to the hot corrosion phenomenon.

Unlike the failures listed above, which arise due to a foreign entity entering the system, some forms of degradation come from within the blades themselves. Most often this failure occurs near the interface of the TBC and coating to which it is attached, and is characterized by spallation of the TBC/oxide layer from the bond coat. This delamination can occur by several different means. The first is from oxide formation between the TBC and the bond coat. As the oxide increases in thickness it is more likely to crack and eventually break off from the substrate, leading to spallation. The second form is from creep of the bond coat and/or the nickel super alloy substrate. This can be reduced through the use of TBCs, as a

reduction of only 10-15°C can decrease the creep life by half [1]. Another likely and related cause of failure is through coating/substrate interdiffusion which can deplete the bond coat in elements that are necessary for the adherence of the oxide.

Finally, phase changes within the bond coat, which will be discussed in more depth later, can lead to spallation. This is shown to result in changes in creep strength and coefficients of thermal expansion. The phase changes occurring in the bond coat are a result of the oxide formation as well as interdiffusion of the bond coat into the substrate.

Encompassing all the internal failure mechanisms listed above is a rumpling of the bond-surface observed after oxidation. However, it is not clearly understood which of these factors truly is the dominating mechanism associated with this phenomenon. The focus of this research, therefore, is to more clearly define these parameters as they relate to rumpling such that it may be more easily understood.

This proposal begins by first giving a review of the turbine blade system. This includes the TBC layer and the bond coats to which it is attached. The next section will deal with the oxidation and diffusion process that occurs. Within this section, several of the phase changes that occur in the bond coat will be discussed. This includes the formation of the γ'-Ni_3Al phase, together with the martensitic $L1_0$ structure of NiAl. A review of the martensitic transformation will be given. This transformation will be explained in terms of the binary NiAl system followed by the Pt-modified NiAl series, which is used in many commercial bond coats today. Section 5 will present the rumpling phenomenon seen in Pt-modified NiAl bond coats and explain how the formation of martensite may be a mechanism contributing to the formation of bond-coat surface rumpling. Section 6 will give the objectives of this current project while Sections 7 and 8 will give the procedures used and preliminary results found, respectively. The final section will explain what has yet to be accomplished and suggested changes/modifications to the current project (if any).

Section 2: Commercial Turbine Blade System

A commercial high-temperature turbine blade is composed of several complex layers. The innermost section is the superalloy substrate. This substrate is a nickel-based alloy whose composition will vary depending on the manufacturer, but is invariably of a γ-Ni and γ'-Ni_3Al phase constitution and is designed primarily for strength rather than oxidation resistance. The next layer is the bond coat. This layer is used as an aluminum reservoir for the thermally grown oxide (TGO) layer of Al_2O_3. The final layer is ceramic top coat known as the thermal barrier coating (TBC), which is used as a thermal insulating layer. A schematic cross-section of a typical TBC system is shown in Figure 2.

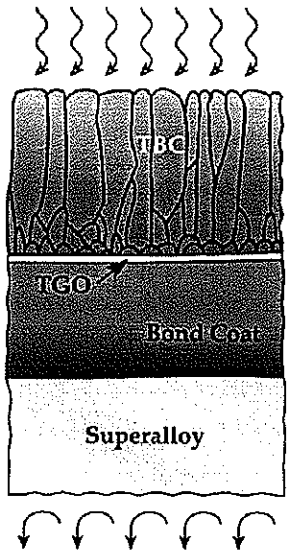

Figure 2: Cross section of TBC system [3]

2.1 TBCs

A thermal barrier coating is typically made up of yittria partially stabilized zirconia (YPSZ) with yittria usually comprising about 7-8 wt% of the ceramic system [2]. YPSZ is chosen over other ceramics for a number of reasons. Most importantly, it has a low thermal conductivity (~1.8W/mK) that will impose high thermal gradients across the surface region of the air-cooled blade [2]. In addition, YPSZ has a relatively high thermal expansion coefficient (~10 ppm/°C), which closely matches the metallic substrate rather closely [3].

This low CTE mismatch, working in conjunction with a high strain compliance, is ideal in the case of thermal cycling (i.e. normal operating conditions). The reason for this is due to the fact that the system is more able to accommodate imposed strains during service. The thicknesses of the TBCs can range from ~150 μm to ~500 μm, depending on the method by with it was deposited.

There are two primary modes of TBC deposition onto a metallic substrate. The first is using the electron-beam physical vapor deposition process (EB-PVD). This technique is most often used on smaller components where a high amount of thermal and mechanical strain is likely to occur (i.e. blades in hot zone) [3]. In EB-PVD, the TBC appears as a columnar structure on the bond coat (Figure 3). This columnar structure leads to several advantages over a solid layer. Between columns, and even within the columns themselves, small pores exist [3]. These pores work to lower the thermal conductivity of the bond coat even further, thereby reducing the overall temperature of the metal underneath. In addition, the affects of differences in thermal expansion between the TBC and the substrate is alleviated somewhat due to the weakly bonded nature of the columns to one another, which confers strain tolerance.

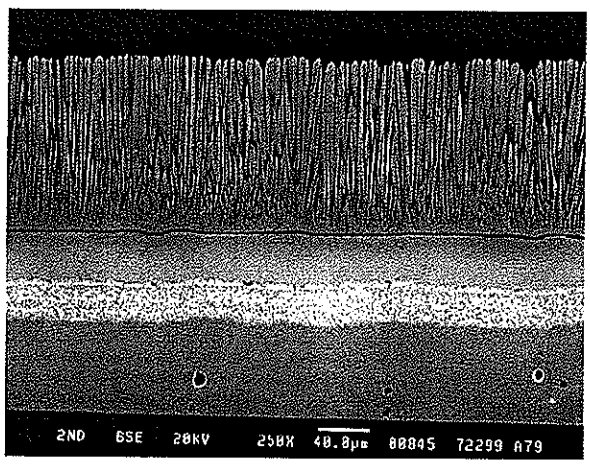

Figure 3: EB-PVD thermal barrier coating on superalloy substrate [3]

The second means of TBC deposition is through the use of air plasma spraying (APS). In this technique, YPSZ is sprayed directly on the surface of the metal. The deposited YPSZ forms a layered structure which tends to be more porous than the EB-PVD technique (Figure

4). While these pores do help in insulation, increasing fracture toughness, and strain tolerance, the APS technique has become overshadowed by the newer, more effective, EB-PVD process within the first and second stages of the aero-engine. However, this deposition technique is still used in other sections of the aircraft engine.

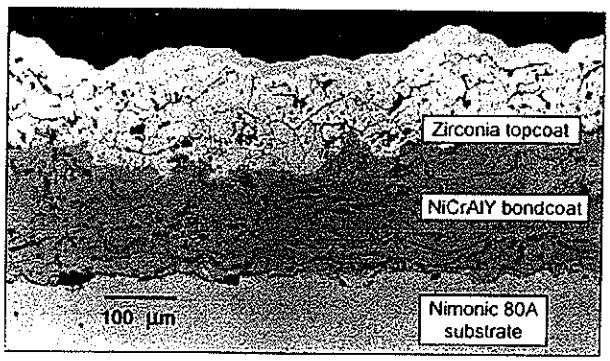

Figure 4: APS thermal barrier coating on superalloy substrate [4]

2.2 Bond Coats / TGO

The primary purpose of the bond coat in the TBC system is to provide oxidation resistance to the substrate as well as to create an oxide layer to which the ceramic topcoat can affix itself. While there are three major types of bond coats used today, their purpose remains the same; the formation of an Al_2O_3 (alumina) scale. Alumina is chosen over other oxides for a number of reasons. The first is that α -Al_2O_3 is phase compatible with YPSZ, ensuring long-term thermodynamic stability of the coating [3]. Because of its high thermodynamic stability and low oxygen and aluminum diffusitivity, alumina is considered to be the slowest growing of the high-temperature oxides able to form [5]. As a large TGO layer will most likely lead to spallation, this makes alumina even more desirable.

In addition to the formation of alumina, the bond coat may also be used to protect the base material from oxidation and hot corrosion effects. If left exposed to high temperatures, a multilayered alumina/spinel section would most likely form. Unlike α -Al_2O_3, these oxides are not thermodynamically stable with the YPSZ and would possibly lead to spallation of the TBC [3].

Deposition of the bond coat to the superalloy can be done in a number of different ways. The most common means are low pressure plasma spraying and electron beam particle vapor deposition (EB-PVD); although, chemical vapor deposition (CVD) and the related powder pack cementation have often been utilized.

2.2.1 MCrAlY Bond Coats

The first series of bond coats to be discussed is the MCrAlY group (M=metal, usually Ni and/or Co). A typical composition is ~20 at% Cr, 20 at% Al, 0.1-0.2 at% Y, with the remainder of the alloy using Ni, Co, or both. When using this type of bond coat the TGO usually exhibits a heterogeneous morphology. This is especially true during the initial heating of the TBC system. The primary reason for the inhomogeneity is that the MCrAlY series is two-phased, consisting of β-NiAl (cubic) and γ-Ni (FCC) [6]. It should be noted that other phases may be present depending on the composition being used, but the β-NiAl and γ-Ni are present in the greatest amount. Figure 5 shows a ternary phase diagram for the Ni-Al-Cr system at 1100°C. Upon heating, all phases present in the bond coat will tend to form their own oxide. As heating continues, these phases will eventually give rise to a more homogeneous α -Al_2O_3 oxide layer, but stresses induced during this transformation can ultimately lead to crack formation.

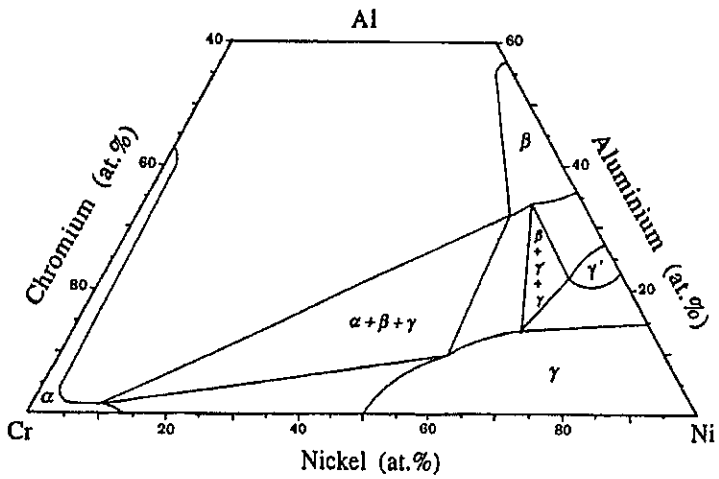

Figure 5: Ni-Al-Cr ternary phase diagram [8]

Problems of inhomogeneity can be alleviated through the use of alloying additions. Various studies [6-7] found that the formation of other, less desirable oxides can be prevented by adding a thin layer of Pt to the surface. In a study by Quadakkers et al. [7], cyclic oxidation was conducted at 1000°C on several MCrAlY coatings. After 1000 hours alumina remained the only oxide present, although substantial amounts of the metastable θ-Al_2O_3 remained on some samples. The disappearance of other oxides was thought to be due to the low oxygen permeability from the presence of Pt at the surface.

The major advantage of the MCrAlY coatings is their ability to resist hot corrosion. Meelu and Loretto [9] reported that the addition of Cr to the NiAl system provided much greater resistance to degradation compared to those samples that simply had been alloyed with Pt. In addition, it was also found that further corrosion protection was achieved by adding Hf to the MCrAlY bond coats.

2.2.2 β Aluminide Bond Coats

Aluminide coatings based on β-NiAl (B2 crystal structure) are similar to the MCrAlY series in that they can suffer from poor oxide scale adhesion. With the addition of platinum, they are not only able to form a slow growing and homogenous Al_2O_3 scale, but also one that is extremely adherent [10, 11]. In many cases, this oxide scale is more adherent than that found in the MCrAlY series because of the lack of heterogeneous to homogeneous oxide transformation. While it seems that this particular bond coat may be superior to the MCrAlY series, Pt-modified β do not have the hot corrosion resistance of the MCrAlY series and suffer from rumpling which, as described further in Section 5, may be due to extensive interdiffusion between the coating and the substrate causing phase changes such as β → martensite, β → γ', or both.

As the stability of alumina is much higher than that of the nickel oxide, alumina is most likely to form in β coatings. However, in order to be used as a coating correctly, spallation must not occur. There is little doubt that the presence of Pt in the β system helps to create a

slow growing scale. What is debated is the reason for this effect. One theory is that the oxygen solubility is extremely low due to the presence of Pt [12]. This causes very selective oxidation in the material during heating. Another theory suggests that the addition of Pt to nickel aluminides increases the amount of aluminum present at the oxide/metal interface [12, 13].

Figure 6 shows the Ni-Al-Pt ternary phase diagram. For a commercial bond coat, the initial aluminum composition is generally around 46-49at%. The amount of platinum can vary with manufacturer, but is usually around 10 at%.

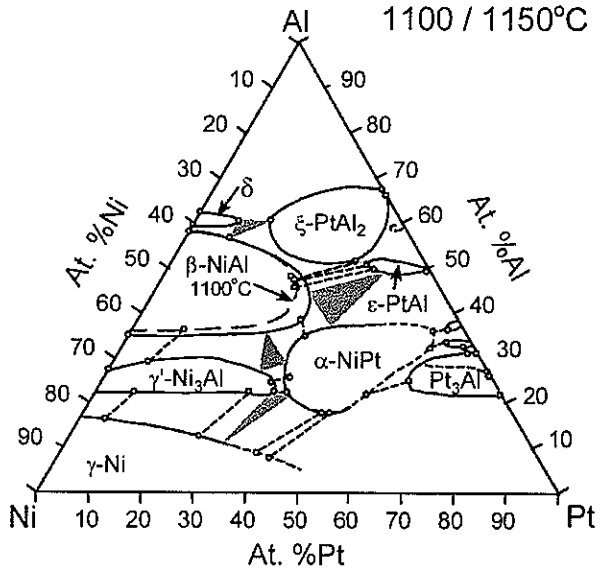

Figure 6: Ni-Al-Pt ternary phase diagram [10]

2.2.3 Pt-Modified $\gamma + \gamma'$ Aluminide Bond Coats

The Pt-modified $\gamma + \gamma'$ bond coat series is the newest type of bond coat available and, as such; few data are available. As can be seen from the phase Ni-Al-Pt diagram (Figure 6), these alloys have lower aluminum content than β but can still maintain similar amounts of platinum. It is hoped that one day these next generation bond coats will surpass the β series due to their higher creep strength and higher compatibility with the substrate.

In papers written by Gleeson et al. [10] and Pint [11], oxidation experiments were conducted on $\gamma + \gamma'$ bulk alloys. It was found in both studies that the oxidation effects to promote scale adhesion of $\gamma + \gamma'$ were similar to those seen in the Pt modified β coatings (Figure 7). It was also determined that Pt has the additional beneficial role within the new bond coats promoting the formation of alumina as the prominent oxide in the TGO.

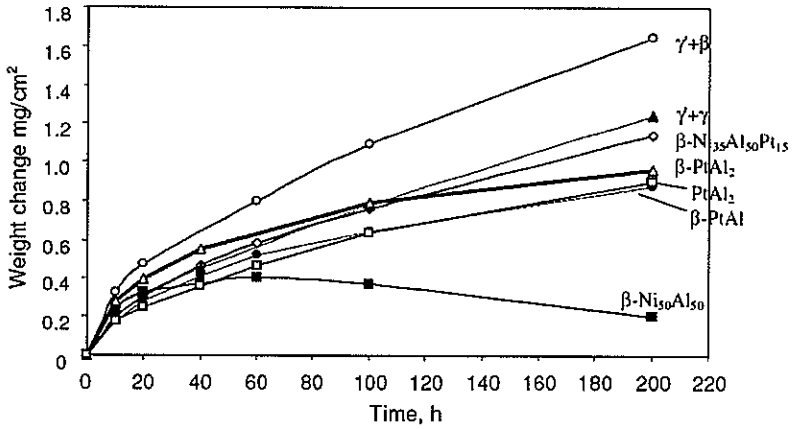

Figure 7: Weight changes for Ni-Al-Pt alloys with different phases after isothermal exposure at 1150°C [10]

One interesting characteristic of the $\gamma + \gamma'$ series is how Pt affects the interdiffusion of aluminum into the substrate. It was found that as Pt is added to the alloy, the chemical activity of the aluminum decreases to the extent that there is uphill diffusion from the substrate to the bond coat [10]. This is significant in that the coating could theoretically have a significant reservoir of aluminum (i.e. the substrate) to aide in the formation of a TGO layer.

Finally, it should be noted that unlike the β bond coats the $\gamma + \gamma'$ series does not seem to contain a large, well defined, band of brittle topologically closed packed (TCP) phases at the coating/substrate interface. This is due to the fact that interdiffusion between the coating and the substrate is reduced between the two layers. While the formation of TCP phases exist in these coatings, the extent to which they are observed is severely diminished compared to the β coatings previously discussed.

Section 3: Affect of Oxidation and Diffusion on Commercial Bond Coatings

While the various layers encompassing a TBC system have already been briefly discussed, more should be discussed on the overall affect of diffusion and oxidation on the strength and durability of the bond coat layer. Many reports have shown that large stresses can form due to the TGO growth and void formation can occur from oxidation and interdiffusion between the TGO, coating, and substrate [14, 15]. In this section these effects and subsequent consequences will be discussed so that a better understanding of TBC failure can be obtained.

3.1 Oxidation Driven Stresses in Metal Alloys

Oxidation at an interface can proceed only by diffusion of ions across the surface. This criterion suggests that diffusion is the rate-controlling step in the formation of oxides. While in many cases this is true, surface reaction control also may play a role in the formation of oxides on the surface. Metal ions can migrate through a material and react with the oxygen at the surface or oxygen can diffuse into the sample and react from within. The desired oxide for high temperature applications is an adherent, slow growing layer that follows a parabolic relationship (Equations 1,2) and does not oxidize within the specimen (i.e. internal oxidation) [16,17]. This requires that there be sufficient amounts of the reactive element and that the desired oxide be the only one to form.

$$dx/dt = k_p'/C \quad (1)$$

$$\Delta W_S^2 = k_p t \quad (2)$$

Where ΔW_s is the weight change due to oxide pick up to form the scale, k_p' and k_p are the parabolic rate constant, x is the instantaneous scale thickness, and t is time

The formation of stress and ultimately spallation due to oxide formation is not limited to the turbine blade system. Any material which forms an oxide that puts the system in a state of tension or compression is susceptible. In addition, other factors such as thermal expansion mismatch, creep, and heterogeneous oxidation may influence the final stress state.

Suo et al. [14] numerically showed how a binary alloy can generate stress due to preferential oxidation of one of the constituents. The authors explains that in an alloy containing A and B atoms, with A forming an adherent oxide a flux divergence occurs (known as Kirkendall effect). While A continues to migrate to the surface, B atoms move further into the substrate. This nonreciprocal diffusion causes a mass gain or loss in the material, generating a strain-rate field. In order to relieve the stress, coalescence of the voids or creep must occur. If the stress is tensile, the coalescence of the voids is apt to occur at the metal/oxide interface. An example of such void formation is shown below in Figure 8. The sample is a Pt modified (NiAl) bond coat but void formation can occur in any metallic system where nonreciprocal diffusion can occur.

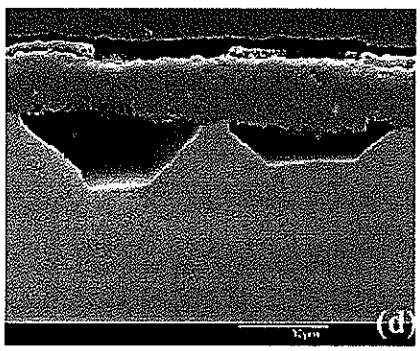

Figure 8: Void formation after oxidation [14]

3.2 Affect of Oxidation on β-NiAl Bond Coats

Oxidation of β-NiAl causes stress build up in a very similar manner to the simple metallic system discussed in the previous section. During initial oxidation a transient form of alumina, Θ–Al_2O_3, is apt to form. This oxide is known to grow primarily by the outward diffusion of the aluminum cations [18]. The formation of this oxide imposes a large compressive stress on the unconstrained sample on the order of 0.5 GPa at 1000°C and

1100°C for binary systems Ni-40Al and Ni-55Al [18]. At different locations along the oxide/alloy interface the desired α-Al_2O_3 will eventually form at the expense of the transient oxide. The formation of this new phase results initially in an extremely high tensile stress, which causes scale cracking [18]. While these cracks may be detrimental to the system they also serve as nucleation sites for further α-Al_2O_3 formation. As the oxide continues to grow the tensile stress in the α-Al_2O_3 and the compressive stress in the Θ–Al_2O_3 eventually decreases to almost zero. Continued growth at 1100°C eventually causes low compressive stresses to form but this stress reaches a steady state of 75 MPa (compression) due to stress formation and relaxation occurring simultaneously [18]. Relaxation will most likely occur through spallation and reformation of the oxide or through creep.

While these results serve as a reference as to how oxidation and stress formation occur in the β-NiAl system, it does not fully represent a real bond coat system. The presence of a top coat creates a system which is constrained and, therefore, unable to creep dramatically. The superalloy substrate may also contribute to stress formation due to CTE mismatch. Finally, these values represent a binary system as opposed to a ternary system (Pt additions) that is traditionally used in commercial bond coats.

The affects of Pt additions on the oxidation growth rate was investigated by Cadoret et al. [19]. In their paper binary β-$Ni_{50}Al_{50}$ was compared to ternary $Ni_{40}Al_{50}Pt_{10}$ alloys using isothermal oxidation at 900°C and 1100°C. At both temperatures (and both sample types) void formation was noted to occur, however, the number of voids was greatly decreased for the ternary system. The differences in the samples were attributed to Pt increasing the diffusivity of Al through the bond coat. The void formation observed in both specimens was in agreement with previous findings [20], which concluded that the void formation was due to the Kirkendall effect, vacancy condensation during cooling due to relaxation of the stress built-up during oxidation, and vacancy condensation due to the large change of the vacancy concentration.

Differences in the overall oxide layer were also noted for the β systems with and without Pt additions [19]. At both temperatures the transition between Θ–Al_2O_3 and α-Al_2O_3 occurred much sooner in the binary than in the ternary alloys. This quick transition between oxides imposed greater stress into the system and spallation was shown to occur. In the case of the ternary alloys, where the transformation was slower, the lifetime was greatly improved because stresses were greatly diminished due to the longer relaxation time.

3.3 Affect of Diffusion on β-NiAl Bond Coats

The selective depletion of Al due to the formation of alumina on the surface will contribute to changing the overall microstructure of the bond coat. In addition, the formation of voids within the bond coat and at the interdiffusion zone (IDZ) may also appear. While some of these changes in the coating are agreed upon to cause problems, others are not as clear.

If it is assumed that the bond coat is only composed of three alloying additions, it can easily be seen from the phase diagram (Figure 6) what phase is likely to form. Aluminum will oxidize at high temperature and a net reduction in Al will occur in the coating. This leaves a relatively constant amount of Pt and an increase in the overall Ni content due to interdiffusion from the substrate. An increase in overall Ni will eventually lead to the formation of γ'. This transformation creates a higher density phase which will result in a reduction in volume of between 8% and 38% depending on the relative compositions considered [31].

The model becomes somewhat more complicated when the affects of interdiffusion of other species are introduced. While the formation of γ' is still assumed to eventually occur, other alloying additions will likely begin diffusing from the substrate into the bond coat. Nickel, which has a high diffusitivity, will account for the greatest change in the bond coat; however, small increases in alloying additions such as Cr, Co, W, and Ta are also likely. Because of the high diffusivity of the nickel, regions of plate-like topologically closed packed (TCP) phases will form. These undesired consequences of interdiffusion lower the overall strength

of the system as well as deplete the substrate of elements such as W and Re, which were added to the substrate for their solution hardening properties [21]. Figure 9 shows the formation of TCP phases within the IDZ.

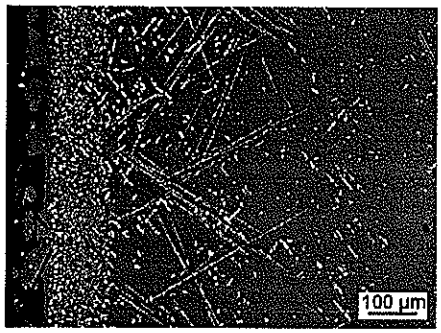

Figure 9: Formation of TCP phases in bond coats [21]

In a paper by Angenete et al. [21] isothermal oxidation was conducted on Pt modified β bond coats at 1050°C. During the first 1,000 hours the bond coat begins to form a noticeable layer of γ' above several voids which had formed. At 5,000 hours a significant portion of the β has transformed to γ'. Finally, after 10,000 hours the bond coat had completely transformed into γ'. The progression from the as-coated structure to that observed after 10,000 hours is shown in Figure 10. This example shows the progression of the bond coat layer for a given temperature at various times. It should be noted, however, that at higher temperatures this transformation can occur much faster due to a much higher diffusivity of Al, Ni and other alloying additions through the bond coat.

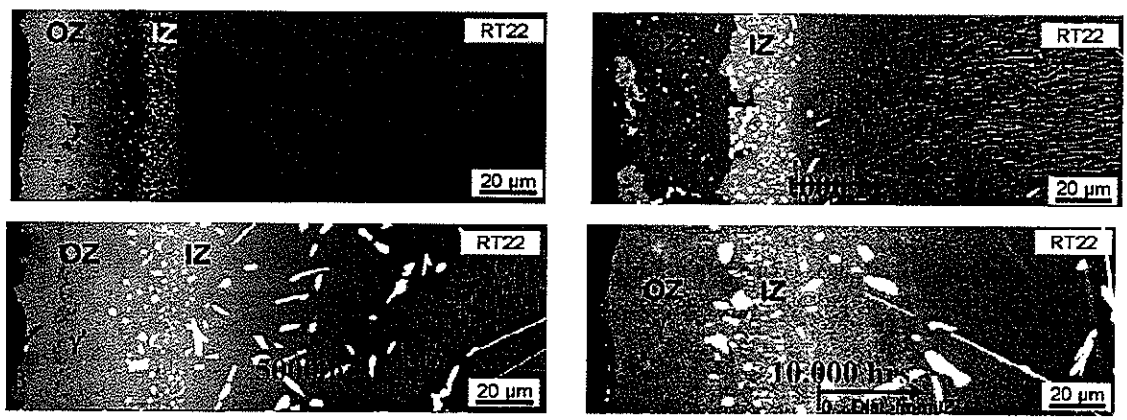

Figure 10: Evolution of Pt-modified NiAl bond coat after isothermal oxidation at 1050°C [21]

The voids experienced in the coating were thought to occur through several means, including diffusion of Al into the oxide and into the substrate as well as Ni diffusion from the substrate into the bond coat [21]. Because the diffusivities of the two species are not equivalent (D_{Ni}/D_{Al} = 3.0-3.5 for Ni rich binary alloys at 1100°C [22]), a vacancy flux is generated and vacancies are formed. These vacancies then coalesce and form voids. This phenomenon was explained previously as the Kirkendall effect. While this theory may successfully be used for high activity (Al rich) alloys, it should not be used to explain low activity (Ni rich) components. In low activity Al alloys the diffusivity of Ni is greater than that of the Al. As the sample is oxidized the Al diffuses into the alumina scale and into the substrate, an even larger flux of Ni moves from the substrate into the coating. This actually causes a noticeable swelling of the bond coating rather than a reduction in volume [23]. Therefore, Kirkendall porosity most likely cannot be used to explain the voids observed in the low activity Al coating

Angenete et al. [21] explained that there may actually be another cause for the formation of the voids. Figure 11 shows how the formation of γ' from the top and bottom of the coating creates voids. When the new phase is created a volume change is likely to occur. In the case of the β to γ' transformation, a reduction in overall volume is created. This reduction creates tensile stresses which can form vacancies. As these vacancies coalesce a void is formed. Voids continue to be created until the β phase is completely consumed. However, as observed by Basuki et al. [23], voids were not necessarily observed in a low activity Al coating even after significant γ' had formed.

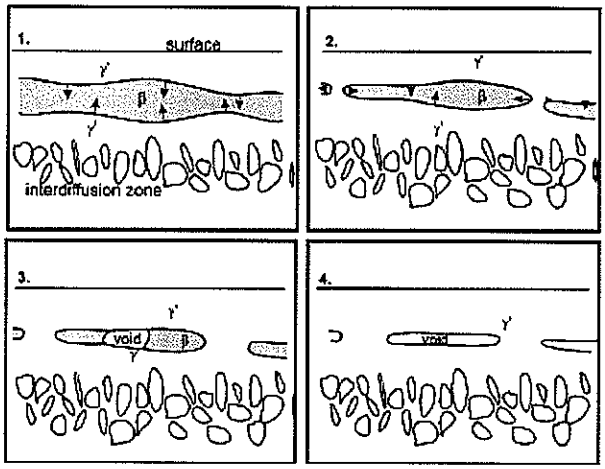

Figure 11: Formation of voids in bond coatings [21]

There is a final phase transformation that may occur for both binary NiAl and Pt-modified NiAl alloys. As the nickel content increases through selective Al oxidation and Ni interdiffusion from the substrate, the composition will progress into a region where it is able to form β', or martensite (Figure 12) upon subsequent cooling. The formation of martensite may have adverse consequences on the longevity of the bond coating due to an overall reduction of volume after the transformation. More detailed information on the martensitic transformation will be presented in the next chapter.

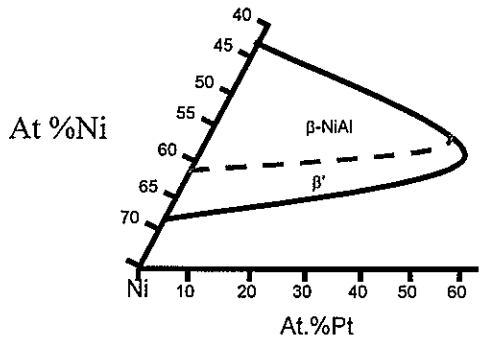

Figure 12: Phase diagram showing martensitic region

Section 4: Martensitic Transformations

The martensitic phase transformation is analogous to twinning in that they both are classified as diffusionless. The difference lies in the fact that martensitic transformations are accompanied with a volume change while twinning is not. In the case of β-NiAl (and Pt-modified β), the B2 phase is cubic, while after the martensitic transformation, the crystal structure becomes face centered tetragonal (FCT). The lattice transformation is shown schematically in Figure 13 below. As Al depletes from the β bond coat layer due to interdiffusion and the oxidation process, the tendency to form martensite on cooling increases considerably. This is because the temperature at which martensite forms, i.e., the Ms temperature, increases with decreasing Al content in the β [24].

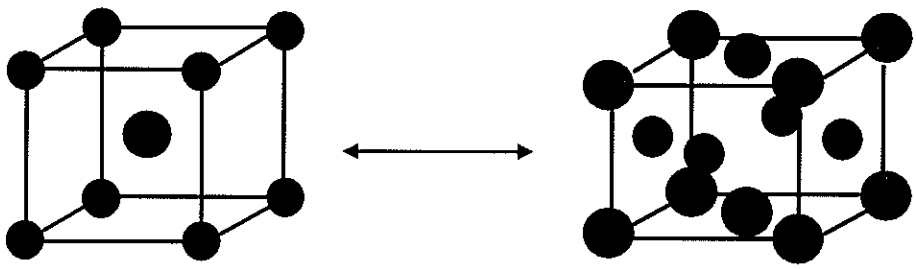

Figure 13: B2-NiAl to martensitic FCT NiAl transformation (blue spheres are Ni while red spheres are Al)

4.1 Martensitic Transformations in β Bulk Alloys

Martensite in binary NiAl was first reported by Maxwell and Grala [25] in 1954. They noticed that alloys containing 17.5 at% and 25 at% aluminum experienced a change in microstructure in what was supposed to be an entirely $\beta + \gamma'$ material. The new microstructure was lamellar in appearance and could be changed (course or fine lamellae as well as relative amounts) depending on the cooling rate used (Figure 14). In addition, some mechanical properties of the material were observed to change. For instance, a 3% increase in elongation occurred at high temperature. Maxwell and Grala [25] compared this martensitic transformation to that seen in the alpha-to-beta transformation for brass and

explained that while the phase change seen in the brass had no real commercial use, the transformation in the NiAl system could aid in the formation of carbides and other intermetallics by creating numerous nucleation sites for growth so long as the correct alloying additions were used. Accordingly, Maxwell and Grala conjectured that the NiAl system would be ideal for high temperature applications.

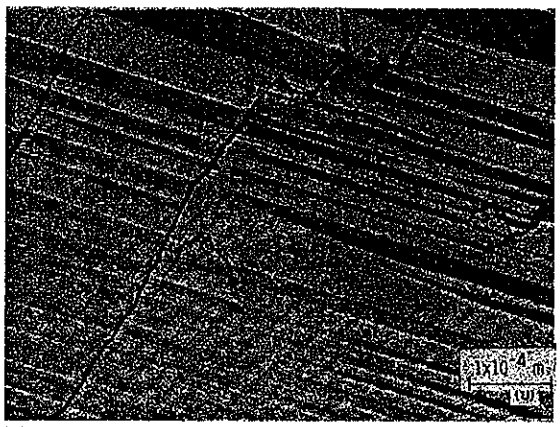

Figure 14: Typical Martensitic Structure in Bond Coatings [24]

Further research by Smialek and Hehemann [24] in the 1970's showed the dependence of the Ms temperature on composition in binary alloys. They determined that increases in nickel content would decrease the ordering forces between the nickel and aluminum, which in turn would lower the amount of shear stress needed to transform the alloy and make martensite the dominant low-temperature phase. They also inferred that because of this ordering affect, stochiometric NiAl would be unable to form martensite. Finally, Smialek and Hehemann determined that the M_S temperature for binary alloys was linear with increasing nickel content. With this observation, the authors were able to generate a general equation relating the two values. This equation, in degrees Kelvin, is shown below.

$$M_S(K) = (124 * at\%_{Ni} - 7410) \qquad (3)$$

While martensite is most often associated with forming through a cooling process, it has also been shown to form from the introduction of stress to the alloy [26]. It was shown in monocrystalline $Ni_{63}Al_{37}$ (B2 structure) that martensite was able to form at the tip of an induced crack. As the crack progressed through the sample the martensite would disappear

and reappear at the new tip (Figure 15). This transformation can be explained in part by the Smialek and Hehemann paper presented earlier. In that paper, it was theorized that a certain amount of shear stress is needed to transform the B2 phase into the $L1_0$ phase. At the crack tip, this stress is high enough for the transformation, but as the crack progresses through the sample, the stress suddenly decreases and the martensite vanishes.

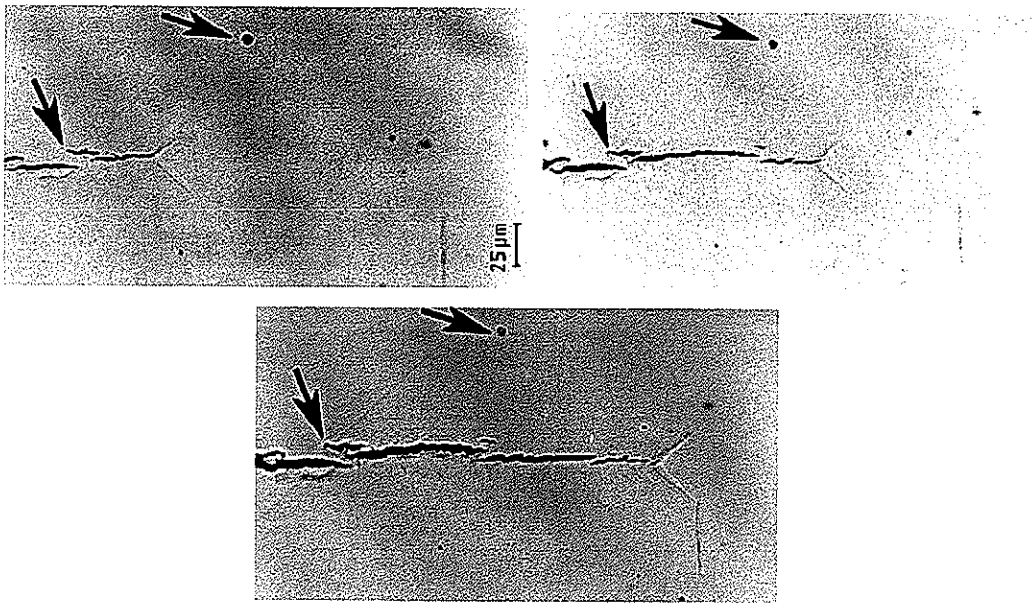

Figure 15: Stress induced martensite in $Ni_{63}Al_{37}$ binary alloy [26]

While the crack-induced transformation results found by Hangen and Sauthoff [26] were significant, another, possibly more important, characteristic of the martensitic transformation was also presented. It was found that martensite does not simply transform en masse at the M_S temperature, (i.e., 100% martensite below M_S) but rather increases in volume fraction as the temperature decreases [26]. A plot showing the volume of martensite in the binary alloy with temperature is shown below. This result suggests that the martensitic transformation in the NiAl system may be athermal in nature, which is generally the case with most martensitic transformations [27]. However, work by Sordelet et al. [28] suggest otherwise. This work focused on the martensitic transformation in ternary Ni-Al-Pt bulk alloys, but the results should be applicable to the binary case. More detail will be presented in Section 4.2 but it was found that holding at a temperature near Ms will cause a progressive increase in the

extent of transformation. Accordingly, the martensitic transformation in β was inferred by Sordelet [28] to be isothermal in nature.

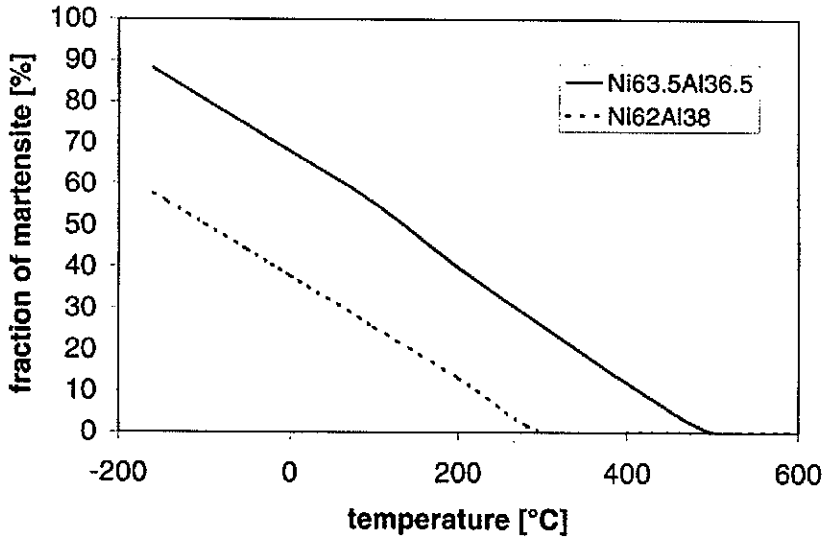

Figure 16: Volume fraction of martensite in binary NiAl alloy at various temperatures [26]

4.2 Martensitic Transformations in Pt modified β Bulk Alloys

The effect of Pt on the martensitic transformation observed in NiAl bulk alloys has only been studied in the last few years and only a small amount of literature data is available. In recent studies by Zimmerman [29] and Jiang et al. [30] it was found that additions of Pt to two alloys ($Ni_{63-X}Al_{37}Pt_X$ and $Ni_{50-X}Al_{50}Pt_X$) would increase the M_S temperature significantly. This phenomenon was explained by Jiang et al. [30] by use of first principles calculations for predicting the effect of Pt on the elastic properties on the β alloys. It was found that if the concentration of Al is held constant and Pt is substituted for Ni, the shear modulus of β will decrease with increasing Pt content. This decrease in modulus indicates a weaker resistance of the B2 lattice to a shear-type transformation and, therefore, a higher M_S temperature is achieved [30, 31]. A plot showing how the transformation temperature and bulk modulus change with Pt additions is shown in Figures 17 and 18, respectively.

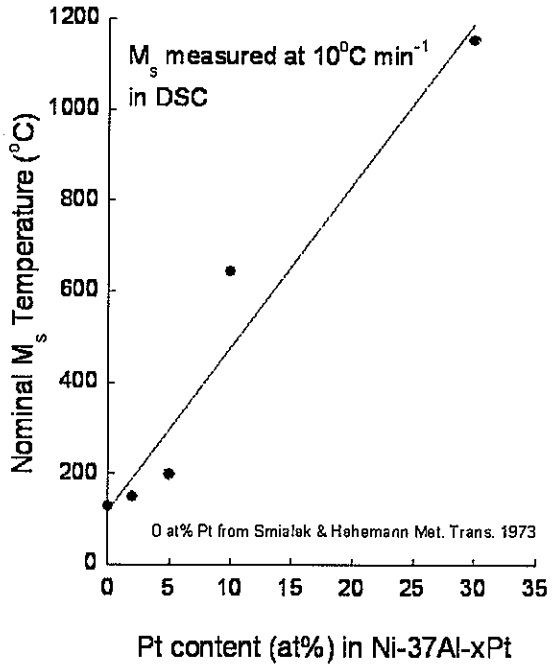

Figure 17: Experimentally determined effect of Pt content on the martensitic transformation in Ni-37Al-XPt Ternary Alloys [29]

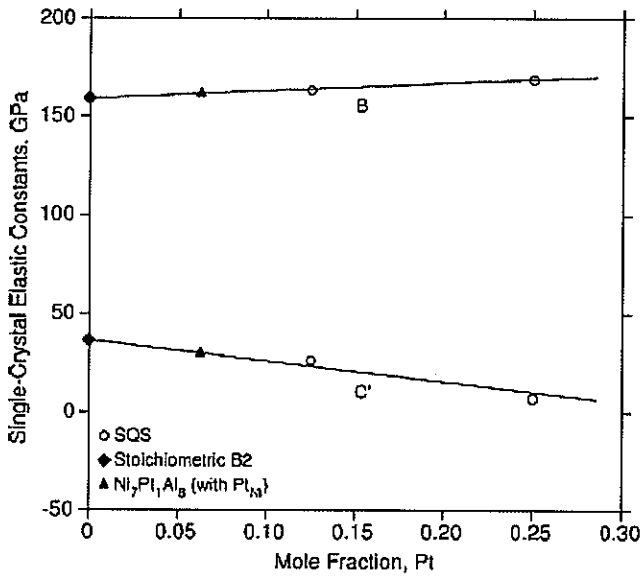

Figure 18: Predicted effect of Pt content on the shear modulus in Ni-50Al-XPt ternary alloys [30]

4.3 Affect of Other Alloying Additions to β Bulk Alloys

While the effect of Pt on the M_S temperature of B2 β is significant, other alloying additions also seem to show variations in transformation temperature. In a study by Kainuma et al. [32] a ternary $Ni_{64}Al_{36}$-$X_{0.5\text{-}1.5}$ system (at%) was alloyed with 14 different elements (denoted

as X) and the resulting change in M_S was recorded using DSC, XRD and TEM. It was found that elements such as Ti, V, Cr, Mn, Fe, Zr, Nb, Mo, Ta, W, and Si decrease the M_S temperature by stabilizing the β phase. In contrast, elements such as Co, Cu, and Ag destabilize the β phase and increase the M_S temperature. Kainuma et al. [32] noted that the variation in M_S temperature between ternary elements was most likely from the lattice stabilities of the BCC and FCC phases of each alloying element.

4.4 Martensitic Transformations in Commercial β Coatings

The martensitic transformation observed in commercial β bond coats has been considered as a major failure mechanism in terms of spallation but, as with the bulk alloys discussed in Section 4.2, little data on the actual martensitic transformation and its consequences are available. A few major papers, however, have modeled the martensitic transformation in some detail [33-35]. Zhang et al. [33] showed the phase transformations that would occur with isothermal and cyclic oxidation experiments of an N5 superalloy having a Pt modified β-NiAl coating. Through the use of optical microscopy, EPMA, and XRD techniques, they determined that an as-coated β coating with a B2 crystal structure would transform into martensite throughout. It was also shown that a section of γ' formed near the interdiffusion zone region after 100 hours at 1150°C. Thermal cycling testing (1150°C 1h + room temp 10 min for 700 cycles) showed similar results, although surface deformation and spallation were shown to occur. The formation of martensite in the coating was thought to occur primarily due to aluminum depletion from oxidation and interdiffusion into the substrate as well as nickel interdiffusion into the coating. The rumpling experienced in the thermal cycling experiment was thought to occur due to the repeated volume change associated with the phase transformation. No experiments were conducted by Zhang et al. [33] to verify this hypothesis, but it was known that some form of volume change does occur during the phase transformation. Figure 19 shows a cross section of an isothermally held coating, as well as the sample which was thermally cycled.

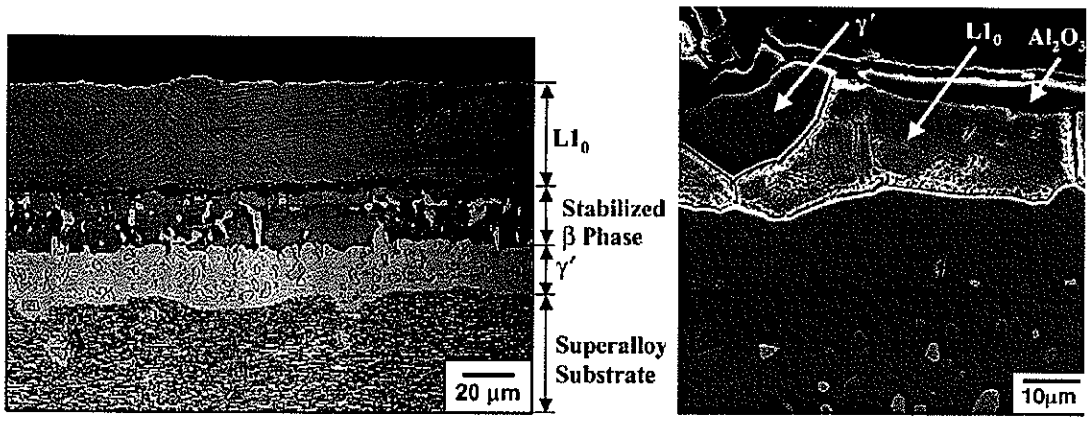

Figure 19: Pt modified coating on N5 substrate: (a) Isothermally held at 1500°C for 100 h (b) Thermally cycled 700 times between 1150°C and 25°C [33]

Work by Chen et al. [34, 35] reinforced the findings of Zhang et al [33]. In the former studies, β coatings were cycled from 1150°C to room temperature to 28% of the furnace cycle test life. These samples were then analyzed using HT-XRD at various temperatures as well as optical microscopy and TEM. The XRD analysis concluded that the austenization temperature (As) for the commercial bond coats was ~680°C for an alloy composition (in at%) of 46.01Ni-35.92Al-8.09Pt-4.45Cr-5.11Co-0.15Ta-0.045Re-0.024W, which was found through microprobe analysis. Using differential thermal analysis (DTA) the As temperature of ~620°C was reinforced and a numerical Ms temperature (530°C) was determined. The DTA plot is shown in Figure 20. Chen et al. noted that by using the equation (Equation 2) generated by Smialek and Hehemann [24] an Ms temperature of 300°C should be expected. However, the equation used to calculate this value is for a simple binary case. Alloying additions such as Pt, as explained earlier, can be expected to raise the Ms temperature significantly while others such as Cr are known to lower it.

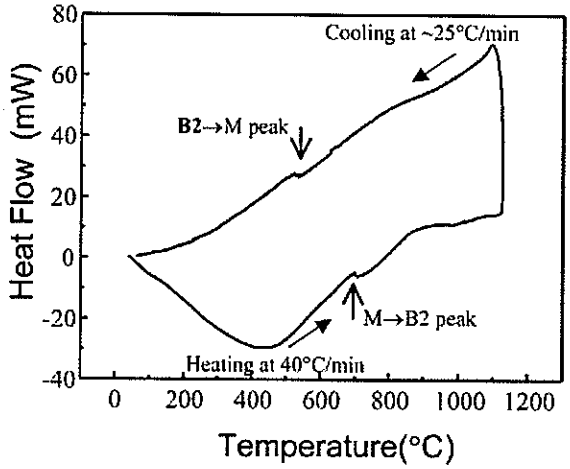

Figure 20: DTA curve of commercial β coating showing β to L10 transformation [34]

Finally, Chen et al. [35] hypothesized about a volume change during the transformation and its effects on the surface quality experienced in the β coating. Through the use of HT-XRD it was determined that the β phase was actually 2% larger than the martensitic phase seen at low temperatures, causing a ~0.7% linear transformation strain. With such large expansions/contractions, Chen et al. [35] explained that stress and strains created during cycling could lead to gross deformation of the bond coat. A plot of the amount of strain generated due to coefficient of thermal expansion (CTE) mismatch and the martensitic transformation in plotted is Figure 21.

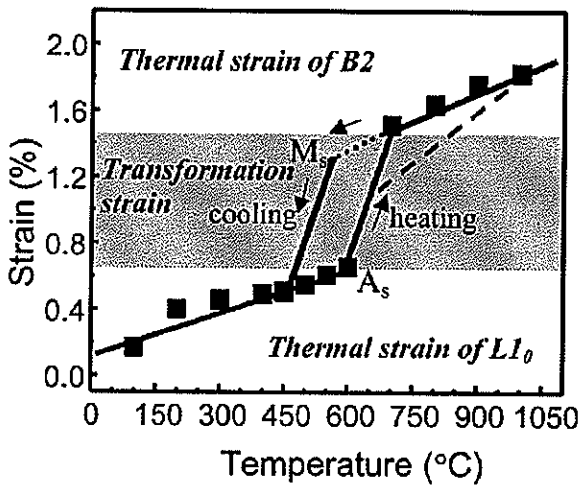

Figure 21: Strain induced in β coatings due to the martensitic transformation and CTE mismatch [35]

Section 5: Rumpling in Pt Modified β Coatings

One of the first papers to discuss the rumpling phenomenon was by Deb et al. [36], who used binary and Pt modified (NiAl) bond coats for isothermal and cyclic testing at 1100°C. After the early stages of cyclic oxidation upheavals on the order of 50 μm (100 μm wavelength) were observed in both coating systems. Later testing showed an increase in the degree of rumpling experienced in the Pt modified specimens (Figure 22). While Deb et al. research does not mention the formation of martensite as the cause for the observed rumpling, some variables may be influenced by the transformation. These variables include coefficient of thermal expansion mismatch, thermal gradient induced strains across the coated specimen, and overall coating strength.

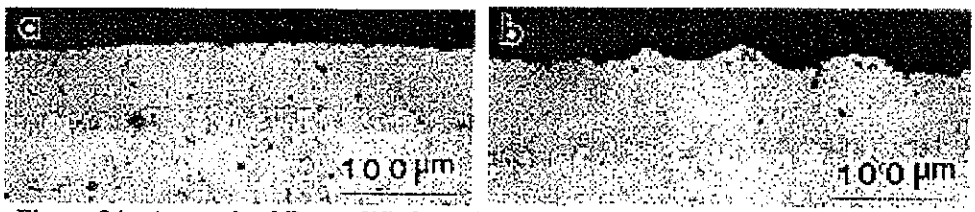

Figure 34: As received Pt-modified coating (a) and coating After 50 Cycles (b) [36]

Accompanying the theories of rumpling, Deb et al. [36] also reported some important characteristics of the rumpling phenomenon that were previously undocumented. The first was that oxide scale adherence was much higher in the Pt modified specimens despite the fact that the degree of rumpling was much more severe. Deb et al. [36] attributed this to the beneficial affects of Pt additions to the binary NiAl system already discussed in Section 2.2.2. It was also mentioned that rumpling only occurred during cyclic oxidation experiments. All isothermal specimens experienced no real measurable degree of rumpling.

The effect of coating thickness on the degree of rumpling was also investigated by Deb et al. [36]. It was found that thicker coatings experienced less rumpling than those that were thinner. This was attributed to an increase in strength of the bond coat which would be needed to overcome the affects of thermal expansion. However, it was noted that the thicker coatings experienced cracking throughout the bond coat while thinner coatings did not.

A 2000 paper by Tolpygo and Clarke [37] further characterized the rumpling phenomenon seen in Pt modified (NiAl) bond coats. Experiments were run using cyclic and isothermal testing at 1150°C and 1200°C. When rumpling did occur, the average amplitude ranged from 30-50 μm and seemed to increase with repeated cycling. These findings were comparable to those published by Deb et al. [36].

One possible explanation for rumpling that had been hypothesized by Deb et al [36] was that relaxation of the growth stresses in the oxide may lead to plastic deformation of the bond coat. In the study by Tolpygo and Clarke [37] two samples were polished using 400 and 800-grit papers and the resulting growth stresses were measured. Interestingly, the small increase in polishing of the bond coat prior to testing lead to a growth stress that was 50% larger than the sample polished using the 400-grit paper. While such an increase in growth stress would likely led to rumpling that was more severe than the underpolished specimen, SEM images clearly showed that, in fact, less rumpling had occurred. These findings indicate that stresses in the oxide do not seem to affect the degree of rumpling observed in the bond coat; however, they do not address whether an oxide is actually needed to facilitate rumpling.

Thermal mismatch between the bond coat and the substrate has also been considered as a contributing factor to rumpling. Coefficients of thermal expansion and relative size differences between the coating and substrate may create thermal strain upon heating and cooling. If this strain is large enough, plastic deformation is likely to occur. Samples held at varying times at high temperature (1150°C) for 100 cycles were studied [37]. While rumpling did occur in both specimens, the sample held at high temperature for a longer period of time was found to have much more severe plastic deformation. This result indicates that the deformation of the sample occurs primarily at high temperature and may not take place during low temperature regimes of the heating and cooling cycle. It should be noted, however, that in this study as well as the one by Deb et al. [36], isothermal oxidation does not yield a measurable degree of rumpling. Therefore, while the time at high temperature is important, temperature changes also seem to play some role.

While the oxide layer was found to be almost identical (rumpling excluded), the bond coat microstructure of the isothermal and cyclic specimens were quite different. In the cyclic testing a well defined, continuous, γ' layer developed near the inner and outer layers of the bond coat (Figure 22c). Samples held isothermally at high temperature showed areas of γ' formation but, unlike the samples run using cyclic oxidation, the layer was not well defined. In addition, large pitting had occurred in the cyclic sample (Figure 22f). Tolpygo and Clarke [37] hypothesized that while rumpling and void formation are different phenomena, they may, in fact, be products of the same process.

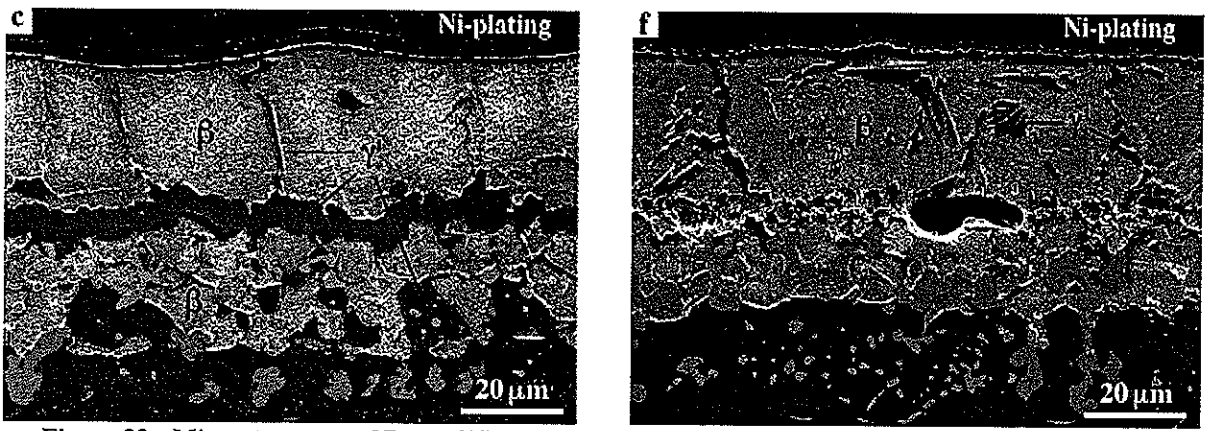

Figure 22: Microstructure of Pt-modified bond coat after cyclic (c), and isothermal (f) oxidation at 1150°C [37]

The formation of rumpling in the bond coat was determined to occur primarily through a reduction in volume [37]. This reduction in volume was postulated to occur through the formation of γ' from the depletion of Al into the substrate and into the TGO. In their modeling the Tolpygo and Clarke [37] determined that an overall reduction of 38% would occur due to this transformation. If this phase change was continuous, the surface would remain planar but as shown in Figure 22a this is not the case upon early cyclic oxidation.

Panat et al. [38] attempted to explain rumpling using a more thermodynamic approach by imploring a method used in the semiconductor thin film industry. These authors proposed that stresses building up in the bond coat due to interdiffusion between the coating and the substrate dictate the lifetime of the system. While this hypothesis was not new, the authors

did suggest that the chemical potential of the bond coat was what drove the rumpling effect. The effects of differences in chemical potential in terms of mass rearrangement were first explained by Freund [39]. Panat et al. [38] explained, the chemical potential is dependent on several factors including elastic strain energy, the surface energy of the bond coat, and curvature of the coating. Accordingly, the chemical potential is not constant throughout the specimen. This variation along the surface then drives the diffusion of the surface atoms along the bond coat/TGO interface but at different fluxes throughout. As atoms accumulate in certain areas, rumpling may occur. The results of this quantitative approach were compared to several experimental results observed in other papers. While the results matched closely, the model seemed to contain several critical assumptions which may prove false. First and foremost, Panet et al. [38] only assumed that the diffusion driven stresses were the cause for rumpling. As discussed earlier, several other factors appear to influence the occurrence of surface rumpling. Also, the authors assumed that their must be a critical curvature on the surface prior to cycling for undulations to form. This critical wavelength then grows at the expense of other smaller undulations on the surface. In bulk alloy cyclic oxidation experiments run by Zimmerman [29] samples polished down to 1 μm were shown to rumple.

A series of three papers by Tolpygo and Clarke [40-42] further assessed the factors affecting rumpling. In the first of these papers [40], a study of the effects of coating thickness on the degree of rumpling was conducted. It was found that a thinner coating would rumple when compared to a thicker one (Figure 23). In many cases, however, thicker coatings could show rumpling along the same order as thin ones, but more cycles were needed to create the similar degree of surface undulations. Using the qualitative results, Tolpygo and Clarke were able to determine that rumpling would be most severe in coatings that were between 100 μm and 150 μm thick.

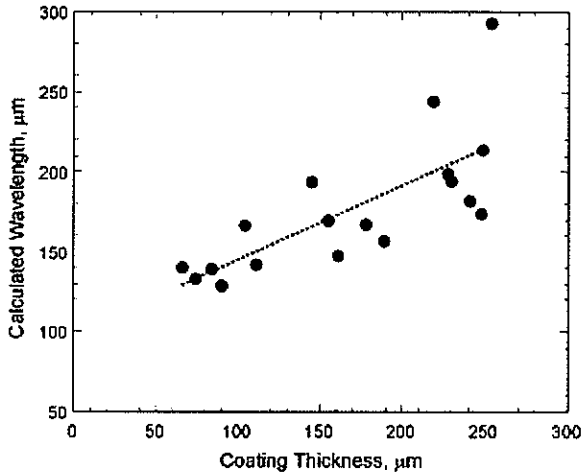

Figure 23: Affect of coating thickness on degree of rumpling observed in Pt-modified NiAl coatings [40]

It has been widely assumed that coating/substrate thermal mismatch is a major cause for the rumpling behavior. If this was the case, though, coating thickness would not affect the degree of rumpling observed. It was also noted that the rate at which the coating changes can be affected due to the coating thickness. The authors explained that as this composition changes different phases such as γ' could form in addition to the volume decrease observed due to the formation of the alumina layer. Finally, it was concluded that because bulk alloys whose composition matches that seen in the bond due not rumple, coatings that were extremely thick or thin would be ideal to use in commercial bond coat systems. This conclusion may be in error; however, as recent work by Zimmerman et al. [29] showed that bulk alloys are, in fact, susceptible to rumpling.

The next paper by Tolpygo and Clarke [41] further dealt with an experimental assessment of the rumpling phenomenon. In that paper, both a commercial bond coat and a bulk alloy with a composition comparable to the bond coat surface were analyzed. The composition used for the bulk alloy was 45.6% Ni, 43.6% Al, 5.5% Pt, 3.6% Co, 1.7% Cr (in at%) . Small amount of Y (~50-200 ppm) were added for greater scale adhesion. As with previous studies it was found that repeated cyclic oxidation of the bond coat leads to rumpling. Oddly enough, though, the bulk alloy was not observed to rumple during the same test. As the degree of oxidation on the surface was similar for both samples, it was suggested that the formation of

the oxide is not a major factor in rumpling. To further show this, the authors pre-oxidized a commercial bond coat so that it formed a very thin TGO scale. It was then wrapped in a tantalum foil and sealed under vacuum in silica ampoules. The specimens were cycled and analyzed. It was found that even though little oxide growth occurred the samples still seemed to rumple.

Tolpygo and Clarke [41] also looked at the martensitic transformation as a factor in rumpling. The authors used the data collected by Chen et al. [34] when determining the M_s and A_s temperatures from which to cycle the coatings. This M_s temperature was found to be ~530°C. In one experiment a bond coat was cycled between temperatures that were well above the M_s for the coating composition. This was then compared to a bond coat which had been cycled above and below the M_s temperature. After comparing the degree of rumpling it was found that the two coatings had undergone similar extents of rumpling. Another experiment was then used in order to verify that the martensitic transformation did not affect rumpling. A bond coat was oxidized in air for 300 hours at 1150°C. This drove the bond coat composition down to one that could easily for martensite. The sample was then cycled from 1150°C 6 min at temperature to 25°C 1h at temperature (100 times) and the degree of rumpling was analyzed. It was found that the degree of rumpling remained unchanged between the isothermal and cyclic exposure experienced by the coating. The authors were careful to rule out the transformation as a mechanism for rumpling, however, because some bulk alloys did experience rumpling that may have been due to the martensitic transformation.

Finally, volumetric changes were considered by Tolpygo and Clarke [41]. A likely reason for these changes was thought to be the formation of γ' owing to Al depletion. The estimated volume decrease due the formation of this phase is between 8% and 38% [41]. If this transformation does not occur homogenously (as is the most likely case) undulations should form due to the decrease in overall bond coat volume. Tolpygo and Clarke concluded that rumpling had been observed in samples before the $\beta \rightarrow \gamma'$ transformation had occurred, and

while the transformation may increase the degree of rumpling observed, it was not the initial cause of the phenomenon.

The third paper by Tolpygo and Clarke [42] offers a more quantitative approach to rumpling. Commercial bond coats were either cycled between 1150°C and 25°C or held isothermally at high temperature. As before, samples that were cycled appeared to rumple more than those held isothermally. Interestingly, however, was how similar the extent of rumpling during the early stages of cyclic oxidation was to that found during the initial isothermal oxidation periods. The degree of rumpling seemed to increase dramatically in the cyclic oxidation periods after approximately 25 hours (Figure 24). In addition, it was found that while the amplitude of the undulations increases with cycling the wavelength remains unchanged. This wavelength (~80 μm) was reported by Tolpygo and Clarke to correspond to the average grain size of the coating.

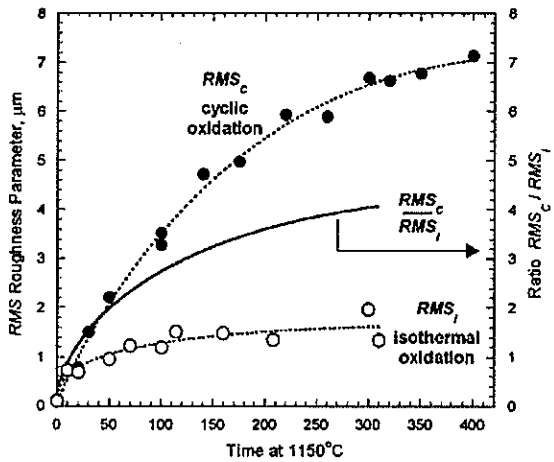

Figure 24: Amplitude of Undulations Seen in Commercial Bond Coating [42]

A more analytical approach to the rumpling behavior was presented by Balint and Hutchinson [43]. While these authors approached the issue in a purely quantitative sense, they did use experimental data derived from the work of Tolpygo and Clarke [37, 40-42] as well as Karlsoon et al [44, 45] as a means of comparison. According to the analytical model developed by Balint and Hutchinson, rumpling is a very complicated process with over 20 different parameters affecting the overall surface quality. That said, these authors decided to

break it down into 5 major effects. These being: thermal history, wavelength and amplitude, the martensitic transformation, and influence of heating/cooling rates.

It has been shown before that isothermal oxidation yields a more planar surface when compared to bond coatings which have undergone cyclic oxidation. Balint and Hutchinson [43] explained that undulation growth is promoted by the equi-biaxial stress in the bond coat. When the sample is heated the stress relaxes and the bond coat is susceptible to undulation growth arising from pressure applied to the coating from the TGO layer. In isothermal oxidation the stress relaxes to almost zero and remains so for the remainder of the heat treatment. While rumpling has occurred to some extent during this relaxation it may be small enough to be considered nonexistent. On the other hand, cyclic oxidation renews the stress levels after each thermal cycle and some growth is produced.

The effects of wavelength and amplitude were already discussed by Panet et al. [38]. Balint and Hutchinson [43] expand on this hypothesis, however, and concluded that when the number of cycles is less than 25, the undulations with the shorter wavelengths grow the most rapidly due to the small thickness of the TGO layer. As the number of cycles surpasses this number, the oxide layer increases in thickness and longer wavelength undulations grow at faster rates. Eventually these undulations coalesce with the shorter ones and rumpling increases.

The thermal mismatch due to the martensitic transformation can have a major effect on the degree of rumpling experienced in the bond coat. Balint and Hutchinson [43] noted that even a small change of -100°C can change the growth stresses by almost 60%. This reduction of stress is highest when the bond coat is the most susceptible to transverse deformation ($T<600°C$).

The final major cause of rumpling was said to occur do to heating/cooling rate effects. Balint and Hutchinson [43] showed that with an isothermal hold at the same temperature during the same amount of time, undulations were predicted to be higher for those samples which took

longer to reach temperature (i.e. lower heating rate). It was concluded that this occurs due to the fact that the bond coat remains at temperatures where the creep strength is low for longer periods of time. This allows deformation to occur at the surface prior to reaching temperature. In addition, during low heating rates there is less time for the growth stresses to decay. Because these growth stresses remain in the coating, the degree of rumpling appears much more severe.

Section 6: Project Aims and Thesis Overview

The primary objective of this project is to further asses the martensitic transformation and how rumpling occurs in commercial Pt-modified coating compositions. The specific aims of this project are as follows:

1. Determine the time and temperature dependence of commercial coating compositions during isothermal heat treatments.
2. Determine the M_S temperatures for various compositions relevant to those found in (1).
3. Determine how the superalloy substrate affects the degree of rumpling experienced in Pt-modified NiAl coatings. Variables considered are interdiffusion, oxidation, phase transformation, and CTE mismatch.
4. Arrive at a clear understanding of the key factor(s) affecting rumpling and, hence, ways to mitigate its occurrence

The results of this thesis work are presented as three separate works that will be published in the future. Each paper contains its own introduction, experimental procedures, results, and discussion. A general conclusion section has been placed at the end of the third paper in order to help tie together results. This section will also be used to suggest possible future research interests.

Section 7: Investigation of the Martensitic Transformation and Rumpling in Pt-Modified β-NiAl Based Coatings

J. Henderkott, B. Gleeson

The effect of depleted β-(Ni,Pt)Al coating compositions on surface rumpling were investigated. This was done be first studying the depletion behavior of commercial Pt-modified β-NiAl based coatings in order to determine relative quantities of alloying additions present in the system. This included primarily Co and Cr additions; however, additions of Ta, W, and Mo were also noted. It was found that while the depletion behavior was time dependent over a 100°C temperature range, the depletion behavior was relatively independent. Nickel rich compositions were chosen because of their ability to undergo the β to martensitic transformation and processed into bulk alloys. By means of different thermal analysis techniques, the martensitic transformation temperature, Ms, was determined and found to be ~100°C, which was 400°C less than what was previously recorded. This was explained to be due to varying amounts of alloying additions such as Pt, Cr, and Co which may alter the Ms temperature. Thermal exposure treatments were then used on depleted coatings to determine what role the martensitic transformation had on the surface rumpling behavior. When cycling exclusively above the transformation temperature, rumpling on the order of what was observed when cycling above and below Ms occurred. This result indicated that martensite was not a requirement for rumpling and that some other mechanism must govern the behavior. Knowing this, differences in coefficient of thermal expansion mismatch are theorized to be the dominating factor associated with the rumpling phenomenon.

7.1 Introduction

Increases in the efficiency and the longevity of materials are essential goals in aero-engine research. With increases in these parameters, higher operating temperatures and, ultimately, lower costs can be expected [1, 2]. The use of thermal barrier coatings (TBC) in conjunction

with internal cooling channels has greatly contributed to this goal. By providing excellent thermal insulation to the metallic Ni-based superalloy substrate, increased service lives of the blades may be achieved [1, 2].

The section of the blade above the superalloy substrate is composed of three independent layers. The first is a ceramic top coat which is made of yittria partially stabilized zirconia (YPSZ); with yittria making up between six and eight mol% of the ceramic [2]. The topcoat is usually deposited by either an EB-PVD or a plasma spraying process [1-4]. Yittria partially stabilized zirconia is chosen over other ceramics for a number of reasons. Most importantly, it has a low thermal conductivity (~1.8W/mK) that will impose high thermal gradients across the surface region of the air-cooled blade [2]. So high are these thermal gradients that a 150 μm thick layer may reduce the temperature felt by the substrate by 75°C [2]. In addition, YPSZ has a relatively high thermal expansion coefficient (~10 ppm/°C), which closely matches the metallic substrate [3]. The resulting low CTE mismatch is ideal in the case of thermal cycling (i.e. normal operating conditions).

The next two layers are the thermally grown oxide (TGO) and the bond coat. Ideally, the TGO is composed of an Al_2O_3 scale, which is desired over other oxides for its compatibility with the ceramic top coat layer and its ability to form a slow growing adherent scale [3, 5]. Formation of a TGO occurs at the expense of the bond coat whose purpose is oxidation and hot corrosion resistance as well as a means of attaching the ceramic top coat. Typically, bond coatings utilize the MCrAlY (M=metal, usually Ni, Co, or both) or the Pt-modified β-NiAl system. Generally speaking, MCrAlY-type coatings are favored when considering the effects of hot corrosion on the coating. This is due to Cr additions which, the Pt-modified β-NiAl system usually lacks [9, 11]. On the other hand, above 1000°C oxidation becomes the dominant surface degradation mechanism and the β-type system becomes the preferred coating [11]. This is especially true when Pt is added to the binary NiAl system, as it creates an oxide scale which has increased adherence [10-13].

If spallation of the TBC portion of the blade should occur, the metallic layer beneath would be subjected to large increases in surface temperature. These increases in temperature would likely cause the metallic layers to creep, ultimately leading to failure. The failure of a turbine system can be catastrophic so there is a large incentive in studying how to predict when failure of a blade can occur and what mechanisms increase the rate of TBC failure.

While there are many mechanisms which may cause a turbine blade to fail, one is of particular interest when considering the Pt-modified β-NiAl coating system. After repeated cyclic oxidation the formation of surface undulations ('rumpling') is observed at the bond coat/TGO interface. As rumpling proceeds, delamination of the TBC layer is likely. Rumpling has been proposed to occur by several different means. These include stress generated by volumetric changes (i.e., swelling), stress generated by oxidation, mechanics of the coating, strains generated due to large thermal gradients across the coating, mismatch in coefficient of thermal expansion (CTE) between the coating and substrate and/or coating and TGO layer, and phase transformations due to interdiffusion and oxidation of the coating [36-43].

Of these mechanisms, phase transformations within the β system are of the most interest for the work presented. The transformation from β to the L10 martensitic phase, as well as the transformation of β to the γ'-Ni_3Al phase, have been shown to cause large decreases in the overall volume of the coating (~2% and ~4% respectively), which are likely to impose large compressive stresses [34, 35]. However, rumpling in the β system has been shown experimentally to occur before the onset of the γ' transformation [41] indicating that it may not be a direct cause of the deformation but rather may help to further the degree of undulations observed. Because of this result, the martensitic transformation will be the focus of this work.

The nature of the martensitic transformation in binary NiAl-based alloys has been extensively studied [24-26]; however, only minimal research has been conducted on the transformation in Pt-modified systems [28-35, 41]. It is known, though, that the addition of

Pt raises the martensitic transformation (Ms) temperature significantly [29-31]. Other alloying additions such as Cr are known to lower Ms by increasing the tetragonal shear modulus (C') of the B2 NiAl lattice [30, 31]. However, these are not the only alloying additions which may affect the martensitic transformation temperature, Co is believed to work much the same way as Pt, while Mo, Ta, and W are known to lower the Ms temperature [32].

Rumpling caused by the martensitic transformation in β coatings has been reviewed in previous studies [36-43]; however, one paper has indicated that bulk alloys do not rumple leading to the belief that the transformation is not a direct cause of rumpling [41]. Recent work by Zimmerman [29] showed otherwise; when using a Ni-40Al-15Pt bulk alloy with an Ms temperature of ~875°C. It was concluded from that work that with a high Ms temperature, the bulk alloy would be able to creep due to the transformation, and rumpling would occur.

With the recent work by Zimmerman [29], there is renewed interest in determining how the martensitic transformation occurs in the β-NiAl system and what affect it has on the degree of rumpling observed in commercial coatings. The occurrence of interdiffusion and oxidation of commercial coatings at high temperature creates a system which is far more complicated than the model ternary systems used previously by Zimmerman. With that in mind, there is a need to understand the depletion behavior of commercial coatings before analyzing the martensitic transformation. In this study, several bulk alloys representing commercial coatings at a given time and temperature were constructed with the aim that they would undergo the β → martensitic transformation. This behavior was analyzed using differential scanning calorimetry (DSC) and X-ray diffraction. Finally, cyclic exposure treatments were conducted on the bulk alloys and associated commercial coatings to determine how the martensitic transformation affects the degree of rumpling. The results from the cyclic heat treatments were then used to determine what factor(s) truly affect rumpling.

7.2 Experimental Procedures

Specimens used in this study were either bulk alloys procured from the Materials Preparation Center (MPC) at Ames Laboratory or commercial Pt-modified β coatings provided by General Electric (GE). In the case of the bulk alloys, specimens were prepared by arc-melting high purity metals under an argon atmosphere and then drop casting the molten alloy into 10 mm or 12 mm diameter castings which were ~ 40 mm long. These castings were then homogenized under argon at 1200°C for 6 hours followed by a treatment at 1150°C for 48 hours. Specimens 1mm long were then cut from the casting and polished down to a 1200-grit finish prior to testing.

The commercial β coatings were deposited onto 25.4 mm diameter René N5 substrate buttons. Unlike the bulk alloys, no homogenization step was performed. However, in some cases the coating surface was polished to a 1200-grit finish in order to achieve a fully planer surface.

Samples were heat treated at 1150°C (unless noted) in still laboratory air either by cyclic or isothermal oxidation using either a horizontal or vertical tube furnace. Both furnaces were programmable; however, the vertical furnace was capable of cycling between two hot zones. Heating rates were ~200°C/min and time at temperature was 1 hour (unless noted). In most cases samples were cycled 100 times.

After a given thermal exposure, surface morphology was analyzed using a Hommelwerke stylus profilometer. Scans were conducted in a 2 mm x 3 mm section of the sample using a TK300 stylus with a vertical measurement range of 80μm. A scan speed of 0.15mm/s and a cut-off length (λ_c) of 0.25mm were used. After completing a scan, two parameters were calculated for the measured area. The first is RzDin, which is an average peak-to-valley roughness for a given scan length. The second, λ_a, which is an average peak-to-peak wavelength calculated using the following equation,

$$\lambda_a = \left(\frac{R_a}{\Delta a}\right) 2\pi \qquad (4)$$

Here, Ra is the average roughness per scan and Δa is the change in slope. Figure 25 is used to define the parameters more closely.

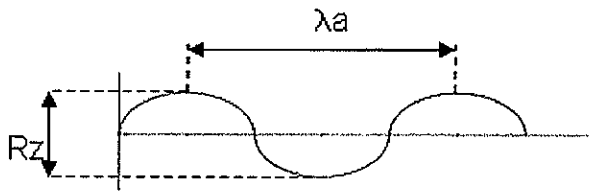

Figure 25: Definition of parameters used in profilometry experiments

After analyzing the sample using profilometry, specimens were studied using scanning electron microscopy (SEM). For all samples, both surface examinations as well as cross-section analysis were conducted. Samples were first sputter coated with gold to ensure a conductive oxide surface and, after analysis of the surface was completed, mounted in an epoxy resin. Specimens were then cut and metallographically polished using standard techniques so that the cross sections could be observed.

In addition to conventional SEM techniques, electron microprobe analysis (EPMA) was used in order to determine compositions of the phases present in both the bulk alloys and coatings. In general, point analysis was conducted on each phase in the bulk alloys while line scans were made on the commercial coatings. In the case of the line scans, an increment of 5 μm was used in the superalloy substrate while a 1 μm step was used in the interdiffusion zone, coating, and TGO layer.

7.3 Experimental Results

7.3.1 Depletion Behavior of Commercial Coatings

In order to determine relative amounts of alloying additions were needed in forming bulk alloys the depletion behavior of a commercial coating on a René N5 substrate was studied.

Isothermal heat treatments at 1150°C were used in conjunction with microprobe analysis in order to determine the composition of the coating.

The resulting aluminum contents are shown in Figure 26 and summarized in Table 1. All compositions were listed in at% rather than wt% in order to better observe how the composition of the coating changed over time. Noting changes in composition using wt% would be difficult as it is dependent on molecular weights of the alloying additions rather than fraction of atoms present. The figure shows the initial Al composition ranged from 51 to 40 at%. This variability in composition was assumed to simply be due to the factors associated with the chemical vapor deposition (CVD) coating deposition process. As CVD is a diffusion type deposition, variations in coating composition may arise under different application conditions [47]. Exposure of the coating at high temperature caused the Al content to steadily decrease by almost 33%. While this was considered the most dramatic change in composition, changes in other alloying additions were also apparent. This included an increase in Ni by almost 20% and increases in Co and Cr from 2.5 at% to 5.1at% and 0.7 at% to 5.2at% respectively.

After 10 hours of exposure, the amount of Al and other components (Figure 26 and Table 1) in the β layer became fixed. However, swelling of the β coating at this time could be observed. This is denoted in Figure 27 as an increase in the overall coating thickness from a thickness of ~ 30 μm in the 'as coated' condition to ~38 μm after 10 hours of exposure. This increase of the β coating thickness is due to interdiffusion of primarily Ni into the coating as discussed by [ref]. Reduction of the β layer thickness was found to occur at 100 hours exposure time (32 μm coating length). Recession of the β coating occurred due to the formation of the γ'phase which occurred as the Al content dropped to 30 at%. This new phase likely formed near the interdiffusion zone where Ni content would be highest. The fact that the coating thickness was the largest at 10 hours and the Al content had reached 30 at% indicates that the phase transformation occurred very soon after this exposure time.

Table 1: Average compositions of β phase in Pt-modified NiAl coating on René N5 substrate after different times at 1150°C (in at%)

Time at 1150°C	Ni	Al	Pt	Co	Cr	Mo	W	Ta
As Coated	44.4	46.5	5.8	2.5	0.7	0.0	0.0	0.0
15 min	42.6	39.4	10.1	3.9	3.4	0.01	0.2	0.4
30 min	45.2	39.0	8.5	3.9	2.9	0.03	0.2	0.3
45 min	46.5	37.2	7.9	4.4	3.5	0.0	0.2	0.3
1 h	48.9	37.0	7.2	3.9	2.9	0.1	0.0	0.1
2 h	50.1	35.0	6.3	4.3	4.0	0.1	0.03	0.2
3 h	52.0	33.0	5.4	4.6	4.5	0.1	0.05	0.4
10 h	52.3	31.2	5.0	5.4	5.4	0.1	0.1	0.5
100 h	53.2	31.2	4.8	5.1	5.2	0.1	0.1	0.3

Further testing of the commercial β coatings at different temperatures (1100°C and 1050°C) yielded compositions analogous to what was observed at 1150°C (see Tables 2 and 3, respectively). However, it should be noted that while the compositions were comparable, the time to reach a given composition did increase with decreasing exposure temperature. Figure 28 shows the diffusion paths for the Pt-modified β coating normalized into a ternary Ni-Al-Pt isotherm.

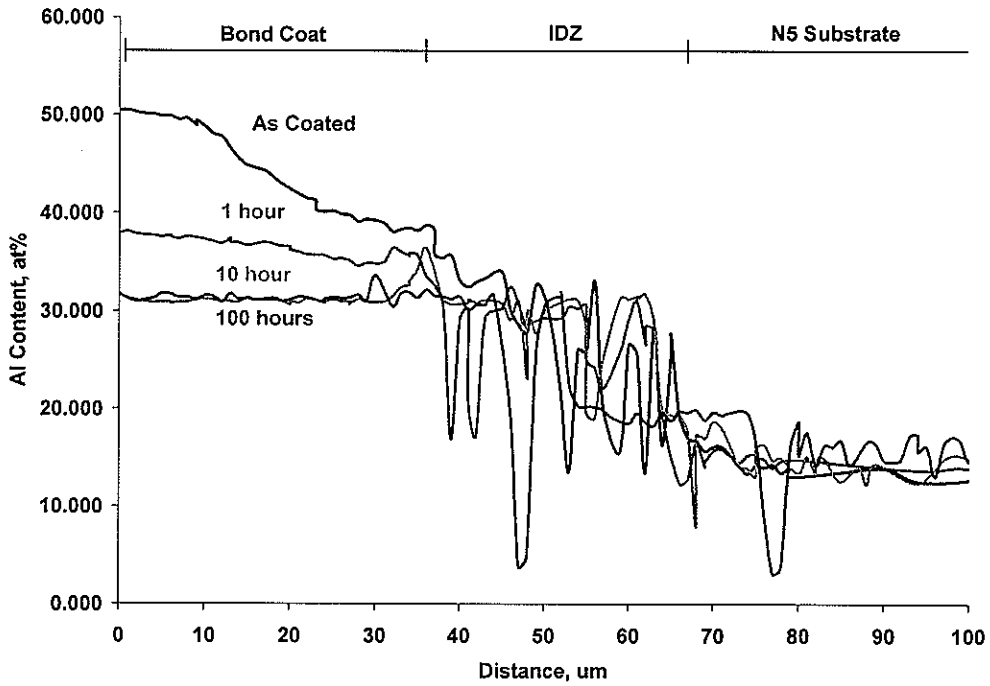

Figure 26: Al content in β for a Pt-modified β-NiAl coating isothermally heated at 1150°C for different times.

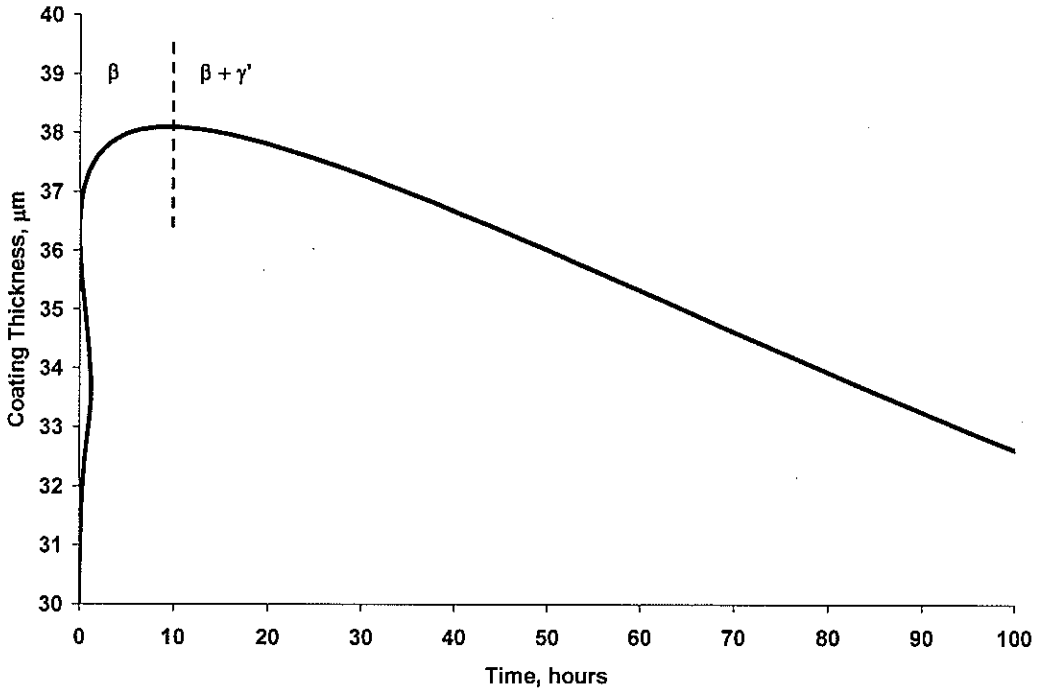

Figure 27: Variations in coating thickness for Pt-modified β coating held isothermally at 1150°C

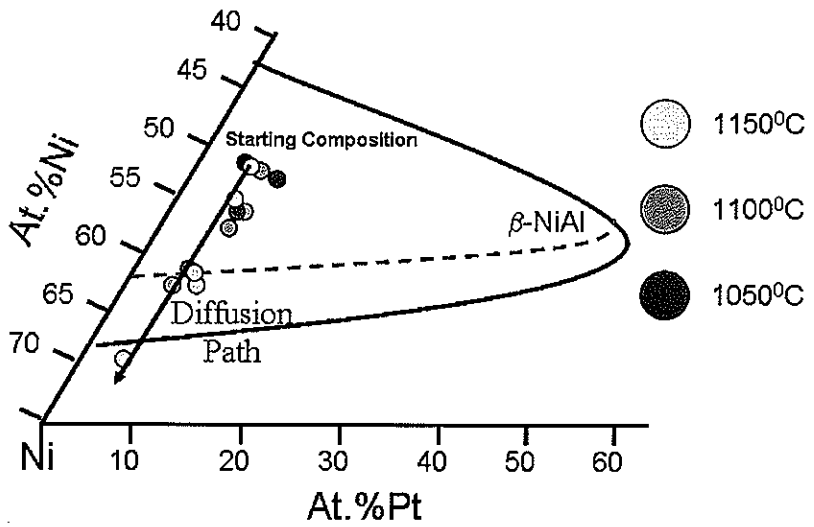

Figure 28: Diffusion path for commercial coatings at different times.

Table 2: Average compositions of β phase in Pt-modified NiAl coating on René N5 substrate after different times at 1100°C (in at%)

Time at 1100°C	Ni	Al	Pt	Co	Cr	Mo	W	Ta
1 h	44.2	40.3	8.1	4.2	3.1	0.04	0.0	0.1
5 h	47.3	35.8	8.2	4.6	3.9	0.05	0.0	0.2
10 h	49.1	35.9	6.6	4.6	3.6	0.05	0.0	0.2
50 h	51.9	32.6	4.8	5.4	4.8	0.1	0.04	0.4
100 h	51.0	32.9	5.5	5.5	4.7	0.0	0.1	0.3

Table 3: Average compositions of β phase in Pt-modified NiAl coating on René N5 substrate after different times at 1050°C (in at%)

Time at 1050°C	Ni	Al	Pt	Co	Cr	Mo	W	Ta
1 h	42.7	41.2	9.3	3.9	2.8	0.0	0.0	0.1
5 h	46.8	37.4	7.7	4.4	3.5	0.01	0.0	0.2
10 h	46.5	36.9	8.2	4.5	3.7	0.04	0.0	0.2
50 h	49.2	34.6	6.3	5.0	4.5	0.1	0.0	0.3
100 h	49.6	34.4	6.1	4.9	4.5	0.1	0.04	0.4

Because the depletion behavior over the 100°C studied was essentially independent of temperature, the depletion path for 1150°C was used as the focus for the bulk alloy study. Several of the compositions listed in Table 1 were of particular interest as they seemed to be potentially prone to undergo the $\beta \rightarrow L1_0$ transformation. This was due to the fact that the composition was entirely β and that the compositions were all Ni rich. Nickel rich β systems have been observed to undergo the martensitic transformation [24-25]. This was particularly true for the composition reached after two hours at 1150°C, as it was very similar to the coating composition looked at by Chen et al. [34, 35] (Ni-35.92Al-8.09Pt-4.45Cr-5.11Co-0.15Ta-0.045Re-0.024W), which was reported to undergo the martensitic transformation. In order to better quantify the transformation behavior, bulk alloys having this composition as well as those found after one and three hours at 1150°C were created. The alloys constructed will be denoted as C1, C2, and C3 for coatings subjected to 1, 2, and 3 hour isothermal heat treatments respectively.

7.3.2 The Martensitic Transformation in β Systems

Differential scanning calorimetry (DSC) was used to investigate the martensitic transformation in a bulk alloy having a composition equivalent to that found for a commercial coating after two hours at 1150°C (Ni-35.0Al-6.3Pt-4.3Co-4.0Cr-0.1Mo-0.03W-0.2Ta in at%), or C2. From Figure 29 it is shown that a transformation had occurred at ~100°C for both a 5°C/min and 10°C/min cooling rate. In addition, while the transformation is clearly a first order event, it does contain several 'burst' transformations indicating that the martensitic transformation has occurred over a range of temperatures rather than a specific point upon cooling. This result is analogous to previous data by Hangen and Sauthoff [26], which observed the presence of martensite to increase in volume fraction with increased undercooling below the Ms temperature, indicating a hysteresis to the transformation. The presence of martensite was verified using x-ray diffraction (CuKα) at room temperature on the bulk alloy. From Figure 30 it is shown that a two-phase system of β and martensite does, in fact, exist.

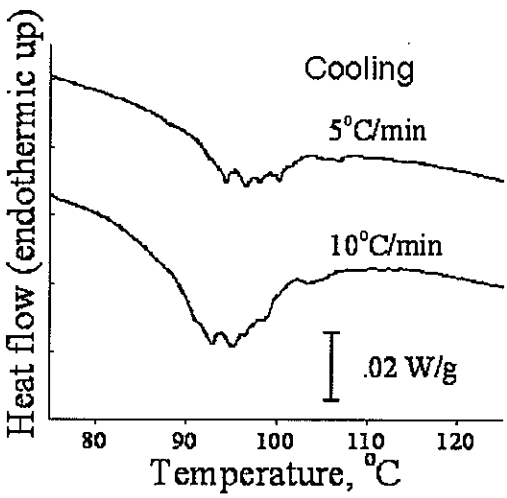

Figure 29: Differential Scanning Calorimetry (DSC) Analysis of Bulk Alloy Coating Composition

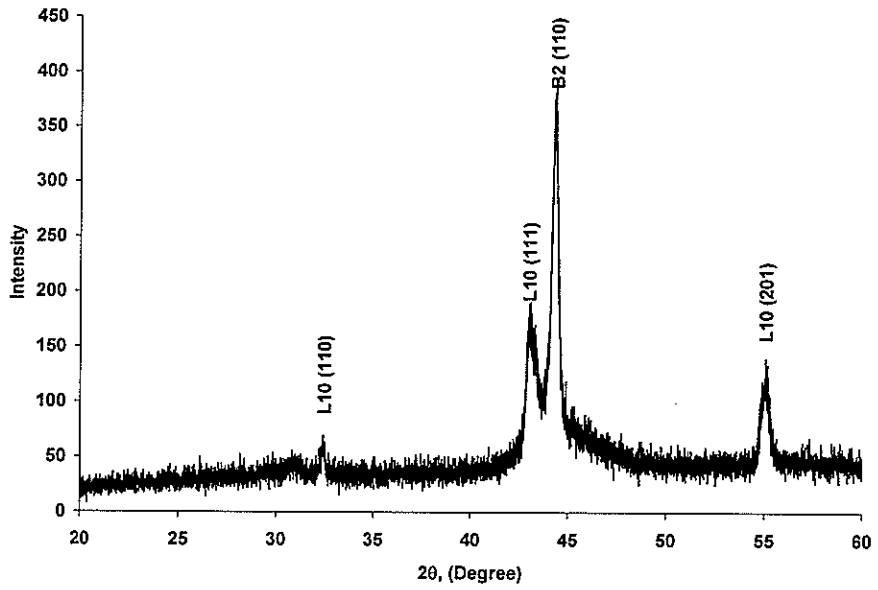

Figure 30: X-Ray diffraction data of bulk alloy with commercial coating composition

The resulting Ms temperature established for the bulk alloy was found to be much lower than that published by Chen et al. [35], who reported an Ms temperature of 530°C. However the DSC analysis performed in this study was for a bulk alloy rather than for a commercial coating as Chen et al. had done. One may speculated that the presence of a superalloy substrate may somehow promote the transformation, creating a much higher Ms temperature when compared to the bulk alloy by adding stress to the bond coat due to CTE mismatch and/or swelling. Because of this discrepancy in comparison between the work presented by Chen et al. and the current study, it was thought that a commercial coating should be depleted down to the composition of the bulk alloy used in the DTA and XRD experiments. This would assure that a proper comparison was conducted.

The Ms temperature was verified through the use of cyclic high temperature x-ray diffraction (HT-XRD) tests that were conducted by heating a depleted commercial coating between 1100°C and 25°C and taking scans at both the high and low temperature. An intermediate temperature of 300°C was also chosen to verify any transformation. A total of 2 cycles were performed. The results are shown in Figure 31. The plots clearly show a transformation lower than 300°C indicating that the Ms temperature found for the bulk alloy may, in fact, be relevant for the commercial coating with the same composition.

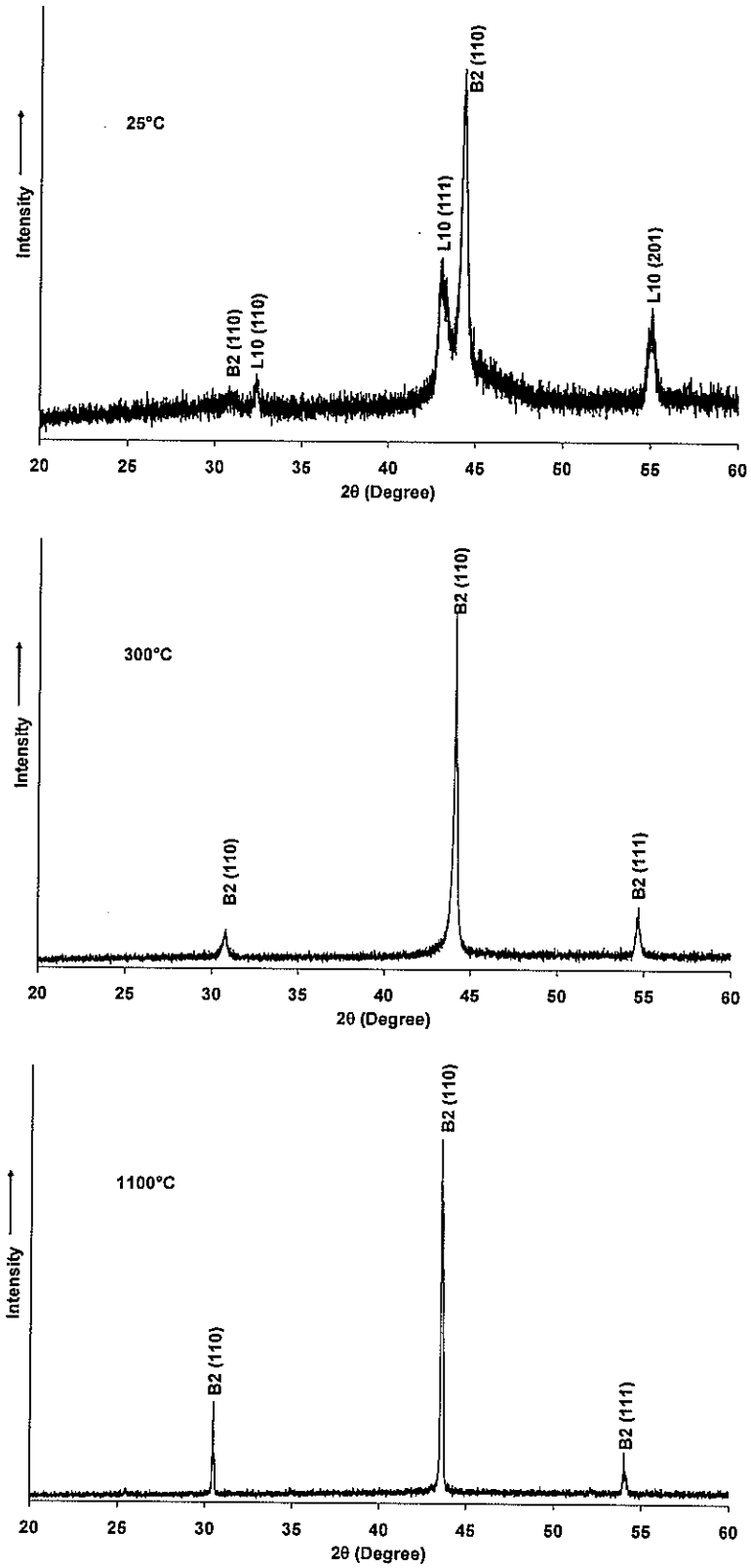

Figure 31: X-Ray diffraction data of depleted commercial coating

7.3.3 Effect of Martensite on Rumpling Behavior

As reported by Zimmerman [29], rumpling in bulk alloys due to the martensitic transformation only occurs if the Ms temperature is high enough to facilitate a sufficiently rapid rate of creep of the specimen. As shown in the previous section, the Ms temperature for a bulk alloy representing a depleted coating was only ~100°C; whereas, the Ni-37Al-15Pt alloy studied by Zimmerman had a Ms temperature of ~875°C. Such a low martensitic Ms temperature in the present study should preclude the martensitic transformation as being the sole cause of rumpling in a bulk alloy as well as a commercial coating.

In order to test this, the C2 bulk alloy was cycled between 1150°C and 25°C ,with 1 h holds at each temperature (cooling rate of 200 °C/min), for a total of 100 cycles. Figure 32 shows a cross section of the sample after cycling. As can be seen in this figure, the sample transformed completely into martensite; however, no significant degree of rumpling had developed. Small undulations are visible, but these are most likely due to oxidation and subsequent spallation of the scale rather than repeated transformations due to thermal cycling.

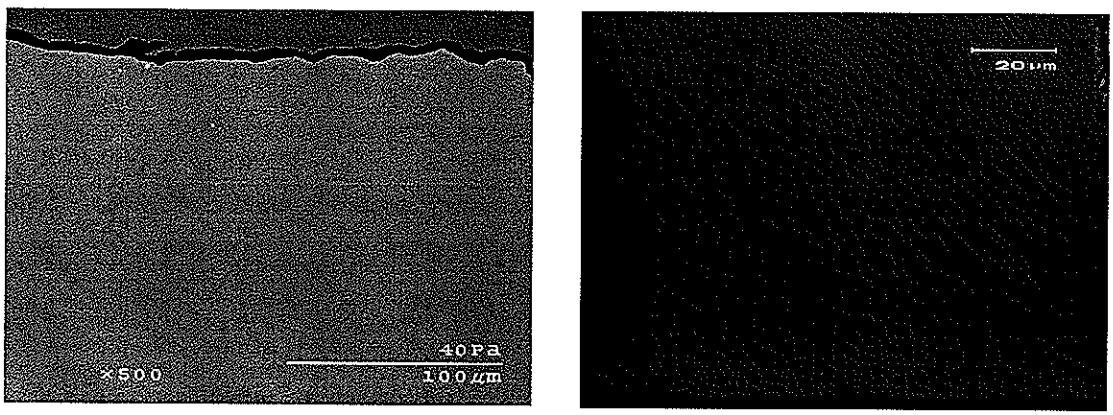

Figure 32: Bulk alloy representing depleted coating composition cycled between 1150°C and 25°C a total of 100 times

Several cyclic exposure treatments were then conducted on commercial Pt-modified β coatings in order to determine the role of the martensitic transformation on the degree of

rumpling. Before testing, the coatings were polished using 1200-grit (course) paper to remove any preexisting undulations. This was then followed by a heat treatment at 1150°C for 1h (water quenched) in order to deplete the coating into one that was likely to be martensite forming. This depleted composition was assumed to be similar to that found in Table 1 after 1h of exposure at 1150°C. All heat treatments were run for 100 cycles.

In the first experiment, a depleted coating was cycled between 1150°C and 25°C. The cross-section and surface images in Figure 33 show the extent of rumpling experienced after cycling. A significant amount of deformation is seen to have occurred, however, this result was not unexpected, as many different variables proposed to cause rumpling are viable for this particular experiment. These include both martensitic and γ' phase transformations, differences in coefficient of thermal mismatch between the coating and substrate as well as the coating and oxide, volumetric changes from swelling, and stress due to oxidation. Therefore, this result was used as a comparison for further testing and rumpling behavior.

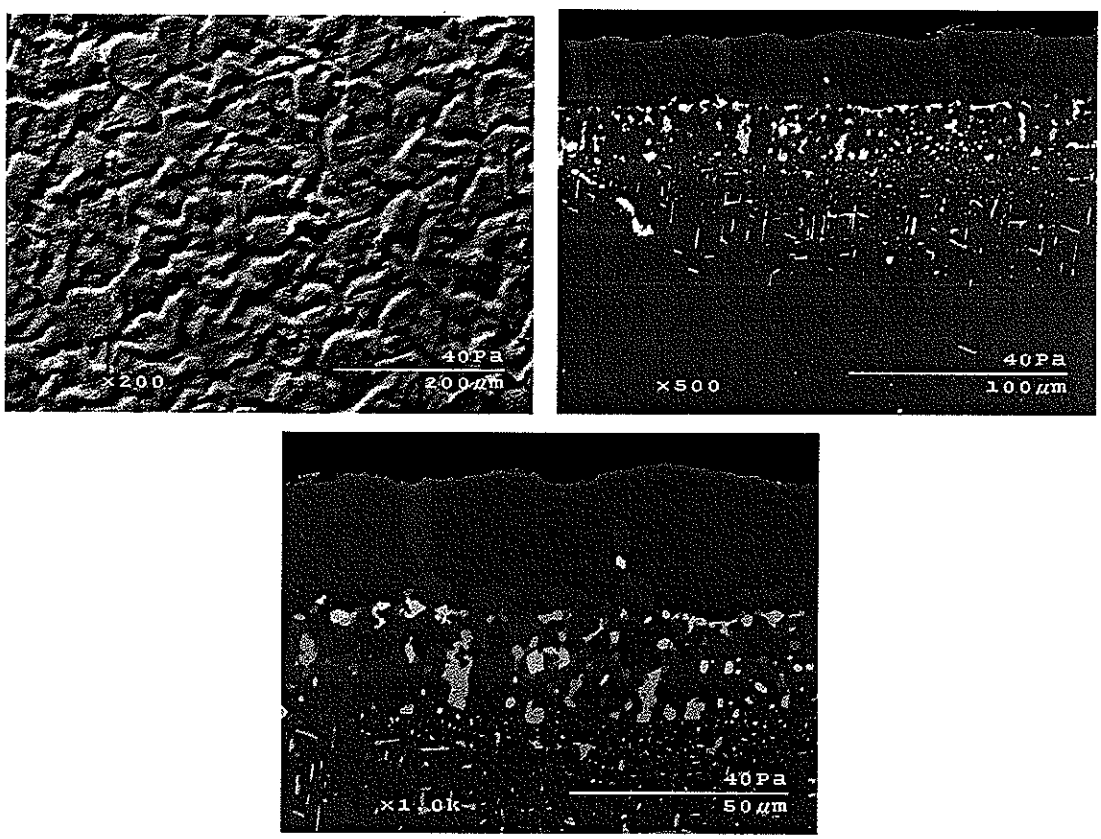

Figure 33: Commercial coating cycled between 1150°C and 25°C 100 times

Next, a depleted commercial coating was cycled between 1150°C and 600°C. As both temperatures were above the Ms temperature for the coating composition, any rumpling due to the transformation would be avoided. Figure 34 shows that a significant amount of rumpling did occur. In fact, the degree of rumpling was comparable to that found in the previous result. This suggests that, much like the results for the bulk alloy, the martensitic transformation is not a necessary criterion for the occurrence of rumpling. However, it may exacerbate the extent of rumpling. Thus, some other mechanism(s) must be dictating the formation of surface undulations

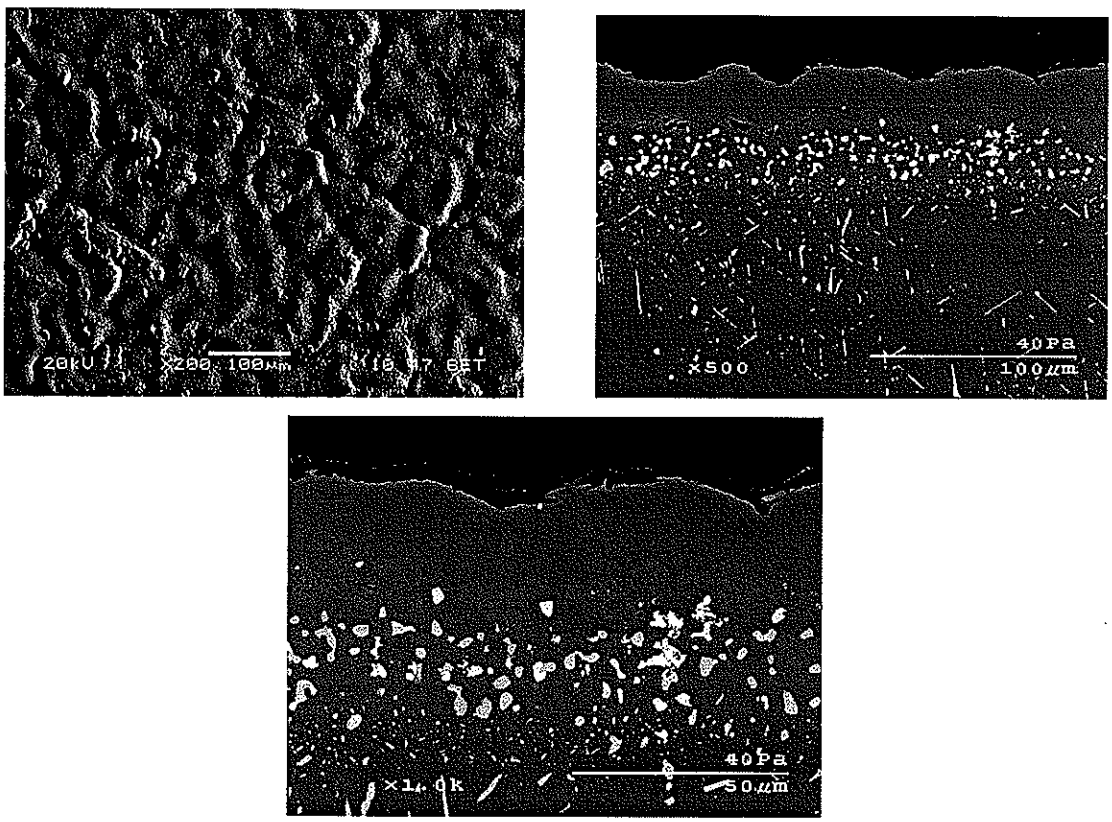

Figure 34: Commercial Bond Coatings on N5 Cycled from 1150°C to 600°C 100 Times

In order to verify the results of the previous experiment, a depleted coating was cycled between 600°C and 25°C. Any deformation of the coating would be due primarily to the martensitic transformation, as the sample was cycled above and below the Ms 100 times. Figure 35 shows that the coating remained extremely planer. Particularly interesting is the formation of the martensitic structure throughout the coating, verifying that the sample was continuously cycled above and below Ms.

Profilometry was used to verify the results of the qualitative SEM analysis of the previous experiments. In Figure 36 both an average peak-to-valley roughness (RzDin) and an average peak-to-peak wavelength (λa) are presented. A baseline roughness and wavelength value for an as-coated, polished sample, is also plotted as a comparison for the experimental results.

When compared to the baseline values of 0.9 μm for the roughness and 1.3 μm for the wavelength, all experiments showed an increase in the average roughness and wavelength. However, the increase is much more dramatic in the two samples that experienced a high-temperature dwell at 1150°C as opposed to 600°C. In these two cases, the wavelength and roughness are nearly identical except for a slight increase in both values for the sample given the low-temperature dwell of 600°C. This increase is most likely due to creep of the coating, which has been shown to occur near 600°C in previous work [48]. In contrast, the sample that experienced a low-temperature dwell of 25°C was unable to creep to a measurable degree.

This creep deformation may also be used to explain the increase in surface parameters observed in the sample cycled between 600°C and 25°C. Bond coat creep may be a direct result of stress generated by the volume change associated with the martensitic transformation, furthering the inference that the martensitic transformation has an effect on the coating surface rumpling, however minimal.

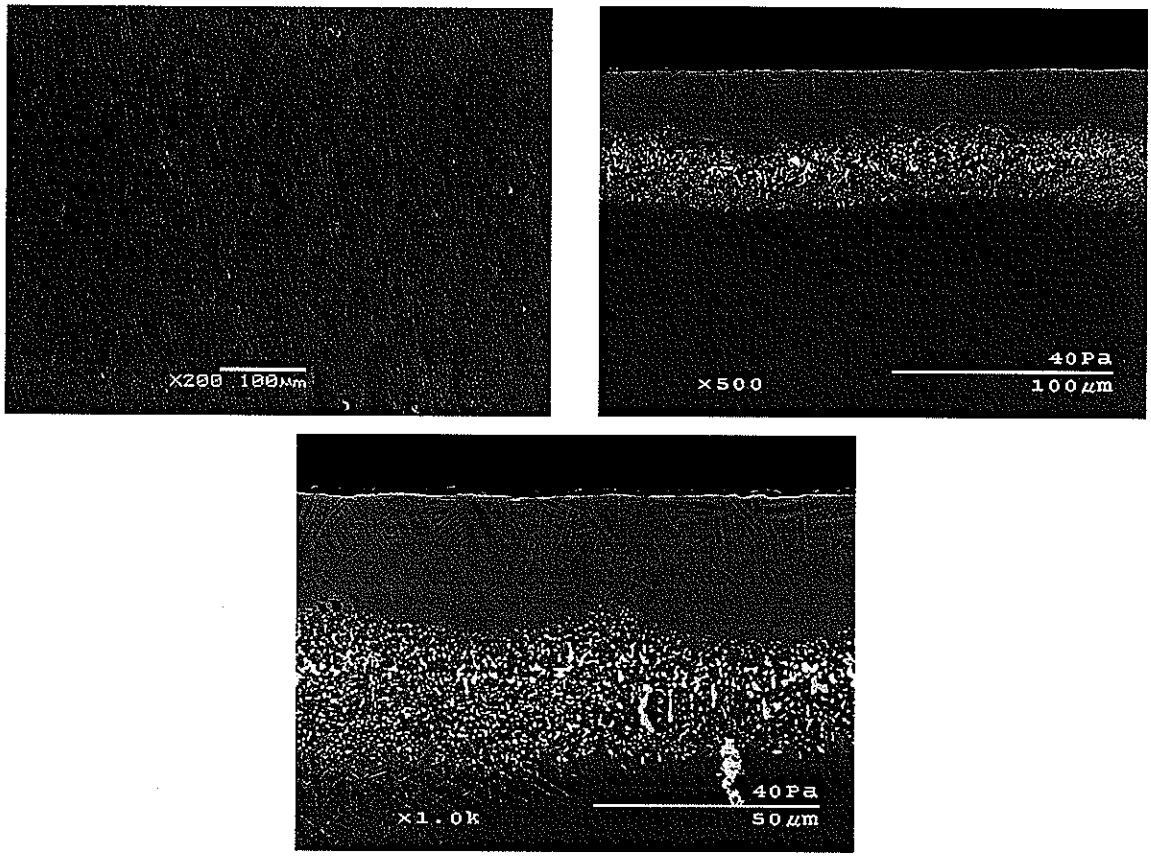

Figure 35: Commercial Bond Coatings on N5 Cycled from 600°C to 25°C 100 Times

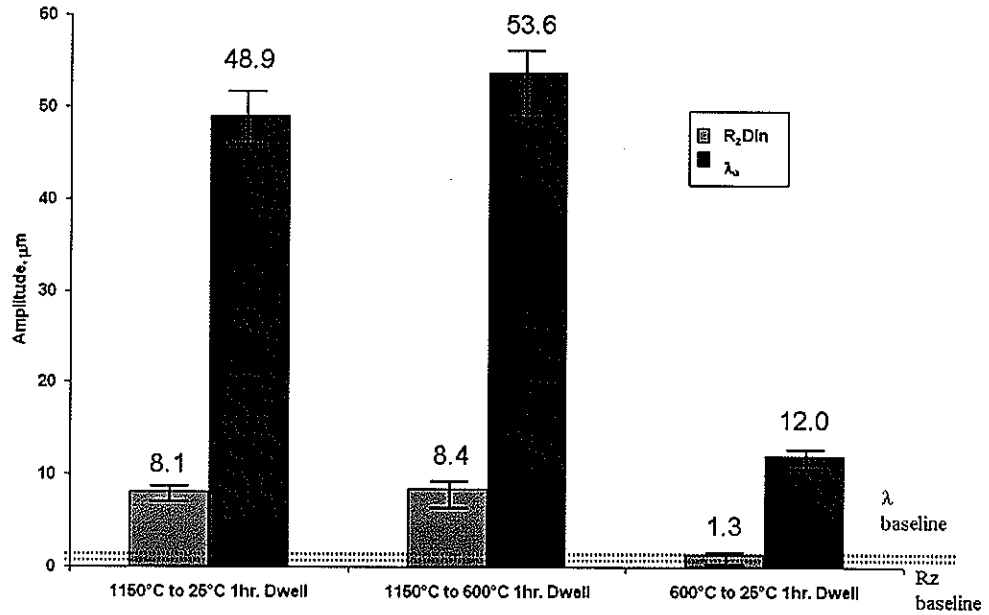

Figure 36: Profilometry results for cyclic exposure treatments: 1150°C → 25°C, 1150°C → 600°C, 600°C → 25°C

7.3.4 Effect of Number of Cycles on Rumpling Behavior

Previous work by Tolpygo and Clarke [37, 41-42] showed that an increase in the degree of rumpling in commercial coatings is expected when a specimen undergoes an increasing number of cycles. In fact, simulations by Balint and Hutchinson [43] confirmed this; however, their model explained that the formation of longer wavelength undulations (i.e., greater rumpling) occurs at the expense of smaller abnormalities. In this current study, depleted coatings were cycled from 1150°C to 25°C with 1h dwell at each temperature for 5 to 100 cycles. Cross-sectional and profilometry analyses were conducted on each coating and the results are summarized in Figures 37 and 38.

In the set of cross-sectional SEM micrographs (Figure 37) a relatively planar surface was observed after five cycles. After 10 cycles, however, some surface distortion was evident. This appeared to be due to swelling of the coating as the β thickness had increased significantly (~52%) compared to the specimen run for 5 cycles. After 25 thermal cycles the presence of γ' was evident and β recession had commenced. This result suggests that the formation of γ' was not the initial cause for rumpling, as increases in surface undulations are evident before the presence of this phase. This result is analogous to that found by Tolpygo and Clarke [41] in a recent study.

Formation of relatively periodic surface undulations was observed to occur after 25 cycles. This is also in good agreement with Tolpygo and Clarke [42], who noted that significant rumpling would occur at ~ 25 thermal cycles at 1150°C. It was also noted by the authors that the average wavelength would remain unchanged while the amplitude of the roughness would increase with increasing thermal cycles. This result is in good agreement with the work presented in this study. After 50 cycles the wavelength remained relatively constant at ~50 μm, while changes in the average roughness were evident. A decrease in the overall roughness after 100 cycles was evident in contrast to Tolpygo and Clarke's work, indicating a possible coarsening effect during thermal cycling.

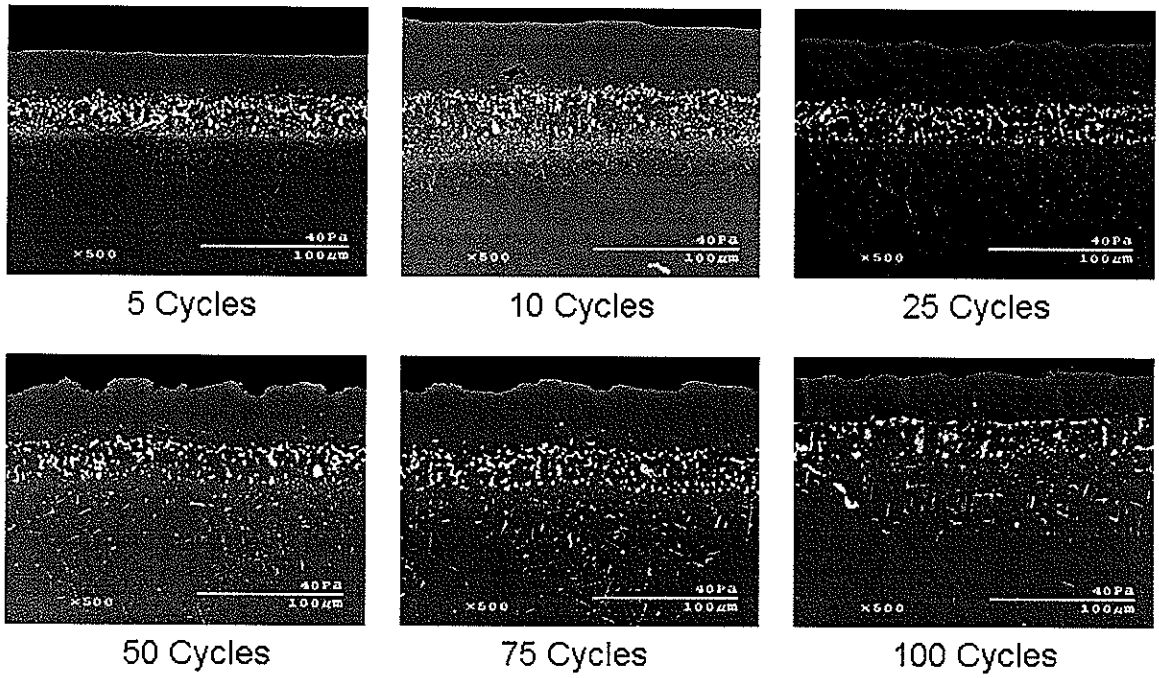

Figure 37: Progression of rumpling behavior in depleted coating after increased number of thermal cycles from 1150°C to 25°C

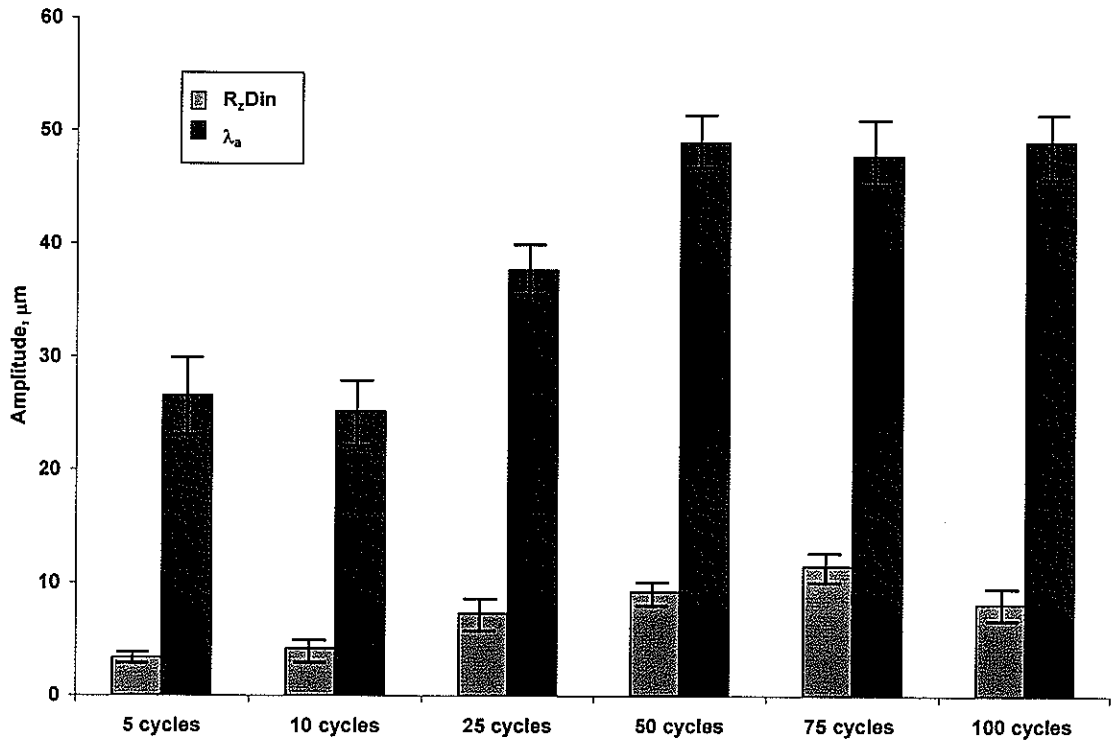

Figure 38: Profilometry results showing progression of rumpling behavior in commercial coatings

7.3.5 Effect of Isothermal Heat Treatment on Commercial Coatings

An isothermal heat treatment of a depleted coating was carried out at 1150°C for 100 hours. From the cross-sectional analysis and the profilometry results presented in Figures 39 and 40 respectively, a significant reduction in the degree of rumpling is observed between the isothermally heat-treated sample and the coating that was cycled between 1150°C and 25°C regardless of the fact that amount of time at high-temperature was identical. Such differences have been observed before in previous studies [37, 43]. It has been suggested that the differences in surface structure is due to stress relaxation occurring at high temperature [43]. Repeated cycling would likely cause stress to accumulate in the coating and oxide due to CTE mismatch and oxidation which would be released in the form of creep deformation.

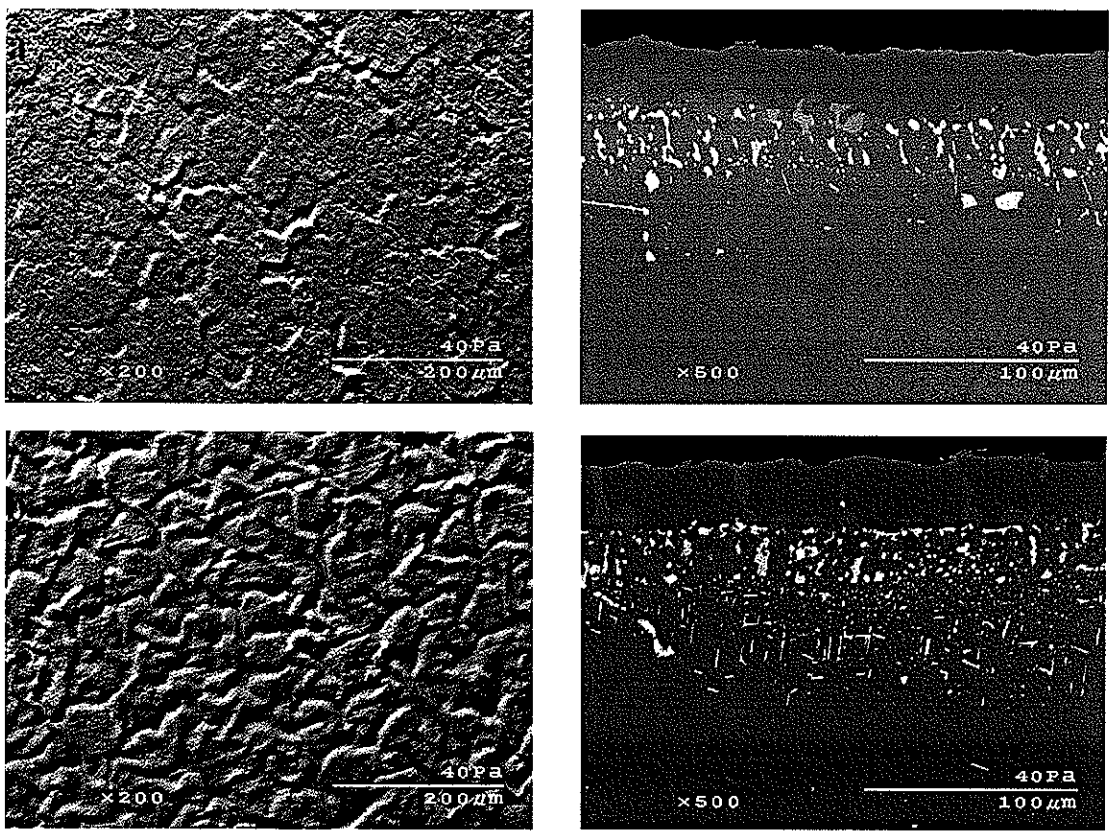

Figure 39: Surface and cross section of a commercial coating isothermally heat treated at 1150°C for 100 hours (a) and cyclically heat treated at 1150°C to 25°C 100 times (b)

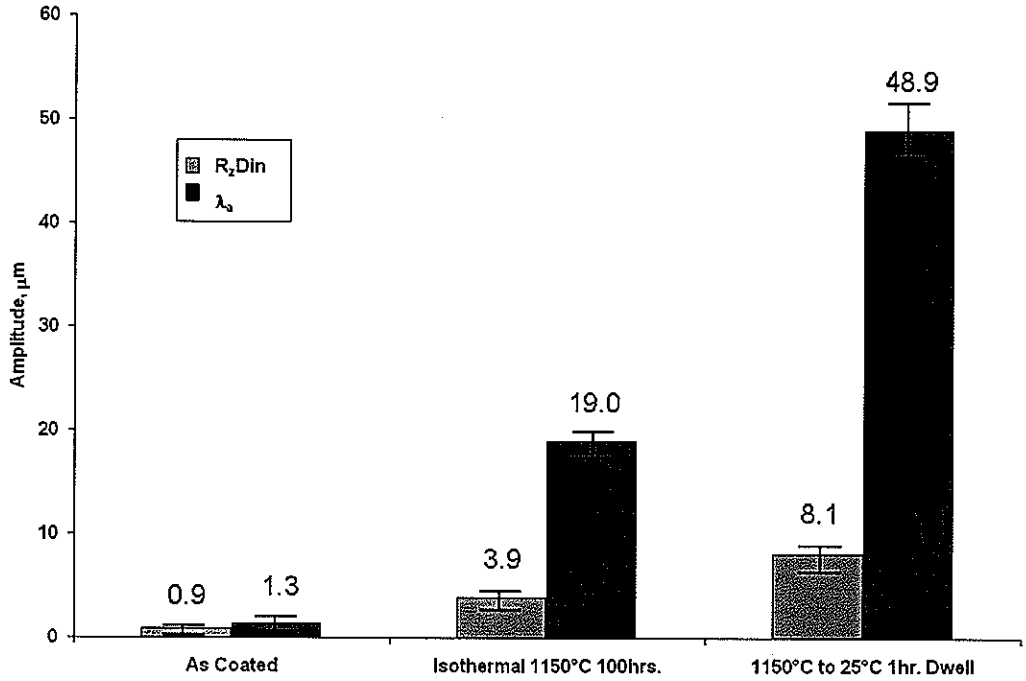

Figure 40: Profilometry results showing polished coating, isothermal heat treatment at 1150°C for 100 hours, and cyclic heat treatment from 1150°C to 25°C

7.4 Discussion

7.4.1 Variations in the Martensitic Transformation Temperature due to Alloying Additions

Composition has been shown to greatly influence the martensitic transformation temperature. In fact, decreases in the binary NiAl system from 39 to 32 at% have been shown to change the Ms temperature by over 700°C [24]. In the commercial system, interdiffusion between the coating and substrate acts to dramatically change the composition of the coating over relatively short amounts of time. This effect is much more influential than oxidation of the coating which has been shown to have very minimal effects [46]

The martensitic transformation for a bulk alloy representing a depleted commercial coating was found to be ~100°C in this study. If taken as a simple binary system of Ni-35Al (in at%)

then the empirical formula presented by Smialek and Hutchinson [24] ($Ms = 4990-124C_{Al}$ in at%) would predict an Ms temperature of 377°C. The large difference in values can be attributed to the presence of other elements, such as Pt and Co which are able to increase Ms dramatically [29-32].

The range of Ms values that is able to occur in the commercial system has been shown to be large. Chen et al. [34, 35], who studied a β composition similar to that used in this study, reported an Ms temperature of 530°C which is significantly higher than our value of only 100°C. As with the comparison to the binary case, the discrepancy in Ms is most likely due to variations in alloying additions. The composition reported by Chen et al. was reported to be Ni-35.92Al-8.09Pt-4.45Cr-5.11Co-0.15Ta-0.045Re-0.024W while ours was found to be Ni-35.0Al-6.3Pt-4.3Co-4.0Cr-0.1Mo-0.03W-0.2Ta. Comparison of Chen et al.'s coating composition to our bulk alloy shows increased levels of Pt and Co (increases of 1.8 and 1.1 at% respectively). As stated previously, these elements are known to raise Ms. In addition, the composition used in this study has a larger amount of Cr (increase of 0.45 at%) which has been shown to lower Ms.

With such a strong composition dependence on the martensitic transformation it is clear that precisely determining an accurate Ms temperature is difficult as the dynamics of interdiffusion and oxidation during thermal exposure remove any notion of a fixed Ms temperature for a coating. Instead, a range of values that is within the instantaneous composition changes would be considered more accurate. This range would ideally fall between 100°C and 700°C. Using this range, modeling the effect of martensitic transformation on rumpling could be considered more accurate as it would account for the evolution of the coating composition due to thermal exposure. In current models, a single Ms temperature is used, which is technically incorrect. It should be noted that the range presented could be reduced significantly if further research detailing the martensitic transformation were perused.

7.4.2 Possible Mechanisms for Rumpling

While the martensitic transformation was the focus of this work, the influence of other factors as they relate to the rumpling behavior was also determined. It is likely that all mechanisms postulated to cause rumpling do, in fact, contribute in some way to form surface undulations. However, some mechanisms may influence the deformation more than others. The results of the cyclic heat treatments help to demonstrate which of these factors play a principal role in rumpling.

The martensitic transformation was shown to have little effect on the degree of rumpling if the Ms temperature is too low for a sufficiently rapid rate of creep. When thermally cycled exclusively above the transformation temperature (i.e., martensite would not form during exposure) the sample suffered from a large degree of deformation. Moreover, the deformation was found to be larger than a sample cycled above and below the Ms temperature. It is important to note, though, that the results of the low-temperature cyclic exposure experiment above and below Ms indicate that martensite may have some small effect on rumpling.

Results by Balint and Hutchinson [43] showed that a martensitic transformation as high as that found by Chen et al. [34, 35] would greatly affect the degree of undulations observed. It was suggested by the authors that a reduction of Ms by as much as 200°C would greatly reduce the amount of deformation present. As the Ms temperature in our study was over 400°C less then the result reported by Chen et al., the suggestion that the transformation has little role on the evolution of rumpling is entirely accurate.

The results showing the evolution of rumpling help to discount two other mechanisms as the primary cause of rumpling. As stated earlier, the formation of the γ' phase was not observed until ~ 25 thermal cycles. Before this, increases in roughness and wavelength were evident Also, after 50 cycles there appears to be little change in the degree of rumpling observed in

the coating, however, the volume fraction of γ' should continue to increase with increasing number of cycles.

In this study, swelling of the coating was thought to be the cause of increased rumpling parameters near the beginning of the cyclic exposure testing. This has been suggested previously; where it was theorized that swelling was the dominating cause of the rumpling behavior in the early stages of oxidation [42, 49]. However, as shown in Figure 11 the degree of swelling diminishes after 10 cycles while the amount of rumpling increases. In the current models on rumpling [43-45], pre-existing roughness in the coating are needed in order to further the extent of rumpling. As samples were polished using 1200-grit paper prior to testing, it was assumed that the surface contained no such roughness. It is possible that the swelling of the sample caused small inconsistencies on the surface which were then used to facilitate rumpling.

Another suggested mechanism that has been considered is stress caused by the formation and continued growth of the Al_2O_3 scale. This growth stress, which is compressive, has been reported to be quite high (~ 3.0 GPa) and would likely lead to deformation of the coating [50]. However, isothermal oxidation of a depleted coating showed only a minor increase in rumpling. This result has been discussed in detail previously by [37, 43]. It is thought by the authors that growth stresses occurring during oxidation are able to be diminished at high temperature through some creep deformation. During isothermal conditions stresses are relaxed and no further deformation occurs. However, during cyclic exposure treatments new stresses develop within the coating/oxide during each cycle which causes gross deformation of the surface.

One final mechanism that has been considered to cause rumpling is differences in coefficient of thermal expansion (CTE) mismatch between the coating and substrate. As the other mechanisms have been shown to only contribute to the rumpling phenomenon rather than dictate it; it would seem that CTE may be the dominating factor. Discussion of the role of CTE on rumpling has been presented briefly by Tolpygo and Clarke [41] when considering

the effects of coating thickness. It was shown by these authors that thinner coatings are more susceptible to rumpling than thicker ones. This, they noted, would mean that CTE could not contribute to rumpling. However, it was conjectured by Tolpygo and Clarke that the depletion/interdiffusion behavior of the coatings may change with coating thickness. This would indicate that, much like the martensitic transformation, a strong composition dependence exists when considering stress generated by CTE mismatch. Further research detailing the composition dependence on the CTE mismatch is, therefore, needed to truly understand what effect it has on the rumpling experienced in β coatings.

7.5 Summary and Conclusions

The rumpling phenomenon found in β-NiAl based coatings was investigated with emphasis on the martensitic transformation as a major cause of the deformation. Several conclusions can be drawn from this work.

1) The diffusion path for a commercial coating, while sensitive to time, is fairly temperature independent over the range 1050-1150°C.
2) The martensitic transformation temperature for commercial coatings is much lower than previously reported; although, it is highly composition dependent, with Pt, Al and Cr contents believed to be important variables.
3) The martensitic transformation is not a necessary criterion for the rumpling of commercial coatings. This is believed to be due to the low Ms temperatures of the coatings, which preclude any creep deformation.
4) Coefficient of thermal mismatch (CTE) is suggested to be the factor most likely to dominate the rumpling behavior.

Section 8: Cracking due to the Martensitic Transformation in Pt-Modified β-NiAl Based Alloys and Coatings

J. Henderkott, B. Gleeson

The effect of a low martensitic transformation temperature on Pt-modified β-NiAl coatings and bulk alloys was investigated. Using a depleted commercial coating as well as a bulk alloy representing the depleted coating, low temperature cyclic heat treatments were conducted. After repeated cycling, cracking was observed on the surface of both systems. These cracks ran along grain boundaries exclusively in the bulk alloy, but were observed to propagate within the grains and along the grain boundaries in the commercial coating. Continued cyclic exposure of the bulk alloy caused it to be easily broken into several sections. In the commercial coating, spallation of the cracked coating from the substrate did not occur. However, cracks were observed to run the entire length of the coating and into the interdiffusion zone. Heat treating a cracked coating at 1150°C caused Al_2O_3 to form within the cracks.

8.1 Introduction

A thermal barrier coating (TBC) system is essentially comprised of three layers above the Ni-based superalloy substrate. The first layer is a ceramic top coat that is typically made of yittria partially stabilized zirconia [1, 2]. In the case of a cooled substrate, this layer creates a large thermal gradient, thus reducing the temperature of the metallic sublayers [1, 2]. The next layer is the thermally grown oxide (TGO) scale that, ideally, is a α-Al_2O_3 in order to provide oxidation resistance and an effective surface to which the topcoat layer attaches itself [3, 5]. The TGO grows at the expense of the metallic bond coat, which is necessarily capable of forming an Al_2O_3 scale. While two primary coating systems exist, the Pt-modified β-NiAl type coatings are thought to have superior oxidation resistance [9-13]. However, due primarily to coating/substrate interdiffusion [46], phase transformations within the β coating

become likely. These transformations include formation of the lower aluminide γ'-Ni_3Al and the martensitic form of NiAl (β').

The transformation between the B2 cubic β-NiAl structure into an L10 face centered tetragonal (FCT) martensitic structure has been investigated previously for binary bulk alloys [24-26]. However far fewer data are available for the Pt-modified ternary bulk alloy and coating systems [28-35, 41]. Due to a volume reduction of ~ 2%, there has been speculation that the transformation can be responsible for the formation of surface undulations, 'rumpling', that has been observed in β coatings [35-43]. In fact, work by Zimmerman [29] showed that if the martensitic transformation temperature, Ms, was high enough, creep of a ternary bulk alloy would occur and the specimen would ultimately rumple as a means of relieving the surface strain imposed by the TGO scale.

Recent work by Chen et al. [34, 35] found an Ms temperature of 530°C for a depleted commercial β coating composition. The commercial coating contained several alloying additions beyond the ternary Ni-Al-Pt system due to interdiffusion with the various constituents of the superalloy. These included primarily Co and Cr, however Re, W, and Ta additions were also noted. Considering this and other Ms temperatures, a simulation model by Balint and Hutchinson [43] showed that the martensitic transformation would, indeed, lead to large-scale rumpling of the coating and that manipulation of this Ms temperature would allow for different degrees of deformation. Specifically it was said that a reduction in Ms of 200°C would create a significant reduction in deformation.

Recent work by Henderkott and Gleeson [51] found an Ms temperature far lower than previously reported (~ 100°C) by Chen et al [34, 35] for commercially relevant Pt-modified β compositions. It was thought that a relatively small increase in the amount of Pt and Co in Chen's et al. system was the cause for the large difference in transformation temperatures. These alloying additions are known to raise Ms by decreasing the shear modulus of the B2 lattice [30-32]. Finally, it was concluded by Henderkott and Gleeson that the Ms cannot be precisely pinpointed in the coating system due to significant sensitivity of the transformation

temperature on coating composition, the latter of which is a dynamic variable. Rather, a range of Ms values between 100°C and 700°C is more realistic.

Henderkott and Gleeson [51] further explained that with an Ms temperature of only 100°C, the ability for the martensitic transformation to cause rumpling in both the bulk alloy and the commercial coating is unlikely. Cyclic exposure treatments between various temperatures above and below Ms clearly showed that the transformation was not a direct cause of the rumpling phenomenon and that some other factor dominated the behavior. This result was in agreement with a similar study conducted by Tolpygo and Clarke [41], who inferred that the formation of surface undulations would occur even without the martensitic transformation.

While the martensitic transformation has been shown to not be the dominating factor associated with rumpling, its occurrence may affect the longevity of bulk alloys and commercial coatings in some other way. For instance, stress generated by the transformation, even at low temperatures, may cause adverse consequences if not removed by creep. The aim of this study was to determine how and to what extent low-temperature martensitic transformations may affect the performance of commercial coatings and bulk alloys representing depleted coating compositions.

8.2 Experimental Procedures

Specimens used in this study were either bulk alloys procured from the Materials Preparation Center at Ames Laboratory, or commercial Pt-modified β coatings provided by General Electric (GE). Bulk alloys of composition Ni-35.0Al-6.3Pt-4.3Co-4.0Cr-0.1Mo-0.03W-0.2Ta were formed by arc-melting high purity metals under argon followed by drop casting the molten metal into 12 mm diameter rods. These rods were then homogenized under argon at 1200°C for six hours followed by 1150°C for 48 hours. The bulk alloy was then cut into small coupons ~ 5 mm in thickness and polished to 0.05 μm.

The commercial β coatings were deposited onto 25.4 mm diameter René N5 substrate buttons. These coatings were then heat treated for 2 hours at 1150°C in dry laboratory air followed by a water quench. This heat treatment was done to deplete the coating composition into one identical to that found in the bulk alloy. In order to observe any surface changes, the sample was polished down to 0.05 μm

Testing of the specimens was carried out using a standard laboratory hot-plate that was able to achieve temperatures of up to 550°C. Samples were placed on the hot plate for ~ 2 minutes. During this time the samples were covered by an alumina crucible. Sample temperatures reached 400°C. After heating, samples were removed from the hot plate and placed on a laboratory microscope to cool in open air. The microscope used in this study was capable of taking digital images so that the transformation could be readily documented. .

8.3 Experimental Results

8.3.1 Martensitic Transformations in Bulk alloys

The martensitic transformation temperature for a bulk alloy whose composition is Ni-35.0Al-6.3Pt-4.3Co-4.0Cr-0.1Mo-0.03W-0.2Ta (in at%) was found to be ~ 100°C using a combination of differential scanning calorimetry (DSC) and x-ray diffraction techniques. This composition is based on that of a commercial coating that had undergone a 2 hour heat treatment at 1150°C [51].

Using a standard laboratory hot plate and microscope, the progression of the β → martensite transformation was able to be recorded over a time of ~185 seconds. The progression of the martensitic transformation is shown in Figure 41. After heating the sample to ~400°C and placing it on the microscope, a combination of β and martensite is visible. After cooling for 90 seconds a significant amount of martensite had formed in some of the larger grains. This transformation continued through to 185 seconds, by which time the majority of the β had undergone the transformation. This result is similar to work by Hangen and Sauthoff [26]

who, for a binary system, concluded that the volume fraction of martensite would increase with increasing undercooling below the transformation temperature.

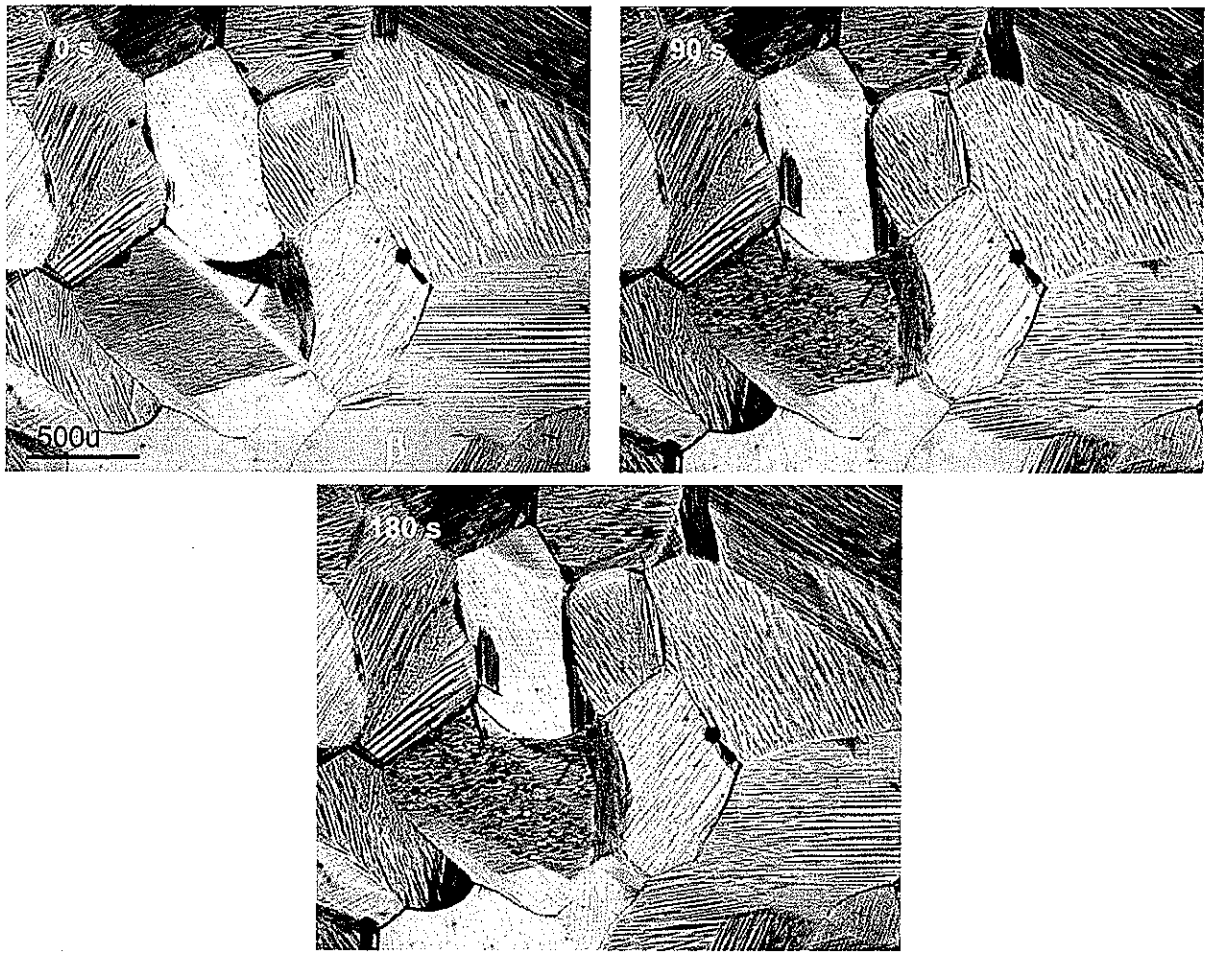

Figure 41: β → martensitic phase transformation in bulk alloy representing a depleted commercial coating

The phase transformation undergone by the bulk alloy was fully reversible using the hot-plate set-up. After repeated runs, however, the effect of the low temperature transformation became evident on the surface. Figure 42 shows the bulk alloy with a large number of cracks running along the grain boundaries (denoted with the arrows). Continuous cycling of the sample allowed the formation of new defects as well the propagation of existing cracks across the surface until, eventually, a 5mm thick sample was able to be broken into several sections by hand. This occurred after ~ 200 thermal cycles.

The destructive nature of the transformation is believed to be due to the brittle nature of β at the low temperatures of the current experiment. It has been shown that the ductile-to-brittle transition temperature of a depleted Pt-modified β system is at ~ 600°C [48]. At this temperature, creep of the coating is possible in the presence of stress induced by the martensitic transformation. In this experiment the sample was subjected to temperatures between 400°C and room temperature. This temperature regime still allowed for the reversible phase transformation to occur, but the β that remained was brittle and hence unable to accommodate any transformation strain by an elastic or plastic relaxation mechanism. Rather, the transformation strains were accommodated by cracking of the sample.

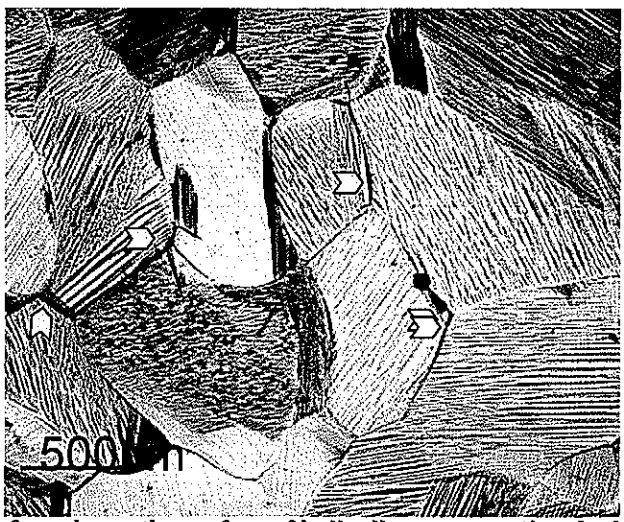

Figure 42: Formation of cracks on the surface of bulk alloy representing depleted commercial coating composition (cracks denoted by arrows

The effect of cycling of a bulk alloy at the ductile-to-brittle transition temperature was explored in Figure 43. The sample was heat treated between 600°C and 25°C 100 times (1 h dwells at each temperature). The cross-sectional and topographical images clearly show the characteristic lath and needle martensitic microstructure; however, no cracking is present. It is believed that strains formed in the alloy due to the martensitic transformation were released at high temperature in the form of dislocation climb and cross slip. Both of these are thermally activated stress reduction mechanisms that manifest as plastic flow of the material. This hypothesis seems acceptable when compared to a previous study detailing the rumpling phenomenon observed in β coatings [51]. It was noted that rumpling of a commercial

coating was noticeably higher for a sample cycled between 1150°C and 600°C when compared to one that had been cycled between 1150°C and 25°C. The study further explained that an increase in average roughness and average wavelength were observed for a sample cycled between 600°C and 25°C compared to an 'as coated' specimen. This indicated that some form of creep occurred during the high-temperature dwell.

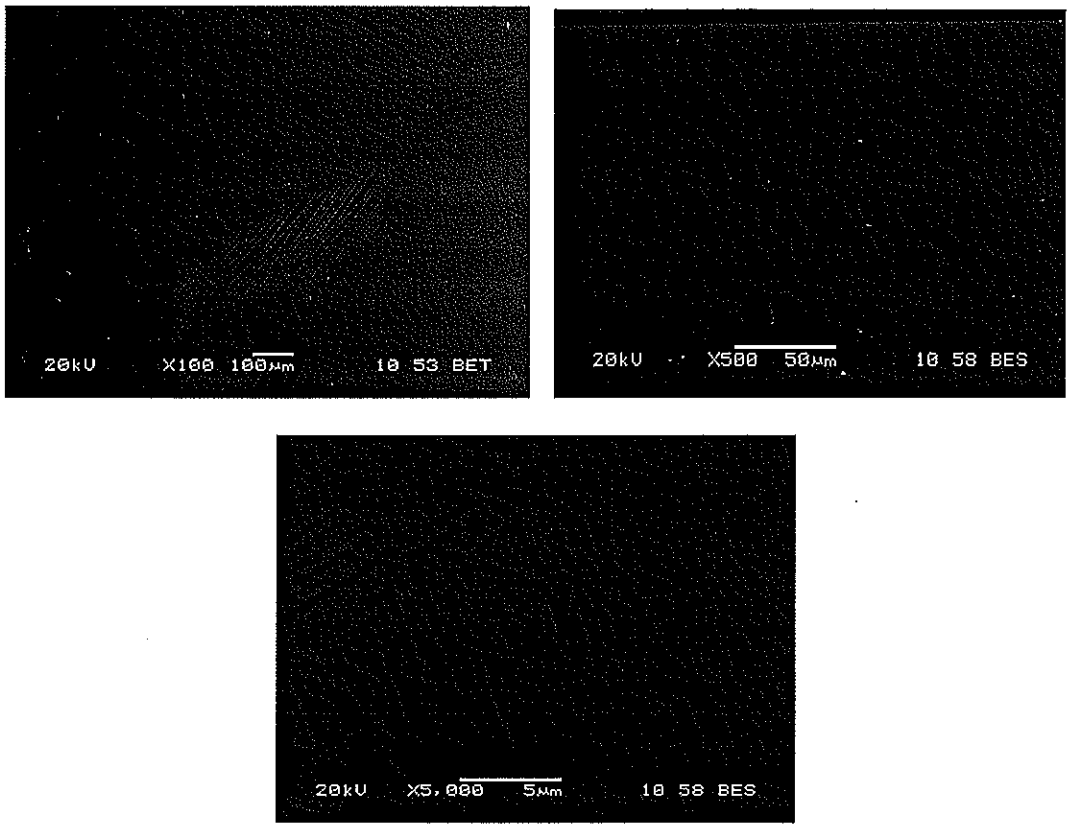

Figure 43: Bulk alloy representing depleted coating composition cycled between 600°C and 25°C a total of 100 times

8.3.2 Martensitic Transformation in Commercial Coatings

The destructive nature of the martensitic transformation was also analyzed using a depleted commercial coating. The coating was heat treated for 2 hours at 1150°C so that it had a depleted composition that was equivalent to that of the bulk alloy used in the previous section. Also, as with the bulk alloy, the sample was polished to a mirror finish to observe the transformation. However, since the superalloy substrate was coated on both sides, a

section of the coating was left with its oxide layer intact to determine what effect it had on the formation of cracks.

Figure 44 shows the effect of 10 thermal cycles between 400°C and 25°C. In the surface image on the left, a large number of cracks are visible. Whereas cracks in the bulk alloy were only observed to run along the grain boundaries (i.e. intragranularly), the cracks in the coating appear to run both inter- and intra-granularly. Also visible is the lath structure of the martensite phase, confirming that the martensitic transformation did, in fact, occur.

The cross-sectional image in Figure 44 shows that cracks originating from the surface were able to travel through the entire thickness of the coating and even into the interdiffusion zone, finally ending at the superalloy substrate. In the presence of a TGO layer, a similar extent of cracking was observed. These observations indicate that the formation of defects within the coating was due to the martensitic transformation exclusively and not from any polishing that had occurred.

The effects of exposing the cracked coating to oxidation at an elevated temperature were also analyzed. After inducing several defects within a coating, it was oxidized at 1150°C for 1h. As shown in Figure 45, cracks still were visible throughout the coating after oxidation exposure. In fact, within the cracks large regions of alumina formation were observed. Thus, during the subsequent heating of the sample, cracks within the coating may sinter together during the high temperature dwell.

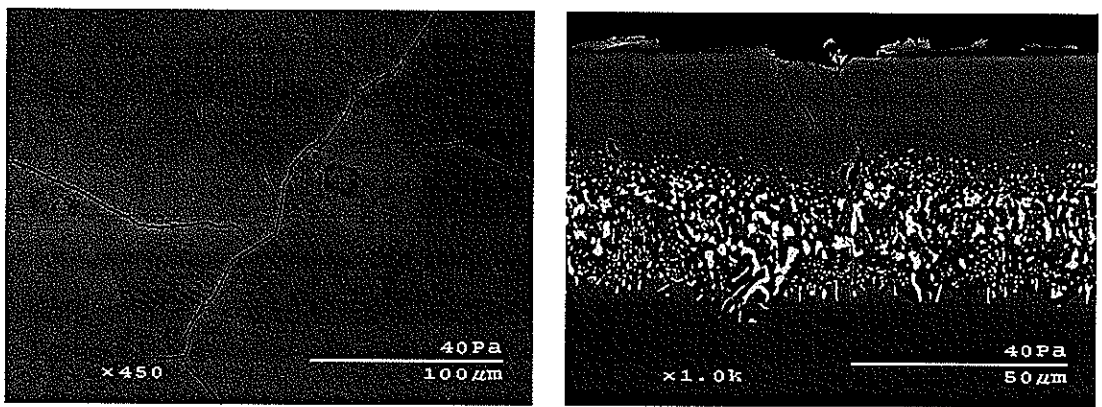

Figure 44: Formation of cracks in depleted coating on René N5 substrate cycled between 400°C and 25°C 10 times (polished surface)

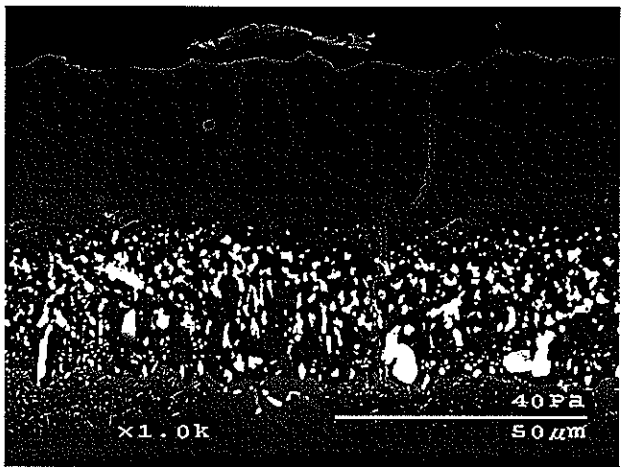

Figure 45: Depleted coating cycled at low temperature 10 times followed by a heat treatment at 1150°C for 1h

8.4 Discussion

It is unlikely that a commercial turbine system would undergo such a large number of low-temperature cycles in service and, therefore, produce the extent of cracking found in this study. However, these results are indeed still relevant when discussing possible failure mechanisms associated with coatings. The formation of even a small fraction of these cracks, in conjunction with repeated high-temperature thermal cycling, may have adverse effects on the longevity of a TBC system. Several papers have dealt with the effects of thermal mechanical fatigue (TMF) and low cycle fatigue (LCF) as failure mechanisms in aluminide coatings [51-57].

At even relatively low strain rates (0.6%) the presence of a coating can be highly detrimental to the fatigue life of a superalloy system as it can aid in the propagation of cracks into the superalloy [52]. Neglecting the martensitic transformation entirely, formation of fatigue cracks have been shown to occur at isothermal test conditions of only 500°C [57]. This result was explained by the fact that testing was conducted below the ductile-to-brittle transition temperature of 760°C, for an 'as coated' commercial coating specimen [58]. Propagation of the cracks occurred due to the inherent brittleness of the β coating at temperatures below 700°C as well as the accumulation of stresses due to mechanical cycling

of the system. Cracks continued through the coating and ended within the interdiffusion zone or at coating/substrate interface where stronger regions of the γ phase were able to blunt the crack [57].

The strain induced by the martensitic transformation has been calculated previously to be 0.7 ± 0.1% assuming a bond coat elastic modulus of 180 GPa and Poisson's ratio of 0.3 [35]. The strain induced by the transformation is less than the low cycle fatigue (LCF) strains used in study mentioned previously [52]. As this amount of strain was found to induce cracking the presence and eventual propagation of cracks in this study seems reasonable.

At higher temperatures (above 800°C) the formation of an oxide layer has been shown to be both beneficial and negative to the properties of the β coating system [54]. Under externally imposed low strain conditions, the oxide layer has been shown to slow crack propagation by blunting the crack tip. The formation of new cracks was able to occur and was initiated within internal micropores in the oxide [52, 54]. Strain levels higher than 1.2% have resulted in growth of oxide within the crack, followed by oxide spallation. New Al-rich oxide was then shown to reform, which resulted in Al depletion around the crack. Repeated oxidation and spallation of the scale resulted in the eventual formation of the γ' phase and, in some cases, the γ-Ni phase [54]. The presence of these new phases in the β system was said to create further stresses due to the inherent volume change associated with the transformation.

Because of the inability of commercial coatings to resist crack propagation during fatigue testing, any cracks generated through the martensitic transformation are likely to have a negative effect on the properties of the coating. This is especially true at high temperatures, where oxidation in the cracked region and stresses generated through CTE mismatch and volumetric changes are contriving factors. It is important to note, however, that the benefits of coatings on a superalloy substrate outweigh most of the negatives. Their superior oxidation and hot corrosion resistance, compared to the superalloy substrate, make them essential in turbine based development and research. As the formation of cracks due to the

martensitic transformation and low-temperature cycling has not been reported, further research is needed to truly understand its behavior and, ultimately, its consequences.

8.5 Summary and Conclusions

Several conclusions can be drawn from this study:

1) For a bulk alloy representing a depleted commercial coating, low-temperature cycling in conjunction with a low Ms temperature can cause eventual failure of the alloy sample due to the formation and propagation of intergrannular cracks. Crack formation was also observed in a commercial coating although no catastrophic failure was observed.
2) Cracks were formed due to cycling below the ductile-to-brittle transition temperature of the β coating which is reported to be ~600°C for a depleted composition. When cycling above the ductile-to-brittle transition temperature no cracks were formed.
3) While it was thought that a commercial coating system is unlikely to undergo such low-temperature cyclic exposures, it is suggested that in the event of initial crack formation due to the martensitic transformation crack propagation could occur by cyclic fatigue of the blade.

Section 9: Effect of Coefficient of Thermal Expansion Mismatch on Rumpling in Pt-Modified β-NiAl Based Coatings

J. Henderkott, D. Balint, B. Gleeson

Differences between coefficient of thermal expansion (CTE) values for Pt-modified β-NiAl coating composition and a René N5 superalloy substrate were determined in order to provide input to a model that simulates the response of a coated system to thermal cycling (i.e., rumpling). Data collected showing CTE differences were found through the use of dilatometry which were conducted on bulk alloys representing depleted coating compositions. Also evaluated was the temperature sensitivity to rumpling, as well as the effect of oxide growth stresses on the degree of rumpling (thought to be a cause of the phenomenon). Both of these experiments helped to reinforce the impact of CTE mismatch on rumpling. Finally, results from the model were compared to previously run cyclic-heat-treatments of commercial coatings to show how CTE mismatch effects influence rumpling.

9.1 Introduction

The use of thermal barrier coating (TBC) systems on Ni-based superalloys has helped to increase overall efficiency of aero-turbine engines by allowing them to run at higher operating temperatures [1, 2]. An important component of the TBC section is the bond coat layer. This layer provides oxidation resistance to the substrate by forming a protective thermally grown oxide (TGO) layer of α-Al_2O_3, which also serves to bond the ceramic top coat. One of the most widely used types of bond coatings is the chemical vapor deposited (CVD) nickel aluminide, which is based on β-NiAl. The binary β-NiAl systems provide good oxidation be creating an adherent scale; however, more recent studies have noted the beneficial effects of Pt additions to the β system. With the addition of ~10 at % Pt, an even more adherent scale is possible [9-13].

While the use of aluminide bond coatings in TBC systems does aid in increasing the longevity of the superalloy substrate, they do suffer from the formation of surface undulations ('rumpling') which may cause eventual delamination of the ceramic top coat [36-43, 49]. Upon delamination, the of the exposed metal increases which, in turn, increases the rates of creep and oxidation to the extents that catastrophic failure can occur. Interestingly, while the formation of surface undulations has been studied in detail, it remains a matter of speculation about what mechanism(s) dominates the rumpling behavior. Phase transformations [29, 37, 40, 41, 43], oxide driven stress [37, 41, 43], and coefficient of thermal expansion (CTE) mismatch [36, 37, 40, 43] have all been suggested to contribute at least in some part to rumpling, but none of these has been conclusively found to be the governing mechanism.

The diffusion driven transformation from a B2-NiAl structure to a martensitic L10 structure has long been considered to be the largest contributor, as a reduction in volume of ~2% is possible [34, 35]. However, recent work has suggested that the martensitic transformation temperature, Ms, depends on the instantaneous composition of the coating and could be as low as 100°C [51]. With an Ms temperature so low, rumpling due to the martensitic transformation was shown not to occur. Speculation of the β–to-γ'-Ni_3Al transformation which has a total volumetric reduction of ~ 4%, has also been considered [35]. Yet in several cyclic-heat-treatment studies, rumpling had occurred prior to the formation of the γ' [41, 51]. This result indicated that it was not the driving mechanism associated with rumpling, but rather a factor that may help to further deformation.

Growth stresses were also considered to be a dominating factor in rumpling, as they can be as high as 3 GPa [50]. It has been suggested by Tolpygo and Clarke [41] that a small amount of rumpling can still occur even under an inert atmosphere, indicating that the source of rumpling comes from the coating itself rather than the oxide. It is interesting to note that although rumpling may still occur without the presence of an oxide layer, the extent of rumpling diminishes by as much as ~30% [41].

With the phase transformations and oxidation of β coatings only seeming to contribute to the rumpling behavior, CTE mismatch may be the dominating failure mechanism. However, little data is available on the differences in CTE mismatch between the coating and substrate. What data is available focuses primarily binary β and ternary Pt-modified β systems [48, 59]. As interdiffusion has been shown to greatly affect coating composition, there is a strong need to correlate depletion behavior of a commercial coating with consequential CTE mismatch. The aim of this work is to determine the CTE misfit between the coating and substrate as a function of representative depleted coating compositions. Using the data obtained by experimental research, a model by Balint and Hutchinson [43] will be used to determine the likely extent of deformation for a commercial system. The results taken from the model will then be compared to cyclic exposure treatments previously conducted [51] in order to better determine the effect of CTE mismatch on rumpling.

9.2 Experimental Procedures

Bulk alloys used in this study were processed by the Materials Preparation Center at Ames Laboratory. Samples were drop cast under argon into 12-mm diameter molds and annealed in an inert atmosphere at 1200°C for six hours and 1150°C for 48 hours. Electro-discharge machining (EDM) was then used to cut dilatometry samples 6-mm in diameter and 25.4-cm long. All dilatometry runs were conducted at General Electric's Global Research Center. Scans were conducted from 25°C to 1250°C at a rate of 5 °C/min.

Commercial coatings used in this study were supplied by General Electric. René N5 buttons 25.4-mm in diameter were coated with Pt-modified β-NiAl using a proprietary process. Before testing, samples were polished using a 1200-grit paper to remove any pre-existing abnormalities. Coatings were then heat-treated prior to experimentation at 1150°C for 1 h in order to deplete the coating composition.

Samples were then heat-treated at 1150°C (unless noted) in still laboratory air either by cyclic or isothermal oxidation using either a horizontal or vertical tube furnace. Both

furnaces were programmable; however, the vertical furnace was capable of cycling between two hot zones. The horizontal furnace was only able to cycle between the hot zone and open air. Heating rates were ~200°C/min and time at temperature was 1 hour (unless noted). In all cases samples were cycled 100 times.

After each heat treatment, surface morphology of the coating was analyzed using a Hommelwerke stylus profilometer. Scans were made within a 2 mm x 3mm area (600 scans). From the profilometry data an average peak-to-valley roughness (RzDin) and average peak-to-peak wavelength λa were calculated. The equation used to calculate the average wavelength was

$$\lambda_a = \left(\frac{R_a}{\Delta a}\right)2\pi \qquad (4)$$

Where Ra is the average roughness per scan and Δa is the change in slope.

9.3 Results

9.3.1 Effect of Oxidation on Rumpling

In order to asses the effects of an oxide layer on rumpling, a commercial coating was first heat treated and polished using 1200 grit paper to achieve a planer surface with no oxide layer present. The coated sample was then positioned into an alumina boat which contained Ta foil. The sample and alumina boat were then sealed in an evacuated followed by Ar-back-filled quartz tube. Using a horizontal tube furnace, the sample was cycled between 1150°C and 25°C.

From the surface and cross-sectional images shown in Figure 46, there appears to be a small level of surface rumpling. Profilometry results shown in Figure 47 compare the sample run under Ar with that run in air under the same temperature and time conditions. It is evident that the sample exposed to laboratory air achieved rumpling parameters almost twice those found for the encapsulated specimen. Given that an 'as coated' polished sample had a

roughness of 0.9 μm and an average wavelength of 1.3 μm, there is an indication that a minor amount of rumpling did occur.

It is very likely that the formation of the oxide layer does play a substantial role in the formation of surface rumpling. Growth stresses due to the oxidation of the coating may facilitate creep of the bond coat in some way. However, as evidenced by the rumpling experienced by the encapsulated sample, some other mechanism must also operate the stress necessary to drive the rumpling process. It has been shown that the various β phase transformations (martensite and γ') are not necessary to create rumpling [41, 51]. Swelling of the coating, another factor mentioned to cause rumpling, has only been shown to contribute stress near the beginning of cyclic exposure, with its effect diminishing significantly after only a few cycles [49, 51]. It is suggested, then, that the dominating cause of rumpling is CTE mismatch between the coating and the Ni- superalloy substrate.

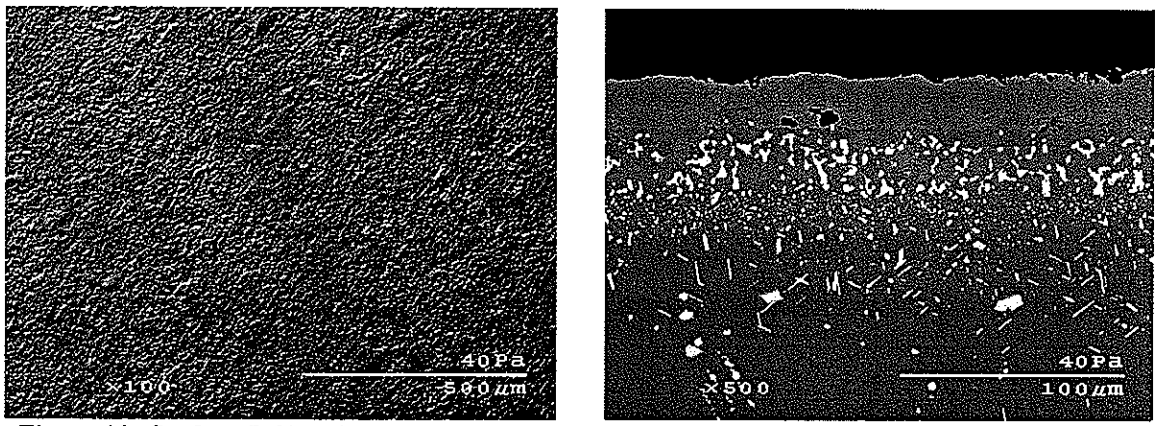

Figure 46: Surface (left) and cross section (right) images of commercial coating cycled between 1150°C and 25°C under Ar

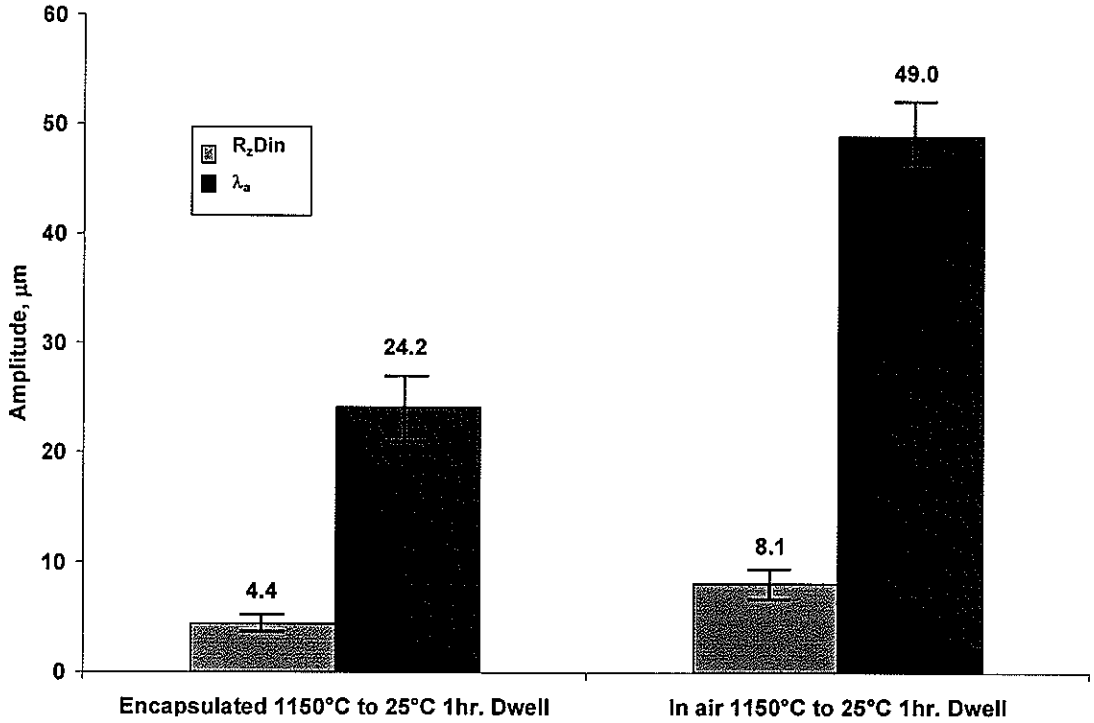

Figure 47: Profilometry results for encapsulated commercial bond coat vs. one cycled in air

9.3.2 Sensitivity of Rumpling due to CTE Mismatch

If coefficient of thermal expansion mismatch is the dominating rumpling parameter, as suggested in the previous section, then it is important to determine under what temperature regimes rumpling will occur. Commercial coatings were depleted for 1hour at 1150°C and subjected to several cyclic heat treatments. Each experiment was run using dwell times of 1 hour at each temperature for a total of 100 cycles. In each experiment, room temperature was used as the low-temperature dwell, with the high- temperature dwells being the controlled variable. Figure 48 shows the cross section of each of the commercial coatings and Figure 49 summarizes the profilometry results.

It is difficult from the results presented to determine precisely when rumpling occurs as increases in the average wavelength are present for each sample run. When determining rumpling, however, both an average wavelength and average roughness are taken into account. For the sample cycled between 1000°C and 25°C, an increase of only 0.6 ± 0.25

μm occurred compared to the 'as coated' specimen. This is in sharp contrast to the more dramatic increases in roughness found for samples cycled at 1100°C and 1150°C (3.2 μm and 7.2 μm respectively). As such, rumpling will be considered to begin at 1100°C.

The results of the cyclic heat treatments show the temperature sensitivity of rumpling. As stated previously, little rumpling was observed on the coating cycled at 1000°C. At 1100°C the roughness parameter increased dramatically, while a small increase in the peak-to-peak wavelength was found. Also present is the formation of the γ'-Ni_3Al phase as determined from EDS analysis. As some rumpling has occurred in the 1000°C where no γ' was found, the formation of the γ' phase can be neglected as the dominate cause of rumpling. The effects of γ' formation on rumpling has been studied previously, where it was found that rumpling was able to occur prior to the phase transformation [41, 51]. Also, several models explaining the phenomenon have shown large scale rumpling may still occur without the phase transformation taken into account [41, 43-45]. At 1150°C the degree of rumpling was shown to have increased dramatically. Large increases in both the roughness and wavelength parameter, as well as an increase in the amount of γ' transformation were evident. In addition, the thickness of the β coating has decreased compared to the previous two samples due to the β → γ' phase transformation

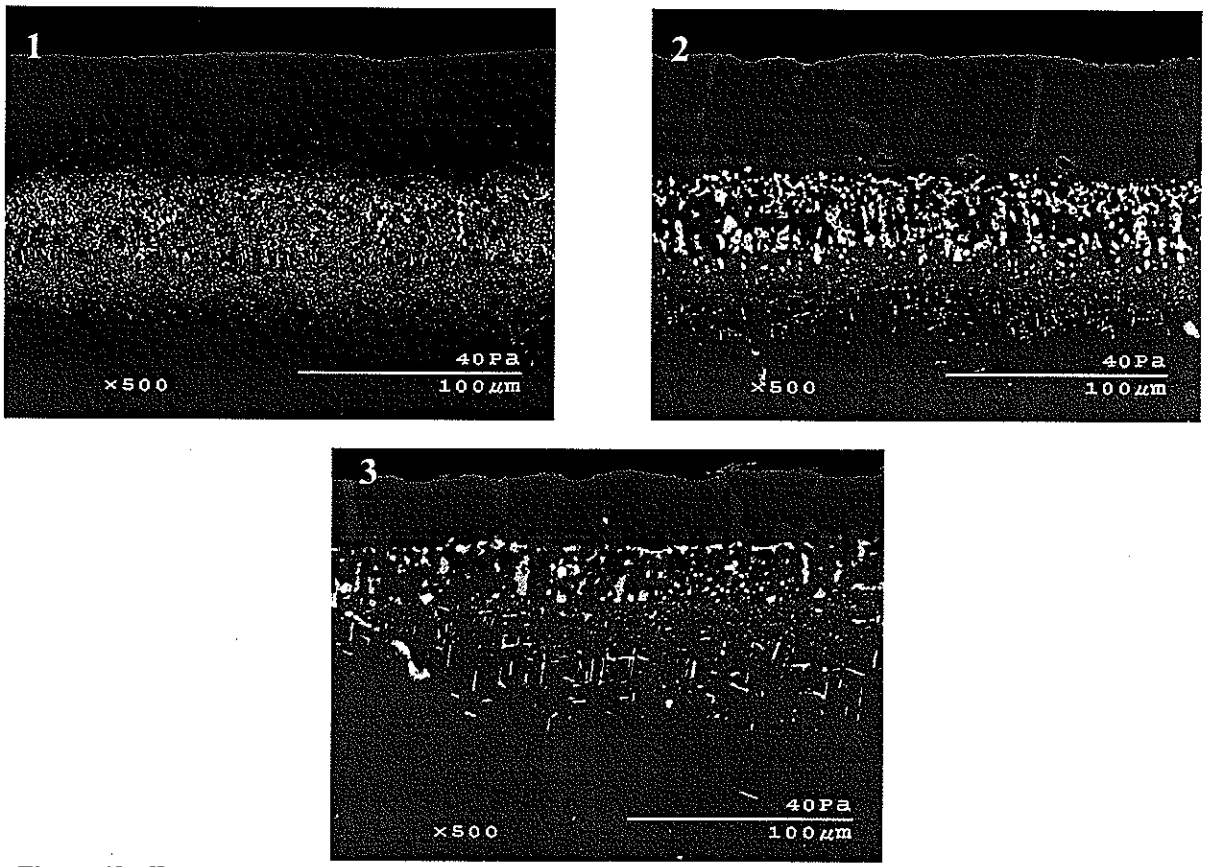

Figure 48: Temperature sensitivity to rumpling. Samples cycled between 25°C and 1000°C (1) 1100°C (2) 1150°C (3)

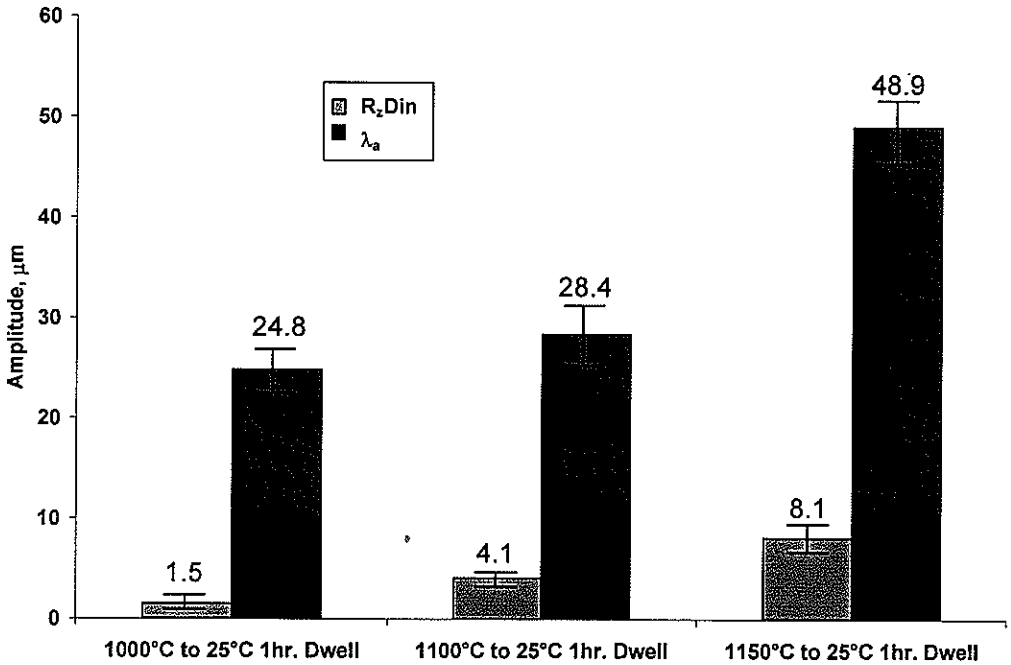

Figure 49: Profilometry results showing the temperature sensitivity of the rumpling behavior

9.3.3 Coefficient of Thermal Expansion Mismatch in Commercial Coatings

Several bulk alloys denoted as C1-C4 in Table 4 were prepared in order to determine the CTE for a commercial coating as a function of depleted composition and over a range of temperatures. Thus, the compositions in Table 1 represent the depletion path of a commercial coating at 1150°C. The exact compositions were determined in a previous paper studying the depletion behavior of commercial coatings over the temperature range of 1050°C to 1150°C [51]. All compositions were calculated using electron microprobe analysis.

Table 4: Bulk alloy dilatometry sample compositions in (at%)

Alloy	Ni	Al	Pt	Cr	Co	Mo	W	Ta
C1	48.9	37.0	7.2	2.9	3.9	0.08	n/a	0.07
C2	50.2	35.0	6.3	4.0	4.2	0.1	0.03	0.2
C3	52.0	33.0	5.4	4.5	4.6	0.1	0.05	0.4
C4	53.9	30.0	4.6	5.4	5.4	0.1	0.1	0.5

Each of the compositions analyzed using dilatometry was compared to a René N5 superalloy substrate that had been studied previously by Pint et al. [59]. Figure 50 shows the results of the dilatometry runs on heating. The superalloy substrate followed a linear relationship until ~825°C when the relation between CTE and temperature became more parabolic in nature. In contrast, each of the four depleted coating compositions follows a linear trend throughout the temperature range considered. Also evident is that as the composition of the bulk alloys become more Ni rich (moving from C1-C4), the CTE values at temperatures above 800°C increase.

One noticeable characteristic of the dilatometry plot is the apparent discontinuity which occurred at around 500°C for each composition. This event was considered of particular interest because of its occurrence at a temperature similar to the Ms reported by Chen et al. [34, 35] using DTA. The discontinuity also appears to be relatively systematic regardless of composition. Temperature variations of the thermal event only occur within ~35°C of each other. In order to determine what transformation was taking place, high temperature x-ray

diffraction was carried out on bulk alloy 'C1'. This alloy was chosen over the others due to its location within the β phase field. It is highly unlikely that the formation of the γ' would occur for this composition, leaving the martensitic transformation as the most likely thermal event. The synchrotron x-ray diffraction spectra in Figure 51 show the alloy on cooling from 1327°C (1600 K) down to 227 °C (500 K). The spectra over this temperature range correspond to a single-phase B2-β structure. As the x-ray diffraction scan clearly passes through the temperature at which the discontinuity occurs, it is difficult to determine what is taking place in the dilatometry run. It is unlikely, though, that the event within this temperature regime is simply a relic of the device used in testing because of its relevance to the previous DTA work by Chen et al. [34, 35].

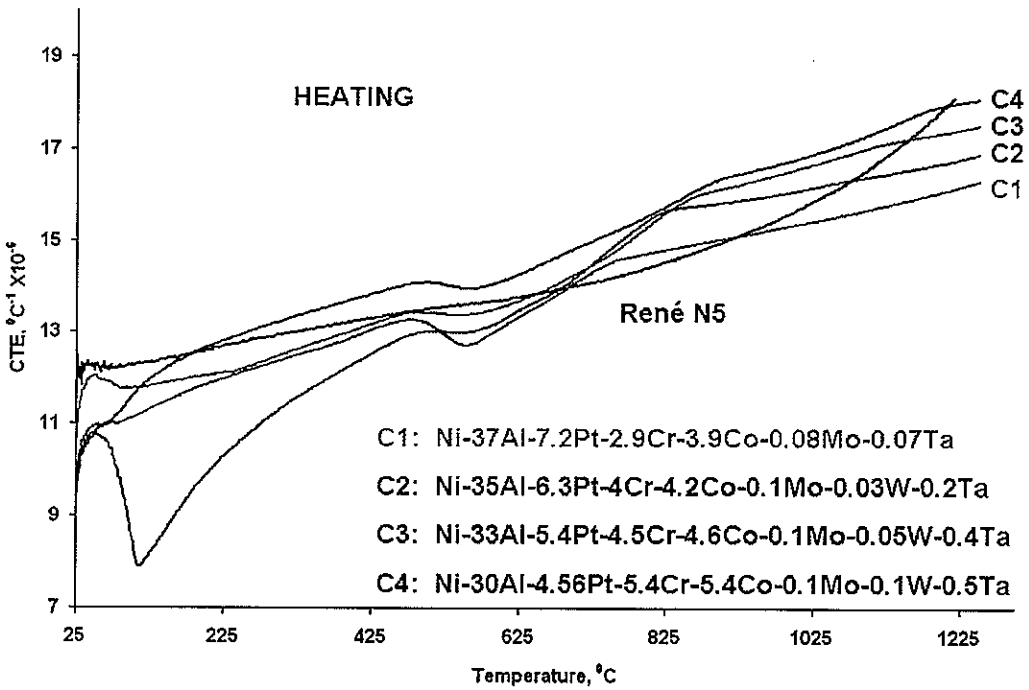

Figure 50: CTE measurements for depleted coating compositions compared to a René substrate over a range of temperatures

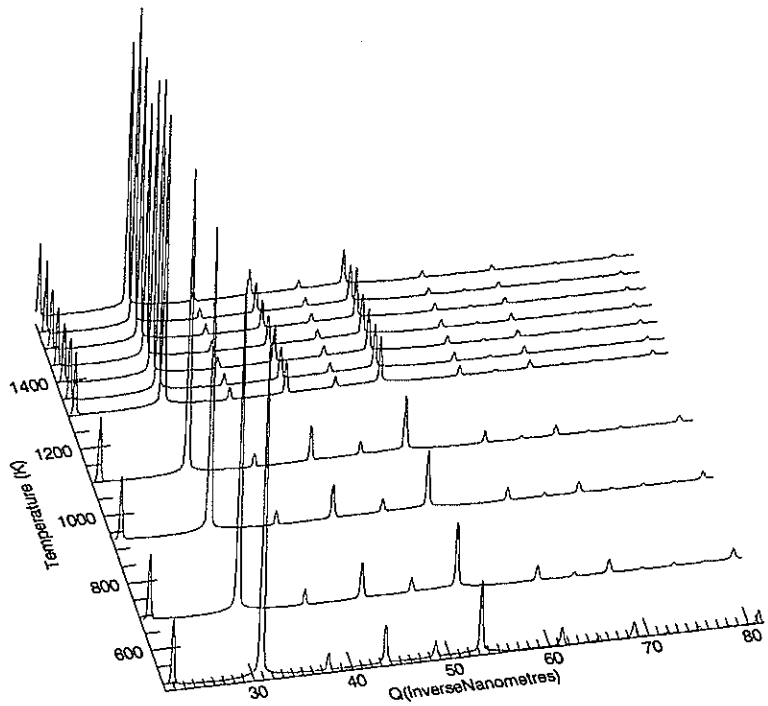

Figure 51: High-temp. synchrotron x-ray diffraction of bulk alloy 'C1' from 1500K to 500K showing only B2 β-NiAl.

The times to reach compositions C1-C4 were noted in a previous study concerning the depletion behavior of commercial coatings [51]. Using this, a plot showing the change in CTE ($\Delta CTE = CTE_{superalloy} - CTE_{bond\ coat}$) over changes in temperature above 900°C was generated. Whether the coating is in compression or tension is also labeled. This is shown in Figure 7. It is evident from Figure 52 that large differences in CTE mismatch occur during the high-temperature portions of cyclic heat treatments. This is especially true for composition C1 which remained in compression throughout the temperature regime analyzed. It is likely that this mismatch produces large strains within the coating that may be alleviated in the form of rumpling of the coating. Dwell times at lower temperature would create less strain of the coating and rumpling would be diminished. This would help to explain the temperature sensitivity of rumpling described earlier.

However, the coating composition is very dynamic due to interdiffusion between the coating and the substrate, and can change dramatically with relatively short times at high-temperature [46]. Because the rate of diffusion is exponentially dependent on temperature, a higher change in CTE values would occur for higher temperature regimes. It is also possible, then,

that the change in CTE mismatch also produces large stresses in the coating. At lower temperatures, where the progression of CTE mismatch is significantly slower, a smaller accumulation of stress would be expected.

From Figures 50 and 52 it is also shown that as the composition of the coating becomes more Ni-rich the differences in CTE mismatch diminish. This is due in part because of the interdiffusion of the coating at high temperatures, but also due to the nature of the change in CTE values with increasing temperature for the superalloy substrate. It is parabolic, rather than linear, in nature which causes a reduced ΔCTE value. For example, after reaching composition C4 the superalloy CTE is actually lower than the coatings (17.2 and 17.7°C^{-1}x10^{-6} respectively). This would cause the coating to be in tension rather than compression, making rumpling of the coating difficult. It is possible, then, that the growth stress of the oxide may help to negate the tensile stress induced in the coating. Large compressive stresses (upwards of 3 GPa [50]) occurring from the formation of the oxide may add compressive stress to the bond coat. If the magnitude of the tensile stress developed by CTE was much smaller than the stress developed by oxidation, then the bond coat stress would continue to be compressive

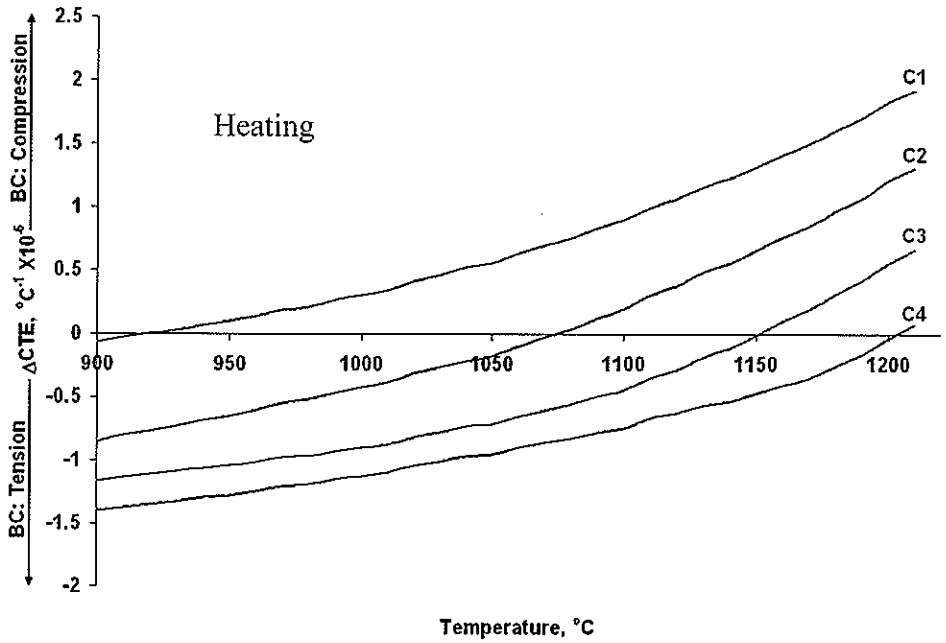

Figure 52: Change in CTE mismatch over time for normalized coating compositions at high-temperature.

9.4 Discussion

The role of CTE has been inferred from this study to be the dominant mechanism for rumpling of β-type coating systems. Several experimental data, both from this study and from another [51], contribute to supporting this inference. In order to provide further verification, a simulation model by Balint and Hutchinson [43] was used to simulate thermal cycling of a commercial coating. The coating system contained a substrate of infinite thickness, a bond coat with thickness $h^{(2)}$, and an oxide layer of thickness $h^{(3)}$. Any deformation is assumed to be sinusoidal with amplitude δ_0. The creep data from Pan et al. [48] and the swelling data from Tolpygo and Clarke [42] are used in the model. Figure 53 details the variables used and the out-of-plane compressive stress in the thermally grown oxide.

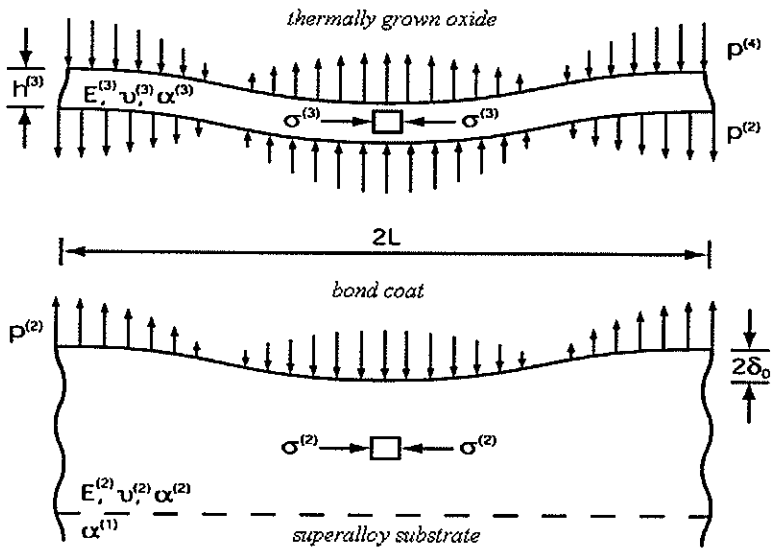

Figure 53: Schematic of variables and stresses present in β-NiAl coating system [43]

The simulation model also contains equations relating the martensitic transformation to the stress in the coating. However, the Ms used in the model is 530°C from Chen et al. [34, 35] rather than the ~100°C found by Henderkott and Gleeson [51]. In addition, coefficient of thermal expansion data for the coating and the substrate were assumed to change linearly

with temperature. While this assumption is reasonable for the coating CTE, it is much less accurate for the substrate which shows an increasing departure from linearity above 1000°C.

Figure 54 shows the results of the simulation model compared to experimental data obtained from this study. The temperature sensitivity of rumpling is clearly seen and the trend is the same for both sets of data. Moreover, the model is in relatively good agreement with the experimental data.

It is thought that the increase in bond coat rumpling occurs due to the lateral strain from the oxide growth. At higher temperatures, the oxidation rate is higher which creates higher strain. In addition, higher temperatures also lower the coating's resistance to creep which makes rumpling less difficult. Variations between heat-treatments also arise due to the 'wavelength effect' theorized by Balint and Hutchinson [43]. In it, they explain that shorter wavelength undulations which grow early during cyclic exposure are quickly overtaken by those having longer wavelengths.

As suggested by Balint and Hutchinson [43], the oxidation of the coating is crucial in creating rumpling. However, stress originating from the coating must also contribute to the formation of surface undulations. This is evidenced by the results of the encapsulated sample presented earlier. While a reduction in rumpling did occur in the encapsulated sample, there was still a substantial difference compared to the profilometry data collected for the as coated specimen. As the martensitic transformation has been shown to not influence rumpling [51], CTE mismatch is thought to be the cause of the stress induced from with the coating.

While the overall trend is the same for both the experimental and simulated data, some deviations do exist. This is especially true for the samples cycled between room temperature and 1000°C/1150°C. It is likely that these deviations arise from the assumptions used by Balint and Hutchinson [43] in their model. The simulations emphasized oxidation of the coating as the dominate cause of rumpling. This causes little change in surface deformation to occur due to stress from within the coating (although some exists). The largest error in

assumption from the model is that the CTE mismatch between the coating and the substrate is linear in nature. This is, in fact, not the case as the superalloy follows a parabolic like increase from linear at temperatures above 1000°C. Therefore, little effect of the CTE mismatch is evidenced in the simulation. This would explain why the experimental results are much higher for the sample cycled at 1150°C where CTE mismatch between the two layers is extremely high. The experimental data is lower compared to the simulation for a sample cycled at 1000°C due to the CTE mismatch being relatively low. It is also likely that the martensitic transformation which, for the model, is considered 530°C creates a simulated rumpling which is higher than if the Ms temperature was 100°C as found by Henderkott and Gleeson [51].

In the future, a better comparison between experimental data and the simulated rumpling calculated by Balint and Hutchinson is expected. This will include alterations in the CTE mismatch between the coating and substrate (namely changing the superalloy to be more parabolic at high temperature and using correct bond coat CTE data) and changes in the martensitic transformation temperature. It is hoped that with these changes the rumpling found in the model will compare more closely to that found in the simulation.

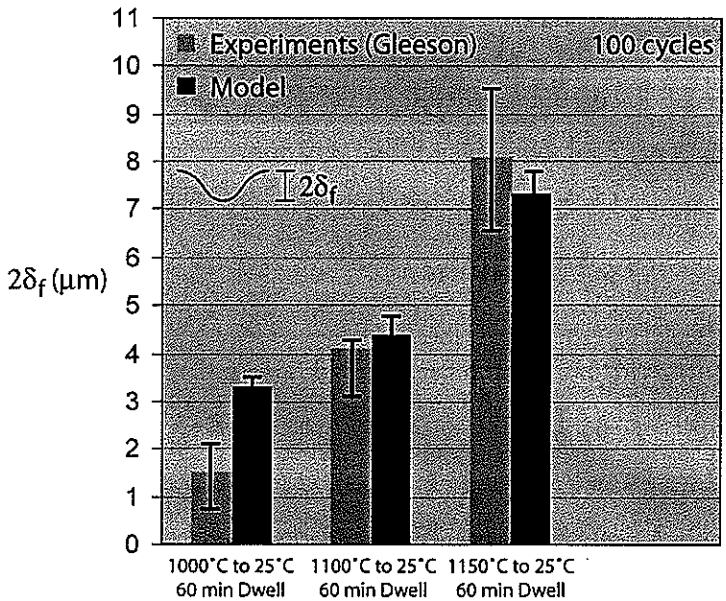

Figure 54: Bond coat rumpling predicted by the Balint and Hutchinson model compared to experimental results [60]

9.5 Summary and Conclusions

The following conclusions can be drawn from this work:

1) The presence of an oxide is not a prerequisite for the formation of rumpling. However, an overall reduction in the magnitude of the deformation is evident when no oxide is present. This indicates that stress needed to form rumpling must come from the oxide formation as well as stress generated in the coating.

2) A temperature sensitivity exists for the formation of rumpling. This occurs at approximately 1100°C.

3) A large CTE mismatch between depleted coating compositions and a superalloy substrate. This difference begins with the coating in compression but progresses to the point where the coating is in tension. It is unclear whether stress generated when the coating was in compression or the significant change in CTE mismatch over a short period of time at high temperature is responsible for the stress needed to form rumpling.

4) Experimental data was found to be in good agreement with data calculated from a model by Balint and Hutchinson [43]. However, more research is needed in order to truly model the system. This includes altering the Ms temperature and assuming a parabolic CTE for the substrate as opposed to one that is linear in nature.

Section 10: Thesis Summary and Conclusions

The formation of surface undulations (i.e. rumpling) on Pt-modified β-NiAl based coatings was studied with special emphasis placed on the martensitic transformation as the dominant failure mechanism. This was due, in part, to previous work which showed that in ternary bulk alloys, rumpling would occur due to the transformation. It was shown in that study that the high transformation temperature facilitated creep of the coating. While these results were meaningful they were thought to be a relatively large simplification of an actual coating system. Alloying additions diffusing from the superalloy substrate and into the coating create a coating with several different additions which may affect the martensitic transformation temperature, Ms, greatly.

In order to study the martensitic transformation for 'real' coatings, several commercial systems were subjected to isothermal heat treatments at various times and temperatures. It was found that the depletion path for the coatings, while time dependent, was temperature independent over the 100°C temperature regime studied. From these results, several bulk alloys were constructed that would undergo the martensitic transformation.

Differential scanning calorimetry (DSC) was then conducted on the bulk alloy systems. It was found that the Ms temperature of ~100°C was far lower than previously recorded for a similar system (530°C) [34, 35]. Differences in these transformation temperatures were thought to be due to small variations in alloying additions such as Pt and Co which are known to increase Ms and Cr which is known to lower it. It was concluded that the Ms temperature could not be an exact temperature but rather should be considered a range of values from ~100°C to almost 700°C.

A low Ms temperature put the ability for the martensitic transformation to cause rumpling in a real coating system in question. This was further emphasized when cyclic heat treatments of a bulk alloy with a low Ms temperature were unable to cause any rumpling beyond that formed simply by oxidation. Several different cyclic heat treatments of the commercial

coating complimented the results of the bulk alloy by showing that the martensitic transformation was not a requirement of rumpling. Cycling exclusively above Ms (no transformation) caused similar rumpling in a coating cycled above and below Ms. Cycling above and below Ms but at lower temperature (600°C to 25°C) presented an extremely planer surface with no real rumpling present. These results suggest some other mechanism must be facilitating rumpling.

While a low temperature martensitic transformation was unable to cause rumpling, it was found to have detrimental effects on the lifetime on both the coating and bulk alloy system. Low temperature cycling between 400°C and 25°C was found to induce cracks in each system due to repeated $\beta \rightarrow$ martensite transformations. These cracks ran exclusively along the grain boundaries in the bulk alloy system but ran both inter- and intra-granular in the coating. Continuous cycling of the bulk alloy results in a sample which could be broken into several sections.

It was thought that the cracking was due to stress accumulation resulting from the transformation. As the ductile to brittle transition temperature for a depleted coating is ~600°C, plastic deformation would be unable to occur. In fact, cycling at 600°C resulted in no crack formation although the martensitic phase was clearly present. Finally, cracks were unable to sinter together during high temperature exposure. This indicated that fatigue could cause continued crack propagation at high temperature.

Coefficient of thermal expansion mismatch was suggested to be the dominating failure mechanism associated with rumpling. This result was verified using several experiments. In the first, an encapsulated sample with no oxide layer was cycled between 1150°C and 25°C. It was found that rumpling was suppressed slightly, but still occurred. It was inferred that the oxide growth stress must also play a role in rumpling, but a stress still would need to occur in the coating to facilitate creep.

Dilatometry measurements were conducted on several bulk alloys representing depleted coatings as well as a René N5 substrate. It was found that as the composition becomes more Ni rich (i.e. interdiffusion and oxidation occur) the CTE values become higher at temperatures above 800°C. All coating compositions followed a linear trend while the superalloy substrate deviated from its linear behavior above 1000°C. An increase in the CTE mismatch between the coating and substrate was found for high-temperature holds. A reduction in this mismatch occurred as the temperature was reduced. A larger CTE mismatch, it was inferred, would create larger stress in the coating. Further analysis of the dilatometry results indicated that at higher temperatures the drop in differences in CTE mismatch was extremely high compared to lower temperatures. It was thought that this dramatic change in CTE mismatch over a short period of time may also help to induce stress in the coating. It was also suggested that, if this was the case, the sign of the stress (tensile or compressive) was irrelevant as large compressive stresses developing from the oxide growth stress would likely maintain a compressive stress in the coating.

Preliminary results using a model by Balint and Hutchinson [43] were found to be in good agreement with experimental data. However, several assumptions used in the model were found to be inaccurate. Foremost was the fact that the CTE data for the substrate was assumed to be linear in nature instead of parabolic. Also, the Ms temperature used in the model was much higher than the one found in this study. Further collaboration with Balint is needed in order to determine the stress imposed by CTE mismatch in the coating.

Section 11: References

1. M. Peters, C. Leyens, U. Schulz, W.A. Kaysser, EB-PVD Thermal Barrier Coatings for Aeroengines and Gas Turbines, *Adv. Eng. Matls.* **3 (4)** 193-204 (2001).

2. P. Seserko, J. Hotz, J. Lemke, P. R. Smith, M. Mede, EB PVD Thermal Barrier Coatings in Production, *ALD Vacuum Technologies AG* (2002).

3. D.R. Clarke, C.G. Levi, Materials Design for the Next Generation Thermal Barrier Coatings, *Annu. Rev. Mater. Res.* **33** 383-417 (2003).

4. H.E. Evans, M. P. Taylor, Delamination Processes in Thermal Barrier Coating Systems, *Journ. of Corr. Sci. and Eng.* **6 (Paper H011)** (2003).

5. Kofstad, Per, ed. "High Temperature Corrosion" Elsevier Applied Science. 121-122 (1988).

6. Kh.G. Schmitt-Thomas, M. Hertter, Improved Oxidation Resistance of Thermal Barrier Coatings, *Surface and Coating Technology.* **120-121** 84-88 (1999).

7. W.J. Quadakkers, V. Shemet, D. Sebold, R. Anton, E. Wessel, L. Singheiser, Oxidation Characteristics of a Platinized MCrAlY Bond Coat for TBC Systems During Cyclic Oxidation at 1000°C, *Surface and Coating Technology.* **199** 77-82 (2005).

8. D.J. Young, B. Gleeson, Alloy Phase Transformations Driven by High Temperature Corrosion Processes, *Corr. Sci.* **44** 345-357 (2002).

9. M.C. Meelu, M.H. Loretto, Development of High-Temperature Corrosion-Resistant Composite Coatings on Gas Turbin Hot End Components, *Materials and Design.* **14** 53-55 (1993).

10. B. Gleeson, W. Wang, S. Hayashi, D. Sordelet, Effects of Platinum on the Interdiffusion and Oxidation Behavior of Ni-Al-based Alloys, *Mat. Sci. Forum* **461-464** 213-222 (2004).

11. B.A. Pint, The Role of Chemical Composition on the Oxidation Performance of Aluminide Coatings, *Surface and Coating Technology.* **188-189** 71-78 (2004).

12. F. Ibegazene, Oxidation of Alumina-forming (Ni,Pd)Al and (Ni, Pt)Al Alloys. Influence of a Thermal Barrier coating. Ph.D. Thesis (Univeristy Paris XI, 200).

13. R. Bouchet, Interdiffusion Study in High Tmerpature Protective Coatings, Ph.D. Thesis (University of Paris XI, 2004).

14. Z. Suo, D.V. Kubair, A.G. Evans, D.R. Clarke, V.K. Tolpygo, Stresses Induced in Alloys by Selective Oxidation, *Acta Mat.* **51** 959-974 (2003).

15. A. Selcuk, A. Atkinson. The Evolution of Residual Stress in the Thermally Grown Oxide in Pt Diffusion Bond Coats in TBCs. *Acta Materialia,* **51** 535-539 (2003).

16. H.E. Evans. Stress Effects in High Temperature Oxidation of Metals. *Int. Mat. Rev.* **40** 1-40 (1995).

17. J. L. Smialek, G. H. Meier. High-Temperature Oxidation Wiley-Interscience, John Wiley and Sons, Superalloys II--High Temperature Materials for Aerospace and Industrial Power, pp. 293-326, (1987).

18. P. Y. Hou, A. P. Paulikas, B. W. Veal, Stress Development and Relaxation in Al_2O_3 During Early Stage Oxidation of β-NiAl, *High Temperature Materials.* 373-380 (2005).

19. Y. Cadoret, D. monceau, M. Bacos, P. Josso, V. Maurice, P. Marcus, Effect of Platinum on the Growth Rate of the Oxide Scale Formed on Cast Nickel Aluminide Intermetallic Alloys, *oxidation of Metals.* **64** 185-205 (2005).

20. D. Oquab, D. Monceau, In-Situ SEM Study of Cavity Growth During High Temperature Oxidation of β-(Ni,Pd)Al, *Scripta Mater.* **44** 2741-2746 (2001).

21. J. Angenete, K. Stiller, E. Bakchinova, Microstructural and Microchemical Development of Simple and Pt-Modified Aluminide Diffusion Coatings During Long term Oxidation at 1050^0C, *Surface and Coatings Technology.* **176** 272-283 (2004).

22. S. Shanker, L.L. Seigle. Interdiffusion and Intrinsic Diffusion in the NiAl (δ) Phase of the Al-Ni System, *Metallurgical Transactions A.* **9A** 1467-1476 (1978).

23. E. Basuki, A. Crosky, B. Gleeson. Interdiffusion Behaviour in Aluminide-Coated Rene 80H at 1150°C, *Materials Science and Engineering.* **A224** 27-32 (1997).

24. J.L. Smialek, R.F. Hehemann. Transformation Temperatures of martensite in Beta-Phase Nickel Aluminide, *Metallurgical Transactions A.* **4** 1571-1575 (1972).

25. W.A. Maxwell, E.M. Grala. Investigation of Nickel Aluminum Alloys Containing 14 to 34 Percent Alumninum, *National Advisory Committee For Aeronoutics.* (1954).

26. U.D. Hangen, G. Sauthoff. The Effect of Martensite Formation on the Mechanical Behavior of NiAl, *Intermetallics.* **7** 501-510 (1999).

27. C. Barrett, T.B. Massalski. "Structure of Metals" 3rd addition. Pergamon Press **35** 529 (1980).

28. D.J. Sordelet, M.F. Besser, R.T. Ott, B.J. Zimmerman, W.D. Porter, B. Gleeson. Isothermal Nature of Martensitic Formation in Pt-Modified β-NiAl Alloys, *Acta Met.* In Press (2007).

29. B.J. Zimmerman MS Thesis, Iowa State Univeristy (2005).

30. C. Jiang, D.J. Sordelt, B. Gleeson. Effects of Pt on the Elastic Properties of B2 NiAl: A Combined First-Principles and Experimeental Study, *Acta Materialial,* **54** 2361-2369 (2006).

31. K. Otsuka, X. Ren. Mechanism of Martensite Aging Effects and New Aspects, *Materials Science and Engineering*, **A312** 207-218 (2001).

32. R. Kainuma, H. Ohtani, K. Ishida. Effect of Alloying Elements on Martensitic Transformation in the Binary NiAl Phase Alloys, *Metallurgical and Materials Transactions*, **27A** 2445-2453 (1996).

33. Y. Zhang, J.A. Haynes, B.A. Pint, I.G. Wright, W.Y. Lee. Martensitic Transformation in CVD NIAl and (Ni,Pt)Al Bond Coatings, *Surface and Coatings Technology*, **163-164** 19-24 (2003).

34. M.W. Chen, M. L. Glynn, R. T. Ott, T. C. Hufnagel, K. J. Hemker. Characterization and Modeling of a Martensitic Transformation in a Platinum Modified Diffusion Aluminide Bond Coat for Thermal barrier coatings, *Acta Materialia*, **51** 4279-4294 (2003).

35. M. W. Chen, R. T. Ott, T. C. Hufnagel, P. K. Wright, K. J. Hemker. Microstructural Evolution of Platinum Modified Nickel Aluminide Bond Coat During Thermal Cycling, *Surface and Coating Technology*, **163-164** 25-30 (2003).

36. P. Deb, D. Boone, T Manley II. Surface Instability of Platinum Modified Aluminide Coatings During 1100^{0}C Cyclic Testing. *J. Vac. Sci Technol.* **A 5** (6) 3366-3372 (1987).

37. V. Tolpygo, D. Clarke. Surface Rumpling of a (Ni,Pt)Al Bond Coat Induced by Cyclic Oxidation. *Acta Mater* **48** 3283-3293 (2000).

38. R. Panat, S. Zhang, K. Jimmy Hsia. Bond Coat Surface Rumpling in Thermal Barrier Coatings. *Acta Materialia*, **51** 239-249 (2003).

39. L.B. Freund. A Surface Chemical Potential for Solids. *Journal of Mechanics and Physics of Solids,* **46** 1835-1844 (1998).

40. V. K. Tolpygo, D. R. Clarke. Rumpling Induced by Thermal Cycling of an Overlay Coating: The Effect of Coating Thickness. *Acta Materialia* **52** 615-621 (2004).

41. V. K. Tolpygo, D. R. Clarke. On the Rumpling Mechanism in Nickel-Aluminide Coatings Part I: An Experimental Assessment. *Acta Materialia*, **52** 5115-5127 (2004).

42. V. K. Tolpygo, D. R. Clarke. On the Rumpling Mechanism in Nickel-Aluminide Coatings Part II: Characterization of Surface Undulations and Bond Coat Swelling. *Acta Materialia*, **52** 5129-5141 (2004).

43. D. S. Balint, J. W. Hutchinson. An analytical Model of Rumping in Thermal Barrier Coatings. *Journal of Mechanics and Physics of Solids*, **53** 949-973 (2005).

44. A. M. Karlsson, J. W. Hutchinson, A. G. Evans. A Fundamental Model of Cyclic Instabilities in Thermal Barrier Systems. *J. Mech. Phys. Solids*, **50** 1565-1589 (2002).

45. A. M. Karlsson, A. G. Evans. A Numerical Model for Cyclic Instability of Thermally Grown Oxides in Thermal Barrier Systems. *Acta Materialia*, **49** 1793-1804 (2001).

46. J.L. Smialek, C.E. Lowell. Effects of Diffusion on Aluminum Depletion and Degradation of NiAl Coatings. *Electrochemical Society, Journal*, **121** 800-805 (1974)

47. M.G. Hocking, V. Vasantasree, P.S. Sidky. "Metallic and Ceramic Coatings: Production", High Temperature Properties and Applications. Longman Scientific and Technical, 173-195 (1989).

48. D. Pan, M.W. Chen, P.K. Wright, K.J. Hemker. Evolution of a Diffusion Aluminide Bond Coat for Thermal Barrier Coatings During Thermal Cycling. *Acta Materialia,* **51** 2205-2217 (2003).

49. A.W. Davis, A.G. Evans. Effects of Bond Coat Misfit Strains on the Rumpling of Thermally Grown Oxides. *Metallurgical Transactions A,* **37A** 2085-2095 (2006)

50. D.M. Lipkin, A.G. Evans. Measurement of the Stress in Oxide Scales Formed by Oxidation of Alumina-Forming Alloys. *Oxidation of Metals,* **45** 267-280 (1996).

51. J. Henderkott, B. Gleeson. Investigation of the Martensitic Transformation and Rumpling in Pt-Modified β-NiAl Based Coatings. unpublished work at Iowa State Univeristy (2007).

52. T.C. Totemeier, J.E. King. Isothermal Fatigue of an Aluminide-Coated Single-Crystal Superalloy: Part I. *Metallurgical Transactions A,* **27A** 353-361 (1996).

53. T.C. Totemeier, W.F. Gale, J.E. King. Isothermal Fatigue of an Aluminide-Coated Single-Crystal Superalloy: Part II. *Metallurgical Transactions A,* **27A** 363-369 (1996).

54. B. Moretto, J. Bressers. Thermo-mechanical Fatigue Degradation of a Nickel-Aluminide Coating on a Single-Crystal Nickel-Based Alloy. *Journal of Materials Science*, **31** 4817-4829 (1996).

55. Y.H. Zhang, D.M. Knowles, P.J. Withers. Micromechanics of Failure of Aluminide Coated Single Crystal Ni Superalloy Under Thermomechanical Fatigue. *Scripta Materialia*, **37** 815-820 (1997).

56. B.M. Warnes, A.L. Purivs, J.E. Schilbe. The Manufacture and Fatigue Cracking Resistance of Grit Free Aluminide Diffusion Coatings. *Surface and Coating Technology*, **163-164** 100-105 (2003).

57. S. Stekovic, T. Ericsson. Low-Cycle Fatigue and Damage of an Uncoated and Coated Single Crystal Nickel-Base Superalloy SCB. *International Journal of Materials Research,* **01/2007** 26-32 (2007).

58. M. Eskner, R. Sandström. Measurement of the Ductile-to-Brittle Transition Temperature in a Nickel Aluminide Coating by a Miniaturized Disc Bending Test Technique. *Surface and Coating Technology,* **165** 71-80 (2003).

59. J.A. Haynes, B.A. Pint, W.D. Porter, I.G. Wright. Comparison of Thermal Expansion and Oxidation Behavior of Various High-Temperature Coating Materials and Superalloys. *Materials at High Temperature,* **21 number 2** 87-94 (2004).

60. D. Balint. TBC conferences, University of California Santa Barbara, (2007).